Distribution Agreement

In presenting this thesis or dissertation as a partial fulfillment of the requirements for an advanced degree from Emory University, I hereby grant to Emory University and its agents the non-exclusive license to archive, make accessible, and display my thesis or dissertation in whole or in part in all forms of media, now or hereafter known, including display on the world wide web. I understand that I may select some access restrictions as part of the online submission of this thesis or dissertation. I retain all ownership rights to the copyright of the thesis or dissertation. I also retain the right to use in future works (such as articles or books) all or part of this thesis or dissertation.

Signature:

_____ _____

Valentina Gonzalez-Pecchi Date

Characterization of MYC Interaction with Nuclear Receptor SET Domain Protein 3 (NSD3)

By

Valentina Gonzalez-Pecchi
Doctor of Philosophy

Graduate Division of Biological and Biomedical Science
Cancer Biology

Haian Fu, Ph.D.
Advisor

Yuhong Du, Ph.D.
Committee Member

Maureen Powers, Ph.D.
Committee Member

Paula Vertino, M.D.
Committee Member

Wei Zhou, Ph.D.
Committee Member

Accepted:

Lisa A. Tedesco, Ph.D.
Dean of the James T. Laney School of Graduate Studies

Date

Characterization of MYC Interaction with Nuclear Receptor SET Domain Protein 3 (NSD3)

By

Valentina Gonzalez-Pecchi
M.Sc., Universidad de Concepción, Chile, 2014
B.S., Universidad de Concepción, Chile, 2012

Advisor: Haian Fu, Ph.D.

An abstract of
A dissertation submitted to the Faculty of the
James T. Laney School of Graduate Studies of Emory University
in partial fulfillment of the requirements for the degree of
Doctor of Philosophy
in
Graduate Division of Biological and Biomedical Sciences
Cancer Biology
2019

Abstract

Characterization of MYC Interaction with Nuclear Receptor SET Domain Protein 3 (NSD3)

By Valentina Gonzalez-Pecchi

As genomics advances reveal the cancer genome landscape, a daunting task is to understand how these genes contribute to dysregulated oncogenic pathways. Integration of cancer genes into networks offers opportunities to reveal protein-protein interactions (PPI) with functional and therapeutic significance. The generation of a cancer-focused PPI network termed OncoPPi, identify 397 cancer-associated PPIs. PPI hubs reveal new regulatory mechanisms for cancer genes like MYC.

The MYC transcription factor plays a crucial role in cell growth control. Enhanced MYC protein stability has been found to promote tumorigenesis. Thus, understanding how MYC stability is controlled may have significant implications for revealing MYC-driven growth regulatory mechanisms in physiological and pathological processes. Our previous work identified the histone lysine methyltransferase Nuclear Receptor SET Domain protein 3 (NSD3) as a MYC modulator. NSD3S, a non-catalytic isoform of NSD3 with oncogenic activity. However, the mechanism by which NSD3S regulates MYC remains to be elucidated. To uncover the nature of the interaction and the underlying mechanism of MYC regulation by NSD3S, my research revealed that NSD3S binds, stabilizes, and activates the transcriptional activity of MYC. Further characterization of the binding interface between both proteins narrowed the interface to a 15 amino acid region in NSD3S that is required for MYC regulation. Mechanistically, NSD3S binds to MYC and reduces the association of F-box and WD repeat domain containing 7 (FBXW7) with MYC, which results in suppression of FBXW7-mediated proteasomal degradation of MYC and an in increase MYC protein half-life.

These results support a critical role for NSD3S in the regulation of MYC function and provide a novel mechanism for NSD3S oncogenic function through inhibition of FBXW7-mediated degradation of MYC. The study suggests a novel regulatory axis between NSD3S and MYC and a potential therapeutic approach for treating patients with MYC-driven tumors.

Characterization of MYC Interaction with Nuclear Receptor SET Domain Protein 3 (NSD3)

By

Valentina Gonzalez-Pecchi
M.Sc., Universidad de Concepción, Chile, 2014
B.S., Universidad de Concepción, Chile, 2012

Advisor: Haian Fu, Ph.D.

A dissertation submitted to the Faculty of the
James T. Laney School of Graduate Studies of Emory University
in partial fulfillment of the requirements for the degree of
Doctor of Philosophy
in
Graduate Division of Biological and Biomedical Sciences
Cancer Biology
2019

Acknowledgments

I want to thank my advisor, Haian Fu, for all of his support and dedication over my graduate studies. For repeatedly teaching me to believe in me, to be confident and a critical thinker. I will always be thankful, and I will apply what I learned from him in my future. I want to thank the members of the Fu lab, especially; Cindy, Sean, Albert, Qiankun, Xiu-Lei, Andrei, and Yuhong for sharing with me their experimental knowledge for the completion of this dissertation. Especial thanks to my friends Lauren and MaKendra, for always providing excellent advice, support and an environment where we could get distraction from lab work. I also thank my committee members for their scientific feedback over these years.

I am grateful to my Chilean Atlanta family. All of you have been more than friends to me. Thank you for all of the good conversations, for all of the laughs, hugs and great moments that we shared and that I will always remember. And for giving me love, support and a place to stay during these last months. My dear Argentinian friend, Candela, thank you for the coffee breaks (much needed), the long talks and encouraging me always.

I thank especially my Mom; she has been a constant support in every aspect throughout my life. She is one of the main reasons I am here and now finishing my graduate studies. Also, my grandfather, Nonno, you were so excited during my application process, thank you for supporting and inspiring me to continue my professional training. Grateful also to my sisters, Gina and Paula, the messages and words of encouragement were always welcoming and truly important. To all of my family, extended family and friends back in Chile, who came to visit us to Atlanta, the video calls, the messages, thank you all.

Lastly, none of this would have been possible without the support, help, and love from my husband, Sebastian. Thank you for always believing in me. For making these 5 and a half years in Atlanta, the best, for all of the trips we made, for taking this opportunity selflessly without even knowing what you were going to do during this time. Finally, making this chapter of our life unforgettable and worthwhile. For all of the memories, we take back to Chile. I dedicate this dissertation to you.

Table of Contents

List of Figures

List of Tables

Chapter 1: Introduction

Cellular regulatory systems are interconnected and orchestrated to lead to normal physiological output. Those regulatory systems are often mediated by molecular interactions, such as protein-protein interactions (PPI). PPIs sense environmental cues and transmit them into the cell regulatory machinery to exert defined biological outputs. Malfunctioning of those PPIs may lead to various disease states, such as cancer. My dissertation focusses on two proteins, MYC, and NSD3S in the regulation of cancer cells. This chapter will outline the general properties of cancer, followed by a summary on PPIs with a focus on MYC and NSD3S proteins.

1.1 Cancer

Cancer is the second leading cause of death worldwide, with an estimate of 1 in 6 deaths due to cancer (WHO September 2018). It is a disease characterized by the uncontrolled growth of abnormal or cancerous cells which invade and spread to different parts of the body. Defined also as the imbalance between oncogenes and tumor suppressor genes, genes that when activated or inactivated, respectively, increase the growth advantage of cells (1). Hallmarks of cancer have been described as tumor cells having eight capabilities that enable tumor growth and dissemination. These are: sustained proliferative signaling, evading growth suppressors, resisting cell death, enabling replicative immortality, inducing angiogenesis, activating invasion and metastasis, reprogramming of energy metabolism and evading immune destruction (2, 3). Two enabling capabilities underlie all of these hallmarks, genome instability and tumor inflammation (3). These hallmarks often are determined by aberrant PPIs.

1.2 Protein-Protein Interaction Network

All cells of the body contain proteins, and these are major players in signaling pathways that drive the function of a particular cell type. Because of the relevance of proteins in regulating cell signaling and function, proteins are a major target for the development of new therapeutic options for cancer

and other diseases. The interaction between two proteins is how an external or internal signal is transmitted through the cell, making PPIs the backbone of cellular signaling pathways. In cancer, PPIs form signaling nodes that promote tumorigenesis. Aberrant regulation of essential PPIs in cells can contribute to the acquisition of the eight hallmarks of cancer, described in section 1.1 (4). Understanding the cancer-associated PPI network may help to identify those interactions that are crucial for cancer cell survival. Targeting PPI interfaces has become of interest as it may represent an anti-cancer strategy through cell signaling pathway perturbation (5). However, for many years PPIs were considered undruggable. The large contact interface and the general flatness of the interaction are two reasons that make disruption of PPIs difficult (5). Despite these challenges, there have been successful small inhibitors of PPIs (6, 7), suggesting that targeting the binding interface between two proteins may be a feasible therapeutic approach. Thus, by studying cancer associated PPIs networks, we intend to identify novel protein interaction interfaces that could lead to new intervention strategies.

To establish a PPI network in lung cancer, our laboratory and the Emory Chemical Biology and Discovery Center (ECBDC) developed a cancer genomics high-throughput screening (HTS) assay. This assay will be discussed in more detail in Chapter 2. We selected genes altered in lung cancer from The Cancer Genome Atlas (TCGA) and performed the HTS screening assay using Time-Resolved Fluorescence Resonance Energy Transfer (TR-FRET) technology. From the screening we identified 397 novel PPIs, generating the OncoPPi (v.1) network (8) (Figure 1-1). MYC, a well-studied oncogene, was identified as a hub of the PPI network interacting with more than 20 proteins. MYC is essential for cancer cell survival, thus a promised cancer drug target. However, it has proven difficult to target MYC, partially because it is a disordered protein and lacks enzymatic activity. Until now, no MYC inhibitor has been FDA (Food and Drug Administration) approved. We postulate that by studying MYC PPIs, we can indirectly target MYC function.

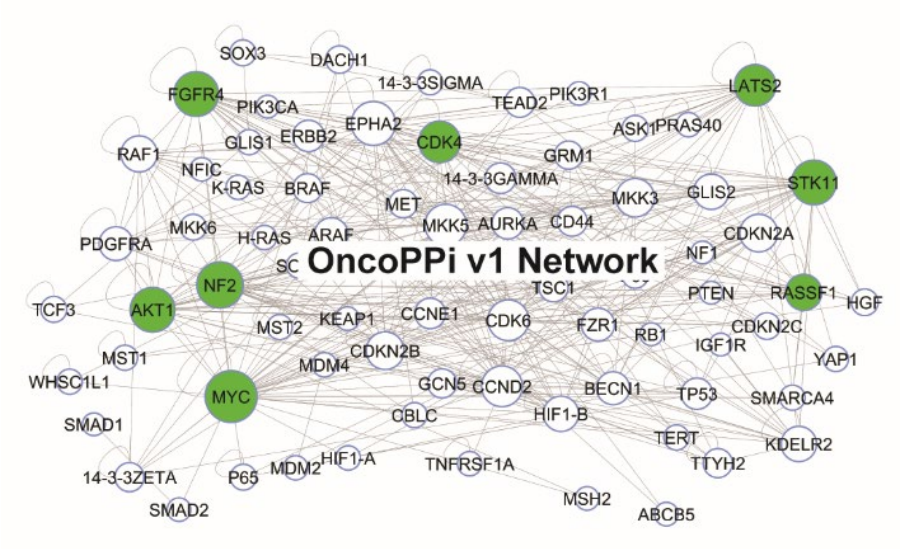
OncoPPi v1 Network
SOX3
DACH1
FGFR4
14-3-3SIGMA
TEAD2
PIK3R1
LATS2
PIK3CA
EPHA2
ASK1
PRAS40
GLIS1
ERBB2
CDK4
RAF1
GRM1
NFIC
14-3-3GAMMA
STK11
K-RAS
BRAF
MKK3
GLIS2
MET
MKK6
MKK5
AURKA
CD44
CDKN2A
PDGFRA
H-RAS
ARAF
NF1
NF2
TSC1
PTEN
RASSF1
HGF
TCF3
AKT1
MST2
KEAP1
CCNE1
CDK6
FZR1
RB1
CDKN2C
IGF1R
MST1
CDKN2B
MDM4
YAP1
WHSC1L1
GCN5
CCND2
BECN1
TP53
SMARCA4
MYC
SMAD1
CBLC
HIF1-B
TERT
KDELR2
TTYH2
14-3-3ZETA
P65
MDM2
HIF1-A
TNFRSF1A
MSH2
SMAD2
ABCB5

Figure 1-1. OncoPPi (v.1) network in lung cancer.

Diagram showing the OncoPPi network generated by the high-throughput PPI screening using TR-FRET assay in lung cancer cells. Shown in green circles are protein hubs on the network (8).

1.3 MYC

MYC was identified in experiments performed around the year 1980. Investigators found homology between an overexpressed gene in human bursal tumors (MYC) and an oncogene carried by the avian Myelocytomatosis virus (v-MYC) (9). Later, three cellular isoforms of MYC were described, c-MYC, N-MYC, and L-MYC, that share between 35 to 50% sequence homology. c-MYC (MYC) is overexpressed in a broad spectrum of hematologic and solid malignancies, while N-MYC overexpression is found in neuroblastoma and glioma, and L-MYC in small cell lung cancer (10, 11).

1.3.1 MYC protein structure

MYC is a 439 amino acid protein, and it consists of a transactivation domain (TAD) in the N-terminus, a central portion, and the C-terminal domain involved in DNA binding. MYC is composed of conserved sequences within the three isoforms, named MYC boxes (MBI to MBIV) (Figure 1-2). The TAD is unstructured unless it is bound to partner proteins to either activate or repress transcription (12) and it is composed of MBI (amino acid (aa) 44-63) and MBII (aa 128-143). MBI and MBII are required for cellular transformation (13). MBII also drives tumorigenesis *in vivo* (14) and activates or represses transcription of target genes by binding with co-activators or co-repressors (15, 16). The central portion of MYC contains MBIIIa (aa 188-199), MBIIIb (aa 259-270), MBIV (aa 304-324) and the nuclear localization signal (NLS) (aa 320-328). MBIIIa is required for *in vitro* transformation, *in vivo* tumorigenesis (17), and for transcriptional repression (18). Until now, no function for MBIIIb has been described (11). MBIV has been linked to MYC pro-apoptotic functions (19). The C-terminal DNA binding domain is composed of the basic-helix-loop-helix-leucine zipper (bHLH-LZ) region (20), that recognizes the consensus DNA sequence "CACGTG," termed "Enhancer box" (E-box). MYC binds the E-box as a heterodimer with MAX protein, as discussed later in section 1.3.4 (21).

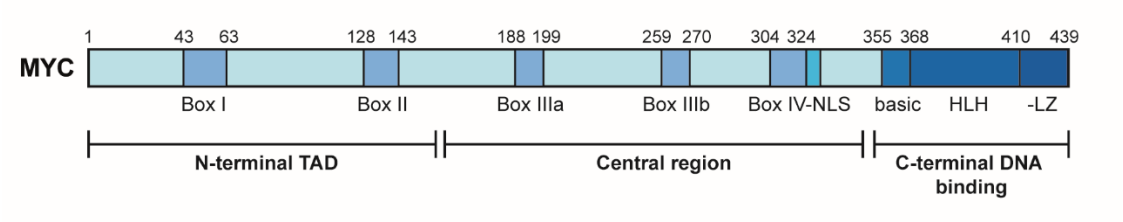
MYC
1
43
63
128
143
188
199
259
270
304
324
355
368
410
439
Box I
Box II
Box IIIa
Box IIIb
Box IV-NLS
basic
HLH
-LZ
N-terminal TAD
Central region
C-terminal DNA binding

Figure 1-2. MYC protein structure.

From the N-terminal of MYC, there are the MYC boxes (MBI, II, IIIa, IIIb and IV) which are conserved across different members of the MYC family of proteins. Right next to MBIV is the nuclear localization signal (NLS) and the basic helix-loop-helix leucine zipper (bHLH-LZ) domain. The amino acids for each domain are labeled on top.

1.3.2 MYC alterations in cancer

Normal cells express a few thousand molecules of MYC (22), but in tumor cells, this number can increase up to 40 folds (23, 24). *MYC* is an "immediate early" gene (24), defined as, not usually expressed in quiescent cells, but its transcription is induced rapidly after exposure to growth factors (25). After transcription, *MYC* mRNA is exported to the cytoplasm under the control of mitogenic signals (26), where it has a short half-life of approximately 20 minutes (27). After protein synthesis, the half-life of MYC protein is also short, about 20 to 30 minutes in normal cells (28). MYC protein turnover is regulated by post-translational modifications (PTM), such as phosphorylation, acetylation, glycosylation, and ubiquitylation (29). Another level of protein regulation is PPIs, which leads to particular states of MYC expression or activity (discussed in section 1.3.3) (30).

For a normal cell to become transformed by MYC, requires only overexpression of the wild-type protein (31, 32). Three mechanisms can lead to MYC overexpression.

(i) Amplification – Amplification of the *MYC* gene is observed in different human cancer types. On average 50% of human cancers have a *MYC* locus amplification. The extent of amplification correlates with a more aggressive tumor (33). *MYC* amplification may be even higher, as the studies do not consider the deregulation of the protein by PTMs or PPIs. These mechanisms can elevate the activity of *MYC* without having a locus amplification (11). As one example, some colorectal cancers have a loss of adenomatous polyposis coli (APC) gene, which leads to β-catenin accumulation and activation of a transcription factor that stimulates constitutive high expression of *MYC* (34).

(ii) Chromosomal translocation – *MYC* locus is translocated in 100% of Burkitt´s lymphoma patients (35). It places *MYC* under the control of the immunoglobulin μ heavy chain enhancer, thus increasing *MYC* mRNA synthesis and overexpression of the protein (36, 37).

(iii) Mutations – Found in about 50% of Burkitt´s lymphoma and AIDS-associated hematological tumors, mutations are often combined with genomic rearrangement that leads to elevated MYC (38-40). Mutations cluster on the MYC TAD domain a region also relevant for MYC degradation; thus, mutations tend to increase MYC stability, leading to protein overexpression (41). MYC amplification is enough to promote tumorigenesis, so it is thought that mutations do not contribute significantly to cancer development (11).

1.3.3 MYC interactome

MYC protein interacts with approximately 10 to 15% of proteins in the genome to regulate numerous biological activities (42). Due to the large number of proteins interacting with MYC, a small fraction of positive and negative MYC regulators and relevant to the current dissertation will be summarized in Table 1-1.

Protein name	The region in MYC where it binds	The function associated with MYC	Ref.
Axin1	N-terminal (1-100)	Facilitates binding of MYC to GSK3β, Pin1 and PP2A for MYC degradation	(43)
BRCA1	HLH (371-412)	Inhibits transcriptional activation	(44)
β-TrCP	278-283	Ubiquitylates MYC antagonizing FBXW7-degradation	(45)
ERα		Transcriptional activation	(46)
ERK	N-terminal	Increase MYC stability	(47)
FBXW7	MBI (phospho-T58)	Ubiquitylates MYC for proteasomal degradation	(48, 49)
FOXO3		Transcriptional repression	(50)
GCN5	MBII	Transcriptional activation through the complex with TRRAP	(51)
GSK3β	N-terminal (1-100)	Phosphorylates T58 and promotes MYC degradation	(52, 53)
HDAC1	bHLH-LZ	Transcriptional repression	(18)
HIF1α		Inhibits transcriptional activation	(54)
MAX	HLH-LZ (368-435)	Required for transcriptional activation and repression	(21)
Miz-1	HLH (371-412)	Transcriptional repression	(55)
p-TEFb	N-terminal (36-70)	Transcriptional activation through elongation pause release	(56, 57)
Pin1	Phospho-T58	Isomerization of MYC for PP2A dephosphorylation	(58)
PP2A	Phospho-S62	Dephosphorylates p-S62 of MYC	(58)
RPL11	MBII	Inhibits transcriptional activation	(59)
Skp2	MBII, HLH-LZ	Ubiquitylates MYC for degradation and transcriptional activation	(60, 61)
SMAD2/3	Internal region (251-360)	Transcriptional repression	(62)
SMARCA4		Inhibits transcriptional activation	(63)
TRRAP	N-terminal and MBII	Transcriptional activation	(64, 65)
VHL		Transcriptional repression through recruitment of HDAC1	(66)

Table 1-1. Part of MYC interactome.

Relevant MYC binding partners for the dissertation are listed, along with the region where they bind in MYC and the function associated with MYC regulation. Adapted from (42).

1.3.4 MYC transcriptional regulation

MYC is a basic-helix-loop-helix-leucine zipper (bHLH-LZ) transcription factor that heterodimerizes, through the HLH motif, with a second protein belonging to the bHLH-LZ family, called MYC-Associated Factor X (MAX) (20). Unlike MYC, MAX protein is highly stable, but its association with MYC does not increase MYC half-life. In contrast to MYC, MAX is in excess and tends to form homodimers in cells. Therefore, when MYC is present, it competes with MAX/MAX dimers to form MYC/MAX heterodimers (21). MYC by itself cannot bind to chromatin; however, MYC/MAX complex forms a functional DNA-binding domain (DBD) which binds to E-box promoters on the chromatin (67). E-boxes are present at a frequency of one every 4kb, and MYC binding increases on segments where there is tri-methylation of histone 3 lysine 4 (H3K4me3), associated with open chromatin (68, 69). MYC also interacts and recruits co-activators or co-repressors, respectively, to induce or suppress transcriptional activity. A portion of these proteins is listed in Table 1-1.

The discovery of MYC as a transcriptional activator lead scientists to study MYC target genes that would provide the connection of the oncogene to important cancer cell processes. MYC has a preference to bind genes that are actively being transcribed, i.e., genes which have already been activated by other transcription factors (70). The consequence is transcriptional amplification, producing increased levels of gene products. Thus, instead of binding and regulating a new set of genes, MYC usually amplifies the output of the existing gene expression program within a cell. This program may explain the diverse effects of MYC in a cancer cell (23, 71).

1.3.5 MYC degradation

As already mentioned, the abundance of MYC in cells is a highly controlled process due to the numerous relevant functions in regulating tumorigenesis. Thus, MYC degradation is crucial to

maintaining low cellular levels of this oncogenic protein. There are two mechanisms to keep low levels of MYC. One is calpain-dependent cleavage, and the second, believed to have a more significant impact on MYC turnover is the ubiquitin-proteasome system (UPS) (30, 72), which will be discussed in more detail.

MYC is cleaved by proteases called calpains in the cytosol (73), and it eliminates the C-terminal domain of the protein, leaving a portion of the protein termed "MYC-nick" (298 aa), which functions in cytoplasmic reorganization and cell differentiation (74).

UPS is a highly specific process, in which ubiquitin is covalently attached to the target protein on lysine residues. The selectivity of ubiquitination is due to degron elements present in the target proteins, as the enzymes that catalyze the addition of ubiquitin, called E3 ligases, bind to those regions. The resulted poly-ubiquitinated target proteins then are degraded by the proteasome (75). MYC itself has a degron region for E3 ligase binding with the N-terminus that is the main site for MYC ubiquitination (41). Along with the degron domain, there are other regions of MYC that control for protein degradation: the D-element relevant for proteolysis but not for ubiquitination (76), the PEST element (region enriched in proline (P), glutamic acid (E), serine (S) and threonine (T)) deletion of this element stabilizes MYC (77) and finally the "stabilon" element, which stabilizes MYC through binding to Miz-1 and repressed transcriptional activation (41).

There are more than ten E3 ligases that contribute to MYC turnover. However, the most well studied and relevant for the dissertation is the SCF^{FBXW7} (Skp-Cullin-F box). The degradation of MYC by the F-box and WD repeat domain-containing 7 (FBXW7), an E3 ligase, is a controlled and sequential event. First, MYC is phosphorylated on serine 62 (S62) by extracellular signal-related kinases (ERK), which stabilizes the MYC protein (47). Phospho-S62 MYC creates a consensus site for recognition and phosphorylation of threonine 58 (T58) by glycogen synthase kinase-3β (GSK3β),

a phosphorylation event required for subsequent MYC degradation (52). Phosphorylation of MYC at T58 promotes dephosphorylation of S62 by protein phosphatase 2A (PP2A) (58). The peptidyl-prolyl isomerase Pin1 is essential for PP2A action, as it catalyzes the isomerization from *cis* to *trans* Proline 63 of MYC, which facilitates de interaction of PP2A (78). pT58-MYC is recognized by FBXW7 which ubiquitylates MYC with K48 linkage and marks the oncogene for degradation by the proteasome (48, 49) (Figure 1-3).

Other examples of E3 ligases that control MYC turnover are, beta-TrCP (F-box and WD repeat domain containing protein 1A or FBXW1) which ubiquitylates MYC, building a "heterotypic"-poly-ubiquitin chain (K48 and K63 linkages), stabilizing MYC (45). HectH9 (Homologous to E6AP carboxyl terminus homologous protein 9) ubiquitylates MYC through a K63 linkage, which results in activation of MYC transcriptional activity (79). Examples of E3 ligases that degrade and inactivate MYC are; TRIM32 (Tripartite Motif Containing 32), FBX29 (F-box/WD repeat-containing protein 8 or FBXW8), TRUSS (transient receptor potential cation channel subfamily C member associated 4) and CHIP (C terminus of HSC70-Interacting Protein) (80-83). E3 ligases targeting MYC act under certain cell environments, for example, FBXW7 only acts when MYC is in the nucleolus, HectH9 acts on a subset of MYC dependent promoters and beta-TrCP regulates MYC just in S-phase arrest conditions (72).

UPS is a reversible process; deubiquitylating enzymes (dUBs) prevent the degradation of proteins. For MYC, there have been dUBs described (84), and the combined action of E3 ligases and dUBs will regulate the fate of MYC protein. As an example, USP28 (Ubiquitin Specific Peptidase 28) is a dUB; it binds to MYC and opposes the action of FBXW7 increasing MYC stability in response to DNA damage (85).

There is also fine-tuning between acetylation and ubiquitination of MYC, as both PTMs occurs on lysine residues on a protein. Histone acetyltransferases (HAT) such as CBP/p300 (CREB-binding protein /E1A binding protein p300), GCN5 (general control of amino acid synthesis protein 5-like 2) or TIP60 (60 kDa Tat-interactive protein) acetylates MYC on lysine residues, thus interfering with MYC ubiquitination and increasing protein stability (86-88).

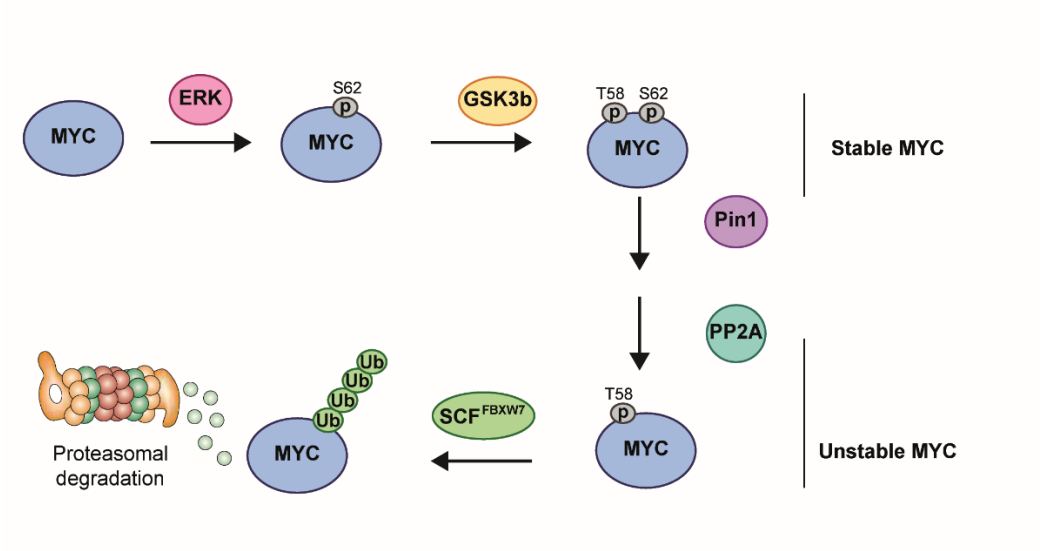
MYC
ERK
S62
P
MYC
GSK3b
T58
S62
P
P
MYC
Stable MYC
Pin1
PP2A
Ub
Ub
Ub
Ub
MYC
SCF FBXW7
T58
P
MYC
Unstable MYC
Proteasomal
degradation

Figure 1-3: SCF^{FBXW7} proteasomal degradation pathway of MYC oncoprotein.

Sequential events of phosphorylation and dephosphorylation lead to ubiquitination of MYC by FBXW7 and proteasomal degradation.

1.3.6 Functions of MYC in tumorigenesis

MYC is involved in the regulation of different hallmarks of cancer, which finally lead to the initiation, maintenance, and progression of tumorigenesis, because of this MYC has been termed "the oncogene from hell" (89).

- Cell Cycle – MYC specifically acts to accelerate G1 and G2 phases of the cell cycle, in the presence or absence of growth factors (90, 91). Part of this role results from activation of cyclin/CDK (cyclin-dependent kinases) expression by MYC transcriptional activity (92).
- Apoptosis – MYC promotes apoptosis only when survival factors are absent (93). MYC induces cell death by diverse mechanisms, one of them by disturbing the balance between pro- and anti-apoptotic proteins (94, 95), and indirectly by stimulating the expression of proteins that activate apoptosis (96). Finally, the most common way of MYC inducing apoptosis is by increasing p53 (tumor protein 53) tumor suppressor activity (97).
- Cell growth – High levels of MYC stimulate cell growth by activating ribosome biogenesis and protein translation (98). The consequence is a cell of twice the size, producing twice the amount of proteins and RNA compared to a cell with normal levels of MYC (11).
- Metabolism – Tumor cells with high MYC levels, became dependent on glucose and glutamine for survival (99, 100), due to the increase of genes involved in glycolysis and glutamine metabolism (101).
- Genomic Instability – High levels of MYC make cancer cells more susceptible to DNA damage, due to the increase of reactive oxygen species (ROS) by MYC (102), and also promote DNA replication stress by disrupting the DNA replication fork symmetry (11).
- Tumor microenvironment – MYC increases expression of vascular endothelial growth factor (VEGF), inducing the development of vascular supply for the tumor (103). MYC also

increases expression of genes related to tumor invasion, cell-cell adhesion proteins and promoting epithelial to mesenchymal transition, processes related to tumor metastasis (104).

1.3.7 Approaches to target MYC

A lot of effort has been directed toward targeting MYC. Studies over time have established that targeting MYC protein could have promising benefits for human tumors, as cancer cells with MYC amplification are "addicted" to the oncogene (105-107). But still, MYC is considered undruggable, primarily because it is an unstructured protein without a defined ligand binding site, and for lacking and inhibitable enzymatic activity.

Until now there have been mainly three approached to inhibit MYC function in tumors. One is direct MYC inhibitors, such as the generation of Omomyc, a dominant negative inhibitor of MYC that has a good response in animal models (105, 108). A second approach is the inhibition of downstream signaling or transcriptional regulation by MYC. A strategy in this category has been interrupting MYC/MAX heterodimer formation and subsequent DNA binding. Although studies have shown promising results *in vitro*, evidence for the efficacy in *in vivo* models is lacking (109-111). Finally, the third category is inhibitors which target upstream regulation of MYC. For example, by targeting the Ub-proteasome system, generating small molecules that increase the rate of MYC destruction or inhibits proteins that stabilize MYC protein (11, 85).

1.4 Novel MYC binding partners

By studying MYC interactors, we can better understand how MYC oncogenic function is regulated on cancer cells. Utilizing the information from the novel MYC binding partners, new avenues on how to target this oncogene can be explored, either by upstream regulation of MYC or downstream regulating the transcriptional activity. Among the MYC binding partners that we found in the OncoPPi screening, known MYC partners validated our assay, and novel MYC PPIs were

identified. One interesting novel PPI that we found, and is the focus of this dissertation, is the interaction with nuclear receptor SET domain protein 3 (NSD3S), which is an epigenetic regulator, specifically a histone lysine methyltransferase. MYC, until now, has been related to epigenetics, but mainly through histone acetylation and DNA methylation. Also, the fact that the interaction involves the isoform of NSD3 that lacks the enzymatic activity (NSD3S) could mean a novel function independent of the catalytic activity of NSD3.

1.5 Epigenetics and NSD3

Epigenetics is the modification of gene expression without involving changes in the DNA sequence. Epigenetics involves covalent PTMs of the DNA (methylation) or histones (methylation, acetylation, phosphorylation, ubiquitination or sumoylation). Histone PTMs occurs on the N-terminal histone tails and have a critical role in chromatin structure, function and gene expression. There are enzymes that deposit modifications in histones called "writers," enzymes which remove these PTMs called "erasers" and finally proteins which recognize the PTMs referred to as "readers." Histone methyltransferases (HMTs) are writers and readers of the chromatin. As writers, they are responsible for catalyzing the addition of methyl groups in arginine (PRMT/CARM) or lysine residues (HKMT). Most of the lysine methylation is carried out by SET-domain containing proteins (112). The different states of methyl groups in lysine residues in the chromatin elicit distinct effects on chromatin function. For example, methylation of H3K4, H3K36 and H3K79 associates with euchromatin, permissive for gene transcription, in contrary, methylation of H3K9, H3K27 and H4K20 links with heterochromatin and transcriptional repression. The nuclear receptor-binding SET domain (NSD) family is a subgroup of the HKMTs, and it is composed by three members: NSD1, NSD2/MMSET/WHSC1, and NSD3/WHSC1L1 (hereafter labeled as NSD1, NSD2, and NSD3) (113-115).

1.5.1 NSD3 protein structure

NSD3 (Nuclear receptor-binding su(var)3-9, enhancer of zeste, trithorax [SET] domain containing gene 3) or WHSC1L1 (Wolf-Hirschhorn syndrome candidate-1-like-1) was first described in 2000, by studying the proline-tryptophan-tryptophan-proline (PWWP) domain of NSD2 (WHSC1 or MMSET), performing a database search for proteins containing this domain in their structure (113). NSD3 shows homology with NSD2 (WHSC1) (116). The gene encoding NSD3 is found in chromosome 8p11.2 (117) with a cDNA size of 5.5Kb, encoding a protein of 1437 amino acids, termed NSD3 long isoform (NSD3L) or full-length protein (Figure 1-4) (118). The NSD3 gene encodes three different isoforms, one of them being the full-length protein. NSD3L contains five plant-home-domain-type zinc finger motifs (PHD), two PWWP domain, and the methyltransferase SET domain. Right next to the SET domain, there is the SET-associated Cys-rich domain (SAC), and finally, near the end of the protein, there is a Cys-His-rich domain termed C5HCH motif (118). There is a smaller isoform, named NSD3 short (NSD3S) generated by alternative splicing of exon 10 and polyadenylation that encodes a protein of 645 amino acids. NSD3S is identical to NSD3L on the first 619 amino acids, including the first PWWP domain, losing the conserved domains between the NSD family of proteins, including the methyltransferase SET domain, that gives the enzymatic activity to the protein (117, 118). Finally, there is the WHISTLE (WHSC1-like 1 isoform 9 with methyltransferase activity to lysine) isoform, a second alternative splice version of NSD3L. This isoform encodes a protein of 506 amino acids that includes the second PWWP, SET, post-SET and PHD5 finger domains of NSD3L (117, 118) (Figure 1-4). Comparing the sequence with other members of the NSD family of proteins, NSD3 shares a similarity of 68% with NSD1 and 55% with NSD2, in regions with conserved domains (on NSD3L between residues 703 and 1409) (118).

Each domain found on NSD3 protein has a different function. The PWWP domains mediate PPIs (116) and also acts as a reader domain for DNA and methylated histone 3 lysine 36 (H3K36me)

(119-121). The PDH domain is also a reader domain which binds to chromatin. The catalytic SET domain is a region conserved between the proteins belonging to the SET family of methyltransferases, giving them the specificity for mono or di-methylation of H3K36. The SET domain itself is separated into three smaller regions, the pre-SET, SET and post-SET segments, all of them required for the catalytic activity (122), however, the post-SET region is relevant for binding to nucleosomes (123). When nucleosomes are used as the substrate, NSD3L is highly specific for mono and di-methylation of H3K36 (124). NSD3L has both the writer (SET domain) and reader (PWWPs and PHDs domains) capacity. However, NSD3S isoform has only the reader function, binding to methylated H3K36 marks through the first PWWP domain.

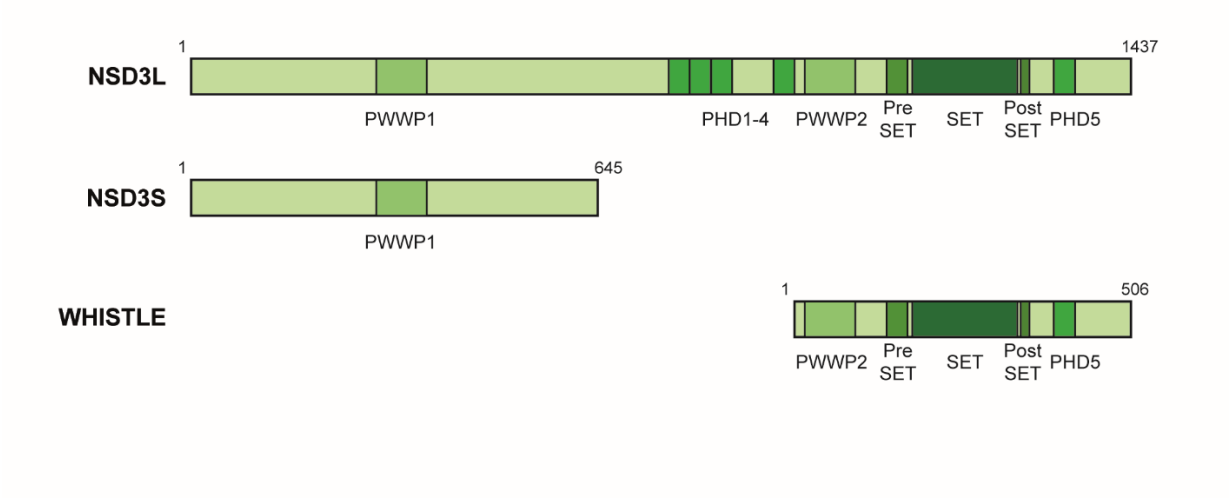
NSD3L
1
1437
PWWP1
PHD1-4
PWWP2
Pre SET
SET
Post SET
PHD5
NSD3S
1
645
PWWP1
WHISTLE
1
506
PWWP2
Pre SET
SET
Post SET
PHD5

Figure 1-4: NSD3 isoforms and protein structure.

NSD3 has three isoforms, NSD3 long (NSD3L) or full-length protein, NSD3 short (NSD3S) and WHISTLE. The protein structure of each isoform consists of different domains; all of them found on NSD3L. From the N-terminal there is a PWWP domain found in both -L and -S isoform, then only in -L isoform there are 4 PHD and a second PWWP domain. More to the C-terminal region, is the SET catalytic domain and the last PHD domain, both of them found in -L and WHISTLE isoform.

1.5.2 NSD3 alterations in cancer

NSD3L and NSD3S are ubiquitously expressed in human tissues with higher expression in heart, brain, and placenta (118). Among the isoforms, NSD3S expression is higher than NSD3L (117, 125). In contrast, the WHISTLE isoform is only expressed in testis (113). The oncogenic role of NSD3 has been supported by locus amplification and translocations generating oncogenic fusions (126).

(i) Amplification - *NSD3* gene is located in the short arm of chromosome 8p11, a region that is commonly amplified in breast cancer, non-small-cell lung cancer (NSCLC), lung adenocarcinoma (AC), pancreatic ductal adenocarcinoma (PDAC) and squamous cell carcinoma of the head and neck (SCCHN) (125, 127, 128). Several oncogenes are encoded by the region 8p11, such as *FGFR1* (fibroblast growth factor receptor 1), *LSM1* (U6 snRNA-associated Sm-like protein), *PPAPDC1B* (Phospholipid phosphatase 5) among others. Amplification of 8p11 is found in about 10 to 15% of breast cancer tumor samples and is correlated with poor prognosis (125, 129-132). *NSD3* is one of the genes amplified in those samples and proposed as one of the major candidate oncogenes, apart from *FGFR1* (125, 133).

(ii) Translocation - *NSD3* gene was first found as part of a fusion with *NUP98* gene in a patient with acute myeloid leukemia (AML) (134). The t(8;11)(p11.2;p15) fuses *NUP98* to the 3´end of *NSD3*, containing the SET and last PHD domain. The fusion transcript includes the FG repeats of *NUP98*, that are known to bind transcription factors, such as CREB-binding protein (134), suggesting a relevant role of the fusion for transcriptional misregulation in leukemic cells. Translocations are often found in hematological cancers; in contrast, epithelial tumors usually are driven by amplification, deletion or mutation of proteins. One exception is nuclear protein in testis (NUT) midline carcinoma (NMC) that is driven by chromosomal

translocations of the *NUT* gene. In about 65% of the cases, *NUT* is fused to *BRD4*, in 25% *NUT* is fused to *BRD3*, with the remaining 10% having unknown partners. Interestingly, recent reports have found *NUT* fused to *NSD3* (135-138). The first NMC patient with *NSD3-NUT* fusion t(8;15)(p12;q15) was identified in 2014. The fusion is defined as a protein comprising exons 1-7 of NSD3 connected to exons 2-7 of NUT protein, encoding a protein of 1694 amino acids, containing residues 1 to 569 of NSD3 and 8 to 1132 of NUT (135). Unlike the *NUP98-NSD3* fusion, the *NSD3-NUT* fusion has only the N-terminal region of NSD3 protein, almost the complete NSD3S isoform, lacking the methyltransferase activity. *NSD3-NUT* oncofusion is necessary and sufficient for the blockage of differentiation and the proliferation of NMC cells (135). *NSD3-NUT* oncofusion has also been described in patients with NMC of the lung including the same 5´ exons of NSD3 described previously (136).

1.5.3 NSD3 interactome

Compared to MYC less is known about what proteins normally interact with NSD3. LSD2 (lysine-specific histone demethylase 2 or KDM1B, an H3K4 specific demethylase) and G9a (histone-lysine N-methyltransferase or EHMT2, an H3K9 specific methyltransferase) are two proteins that bind to NSD3 and together form a tertiary complex, localizing to the bodies of actively transcribed genes. This complex coordinates the methyl modifications at H3K4, H3K9, and H3K36 during elongation for transcription (139).

NSD3 also interacts with BRD4 (bromodomain-containing protein 4), specifically with the ET (extra-terminal) domain, to generate a pTEFb-independent transcriptional activation function in BRD4 and also to regulate the methylation of H3K36 at BRD4 target genes for transcription (140). Later, Shen et al. characterized the binding of BRD4 to a small 11 amino acid region on the N-terminal of NSD3 (aa 152-163). Interestingly, the same publication showed that the short isoform, NSD3S,

was required and sufficient for driving leukemogenesis, indicating a methyltransferase-independent function of the protein. NSD3S also binds to the chromatin remodeler CHD8 (Chromodomain Helicase DNA Binding Protein 8) through the C-terminal region of NSD3S, acting as an adaptor protein, linking BRD4 to CHD8 on the chromatin. NSD3S, BRD4, and CHD8 proteins colocalize in areas of the genome and they are released from MYC super-enhancers using the BRD4 inhibitor, JQ-1 (141).

We recently established that NSD3S interacts with MYC via the C-terminal domain of the protein, and postulate that the interaction can stabilize MYC protein and increase transcriptional activity (details on Chapter 2) (8).

1.5.4 Function of NSD3 in tumorigenesis

HMTs have been showed to methylate not only histones but also proteins. NSD3 mono-methylates Lys721 of EGFR (epidermal growth factor receptor) within the kinase domain. This modification increases the kinase activity and downstream oncogenic signaling independent of interaction with the ligand EGF (epidermal growth factor) and stimulates cell cycle progression (142). NSD3 also mono-methylates IRF3 (interferon regulatory factor 3). The consequence of the protein methylation is an increased IRF3 transcriptional activity. Specifically, methylation of IRF3 sustains phosphorylation of IRF3 by interfering with the binding between IRF3 and phosphatase PP1cc (serine/threonine-protein phosphatase PP1-gamma catalytic subunit) (143).

Numerous studies have supported the oncogenic role of NSD3. As previously mentioned, NSD3 regulates survival, transformation, and invasiveness of breast cancer cell lines containing the 8p11 amplicon (125, 133, 144). Interestingly, a patient with breast cancer harboring 8p11 amplicon contained a deletion in the C-terminal region of NSD3, with specific amplification of exons 1 to 10, encoding the NSD3S isoform, suggesting a role for the short isoform, NSD3S in driving tumorigenesis

(145). In lung, pancreatic and osteosarcoma cancer cell lines, deletion of NSD3 decreases the viability, colony formation capacity and increases apoptosis of cancer cells (128, 132, 146). NSD3, as an epigenetic regulator, has also been implicated in controlling transcription of target genes. NSD3 regulates gene expression of *CDC6* (cell division cycle 6) and C*DK2* (Cyclin-dependent kinase 2), acting on G1 to S transition during the cell cycle (147). Another study reported NSD3 activating expression of *CCNG1* (cyclin G1) and *NEK7* (NIMA Related Kinase 7), showing an essential role in G2 to M phase transition during the cell cycle (148). Combination of these studies shows important functions of NSD3 in regulating proliferation, growth, and apoptosis of cancer cells.

Particularly, NSD3S isoform has been correlated to the oncogenic WNT signaling pathway. Overexpression of NSD3S decreases the expression of *SFRP1* gene (secreted frizzled-related protein 1), a negative regulator of WNT signaling. It also increases the expression of *IRX3* (Iroquois-class homeodomain protein IRX-3), and both, *SFRP1* and *IRX3* have been linked to WNT signaling regulation in embryonic stem cell growth (125, 149).

Although the oncogenic function of NSD3 has been established and validated in multiple cell models, there is one study in 2010 that described NSD3L isoform as a tumor suppressor in human breast cancer cell lines. This study demonstrated that depletion of NSD3L increases pathways related to cell growth, cell cycle, motility and decreased apoptosis (150). Interestingly, the WHISTLE isoform has been proposed as a tumor suppressor also, repressing transcription and promoting apoptosis in an HMT dependent manner in cancer cells (113, 151).

Taken together, the current knowledge concerning NSD3 suggests that the short isoform, NSD3S is a critical mediator of oncogenesis. Further investigation of its downstream effects will inform the rational design of improved targeted epigenetic cancer therapeutics.

1.6 Scope of the dissertation

This dissertation aims to describe the protein-protein interaction between MYC and NSD3S and how it regulates MYC function. In Chapter 2, I will provide evidence of the interaction by orthogonal assays and regulation of MYC stability and transcriptional activity. Chapter 3 will address the identification of the binding interface between the two proteins and describe a mechanism by which NSD3S stabilizes the MYC protein by interrupting binding of MYC to FBXW7. Studying the interaction and mechanism of regulation between MYC and NSD3S adds to understanding the complex regulation of cancer by MYC, and may also reveal the oncogenic MYC/NSD3S PPI as a potential drug target for therapeutic discovery (Appendix A.2).

Chapter 2: The OncoPPi network of cancer-focused protein-protein interactions to inform novel MYC binding partners

A portion of this chapter was published as:

Li Z*, Ivanov AA*, Su R*, Gonzalez-Pecchi V, et al., "The OncoPPi network of cancer-focused protein-protein interactions to inform biological insights and therapeutic strategies." Nature Communications (2017) doi: 10.1038.

2.1 Introduction

Protein-protein interactions (PPI) form the backbone of signal transduction pathways and networks in diverse physiological processes (152). Due to their critical roles in relaying cell growth signals in both normal and cancer cells, once 'undruggable' PPIs have attracted much attention as a potential new class of drug targets (4, 5). In support of this pursuit, large-scale proteomics approaches have been utilized to generate highly informative PPI interactomes (153-155). These studies have resulted in rich resources leading to critical insights into intricate biological regulatory systems. However, the large number of novel PPIs discovered in these large-scale studies demonstrate that only a small portion of the PPI landscape is currently known (153, 156, 157). Further, for specific diseases such as cancer, utilization of these large-scale datasets is limited by lack of inclusion of many disease-specific genes, lack of experimental data in relevant cellular environments as well as inconsistent PPI data quality among various databases. The human interactome space, particularly for disease-focused studies, remains largely open (153, 154, 158). In contrast, cancer genomics studies have advanced towards comprehensive molecular characterization of human cancers, revealing an expanded cancer gene landscape (1, 159) and defining a subset of the proteome that is intimately associated with cancer. Importantly, a large fraction of this cancer genomics space is occupied by non-enzymatic proteins that can only be therapeutically targeted through their molecular interactions (1, 159). To complement large-scale proteomics efforts and leverage cancer genomics data, we undertook a focused proteomics study to discover protein interactions among a set of genes selected for their involvement in lung cancer (160, 161). Our approach is supported by the understanding that proteins involved in a certain disease tend to interact with each other to form a disease-specific interaction network, such as those in cancer (162, 163). In this study, we establish a cancer-associated PPI network, termed the OncoPPi network (version 1), through the implementation of a streamlined time-resolved Förster resonance energy transfer (TR-FRET) technology platform for systematic binary PPI

discovery in an efficient high throughput format. We discover more than 260 high-confidence PPIs not identified in previous large-scale datasets. OncoPPi identifies prominent protein interaction hubs with new PPI partners revolving around key cancer drivers such as MYC, STK11, RASSF1 and CDK4, uncovers interactions for non-enzymatic proteins, suggests crosstalk between oncogenic pathways, implicates novel mechanisms of action for major oncogene drivers such as transcription factor MYC, and reveals connectivity of tumor suppressors with actionable targets. The OncoPPi network expands the lung cancer-associated protein interaction landscape for the discovery of novel cancer targets and connects tumor suppressors to available drugs, offering an experimental resource for exploitation of PPI-mediated cancer vulnerabilities.

2.2 Material and methods

The detailed methods have been published in Nature Communications (2017) doi: 10.1038 (8).

Expression libraries for lung cancer-associated genes

Lung cancer-associated genes collected for the current study were subcloned into the indicated Gateway entry vector (Invitrogen). The integrity of the genes was confirmed by BsrGI restriction digestion and by sequencing, generating the Entry-vector library. Genes in the entry vector library were transferred using the Gateway recombination system to destination expression vectors to produce a GST-gene fusion and a Venus-flag-gene fusion for each gene, generating the OncoPPi expression vector library.

High throughput PPI screening

We utilized the unique spectral overlap of terbium with Venus to develop a TR-FRET system that only requires the addition of one fluorophore during the assay process (164). GST- and Venus-fusion proteins allow the coupling of anti-GST antibody-conjugated donor fluorophore, terbium, to fused Venus for FRET detection in solution to identify direct PPIs (Figure 2-1). For every PPI, GST- and

Venus-only negative controls were included in parallel in every round of screening. To enable HTS for large-scale PPI detection, a cell lysate-based TR-FRET assay in a 384-well HTS format was developed. Briefly, H1299 lung cancer cells (2,500) were cultured in 384-well plates at 37°C before they were co-transfected in wells with Venus-tagged genes in combination with GST-tagged genes using the Fugene HD reagent (Promega, Cat# E2311), assisted by robotic operations with the Sciclone ALH 3,000 liquid handling workstation (PerkinElmer). After incubation for 48 h, whole cell lysates were prepared by replacing the medium with lysis buffer (40 mM Tris-HCl pH 8.0, 137 mM NaCl, 1 mM NaCl, 5 mM NaF, 5 mM NaPyrophosphate, 1% nonident P-40 (Sigma-Aldrich, IGEPAL CA-630) with protease inhibitors and phosphatase inhibitors) followed by a freeze-and-thaw cycle. Anti-GST-terbium antibody (Cisbio Bioassays, Cat# 61GSTTLB, 1:1,000 dilution) was dispensed into each well with Multidrop Combi Reagent Dispenser (ThermoScientific). The lysate-antibody mixtures were incubated at 4°C before the TR-FRET signal was recorded (EnVision reader setting: Ex 337nm, Em1: 520nm, Em2: 486nm; mirror: D400/D505 dual; time delay: 50ms).

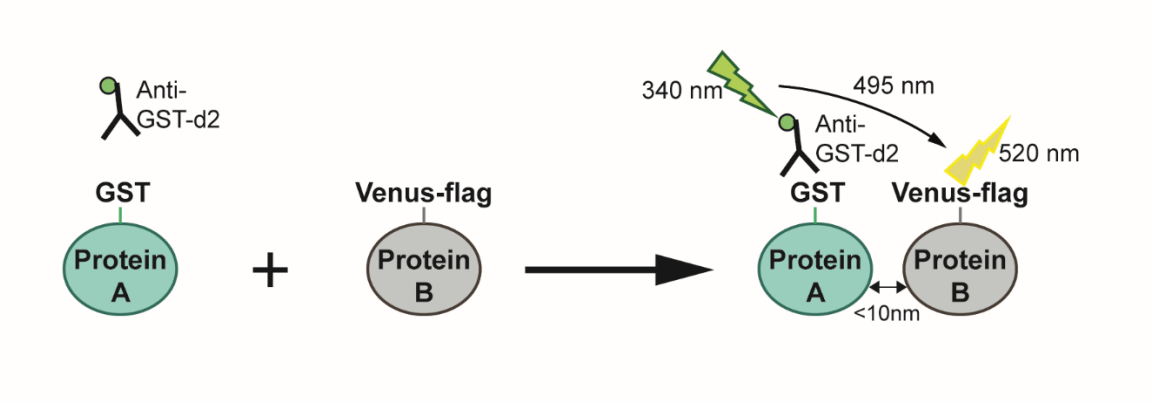
Anti-
GST-d2
GST
Protein
A
+
Venus-flag
Protein
B
340 nm
495 nm
Anti-
GST-d2
520 nm
GST
Venus-flag
Protein
A
Protein
B
<10nm

Figure 2-1. Time Resolved-Fluorescence Resonance Energy Transfer (TR-FRET) principle. Diagram illustrating the principle of TR-FRET used on the OncoPPi HTS. Excitation of GST-Tb antibody bound to GST-protein A (donor protein) generates an energy transfer to the Venus-flag protein B (acceptor protein), only if they are between 10 nm of distance. The energy transfer causes an emission of Venus-tagged protein that is captured by the EnVision Multilabel plate reader.

Cell culture

Human lung cancer cells H1299 (ATCC CRL-5803), H1944 (ATCC CRL-5907) were cultured in RPMI 1640 containing L-glutamine (VWR, Cat# 45000-396) supplemented with 10% fetal bovine serum and 100 units/ml of penicillin/streptomycin. Breast cancer cells MCF-7 (ATCC HTB-22), colon cancer HT-29 (ATCC HTB-38) and embryonic kidney cells HEK293T (ATCC CRL-3216) cells were maintained in Dulbecco's Modified Eagle's Medium (DMEM), with 4.5g/L glucose, L-glutamine and sodium pyruvate (VWR, Cat# 45000-304) supplemented with 10% fetal bovine serum and 1X penicillin/streptomycin solution (CellGro, Cat# 30-002-CI). Cells were incubated at 37°C in humidified conditions with 5% CO_2. All cell lines have been tested for mycoplasma contamination.

Affinity pull-down and co-immunoprecipitation assays

For GST-affinity pulldown assays, cells were lysed in 1% NP-40 buffer (150 mM NaCl, 10 mM HEPES (pH 7.5), 1% nonident P-40, 5 mM sodium pyrophosphate, 5 mM NaF, 2 mM sodium orthovanadate, 10 mg/L aprotinin, 10 mg/L leupeptin and 1 mM PMSF) and incubated with glutathione-conjugated beads (GE, Cat# 17-0756-05) for 2 h at 4°C. Beads were washed three times with 1% NP-40 buffer and eluted by boiling in sodium dodecyl sulfate-polyacrylamide gel electrophoresis (SDS-PAGE) loading buffer.

For immunoprecipitation, cell lysates were collected, quantified and were mixed with respective antibodies. For each co-immunoprecipitation, lysates containing 1.5 mg of total proteins were used, and the antibody/lysate mixtures were incubated overnight at 4°C. Then protein A/G PLUS-agarose beads (Santa Cruz, Cat# sc-2003) were added to the mixture followed by incubation at 4°C for another 4 h. Beads were washed four times with lysis buffer, and proteins were eluted with SDS-PAGE sample buffer and analyzed with indicated antibodies. The following primary antibodies were used for western blotting at the final dilution of 1:1,000 unless otherwise indicated: rabbit anti-GST (Santa Cruz, Cat#

sc-459, 1:2,500 dilution); mouse anti-Flag (Sigma-Aldrich, Cat# A8592, 1:2,500 dilution, or Sigma-Aldrich, Cat# F3165, 1:2,500 dilution); rabbit anti-MYC (Santa Cruz, Cat# sc-764); mouse anti-b-Actin (Sigma-Aldrich, Cat# A5441); goat anti-NSD3 (Proteintech, Cat# 11345-1-AP, 1:200 dilution). The rabbit anti-MYC (Santa Cruz, Cat# sc-764, 1:100 dilution) was used for immunoprecipitation assays.

Protein stability assays

Protein stability assays were performed according to established methods (165). In brief, HEK293T cells were transfected using Xtreme-Gene (Roche, Cat# 06366546001) following the manufacturer's instructions. After transfection, cells were incubated for 48 h in DMEM media supplemented with 10% FBS, then were treated with 100 mg/mL cycloheximide (Cell signaling, Cat# 2112) in DMEM media with 10% FBS at the indicated times. 100 ml of 2X SDS-PAGE sample buffer was added, and the cells were scraped from the wells, boiled for 10 min, then cell lysates were stored at 80°C. After all, lysates were collected, each sample was loaded onto a 10% SDS-PAGE gel and then analyzed by western blotting with rabbit anti-MYC antibody (Cell signaling, Cat# 5605, 1:1,000) to monitor MYC protein level. Protein expression was quantified from the western blot using GelQuant software. For analysis, MYC levels were normalized to tubulin protein levels (Sigma-Aldrich, Cat# T-5326, 1:2,000). Assays were performed three times.

MYC reporter assay

HEK293T cells were grown in six-well plates and transfected using Xtreme-Gene (Roche, Cat# 06366546001) with Venus-flag-NSD3S or Venus-flag-vector along with MYC-E-box-containing luciferase reporter plasmids, with either wild-type (GCCACGTGGCCACGTGGCCACGTGGC) or mutant (GCCTCGAGGCCTCGAGGCCTCGAGGC) E-boxes driving expression of firefly luciferase (166). Renilla luciferase was included as an internal control. After transfection, cells were

incubated for 48 h in DMEM media supplemented with 10% FBS. Cells were harvested mechanically, centrifuged at 1,600 r.p.m. for 10 min, and then re-suspended in 300 ml of DMEM media. The cells were transferred to 384-well plate, and the MYC reporter assay was performed using the Dual-Glo luciferase kit (Promega, Cat# E2920) following the manufacturer's instructions. Firefly luciferase expression was normalized to the internal control Renilla expression. Data were analyzed with GraphPad Prism software. Assays were performed three times.

2.3 Results

2.3.1 Defining the OncoPPi network

To generate a cancer-focused PPI network, a robust PPI detection platform was established using TR-FRET technology to systematically map the association of a library of test proteins in a pairwise fashion (164). A set of 83 genes was selected based on the frequency of alterations in lung cancer and known involvement in cancer signaling pathways (167-169). Our miniaturized, TR-FRET-based PPI platform enables high throughput mapping in a mammalian cell environment. Due to the stringent proximity requirement (<100Å) to obtain a positive FRET signal, the identified positive PPIs generally reflect direct interactions in protein complexes (164). With streamlined workflow for PPI detection, we systematically tested the selected lung cancer gene set in a pairwise manner in H1299 lung cancer cells to characterize their inter-molecular connectivity. H1299 lung cancer cells provide a relevant cellular environment and, with high transfection efficiency, consistent TR-FRET assay performance. A total of 3,486 interactions were examined. To ensure a quality screening dataset, each PPI pair was tested with two fusion tags for each gene, triplicate samples and three independent rounds of screening with fusion vector-only negative controls plus positive controls and expression sensors included in parallel for each PPI pair, resulting in a total dataset of 462,000 data points. We defined a set of statistically significant PPIs and a more stringent set of high confidence PPIs (HC-PPI) based on statistical analysis of FRET signals. The SS-PPI set includes 798 interactions. Through

comparison to publicly available PPI databases including the BioPlex human interactome, we identified 670 novel interactions and confirmed 128 previously reported PPIs as direct interactions in lung cancer cells. A set of 397 high confidence lung cancer-associated PPIs, forms the OncoPPi network (version 1) (Figure 2-2). The experimental HC-PPI dataset is enriched for known PPIs (total 128), with 269 novel interactions, OncoPPi greatly expands the landscape of interactions among this selected set of lung cancer genes and defines interactions with potential significance for cancer PPI target discovery, such as MYC/NSD3S (WHSC1L1). These datasets are freely available through the NCI's Cancer Target Discovery and Development (CTD2) Network Data Portal and Dashboard (http://ctd2-dashboard.nci.nih.gov/) (170).

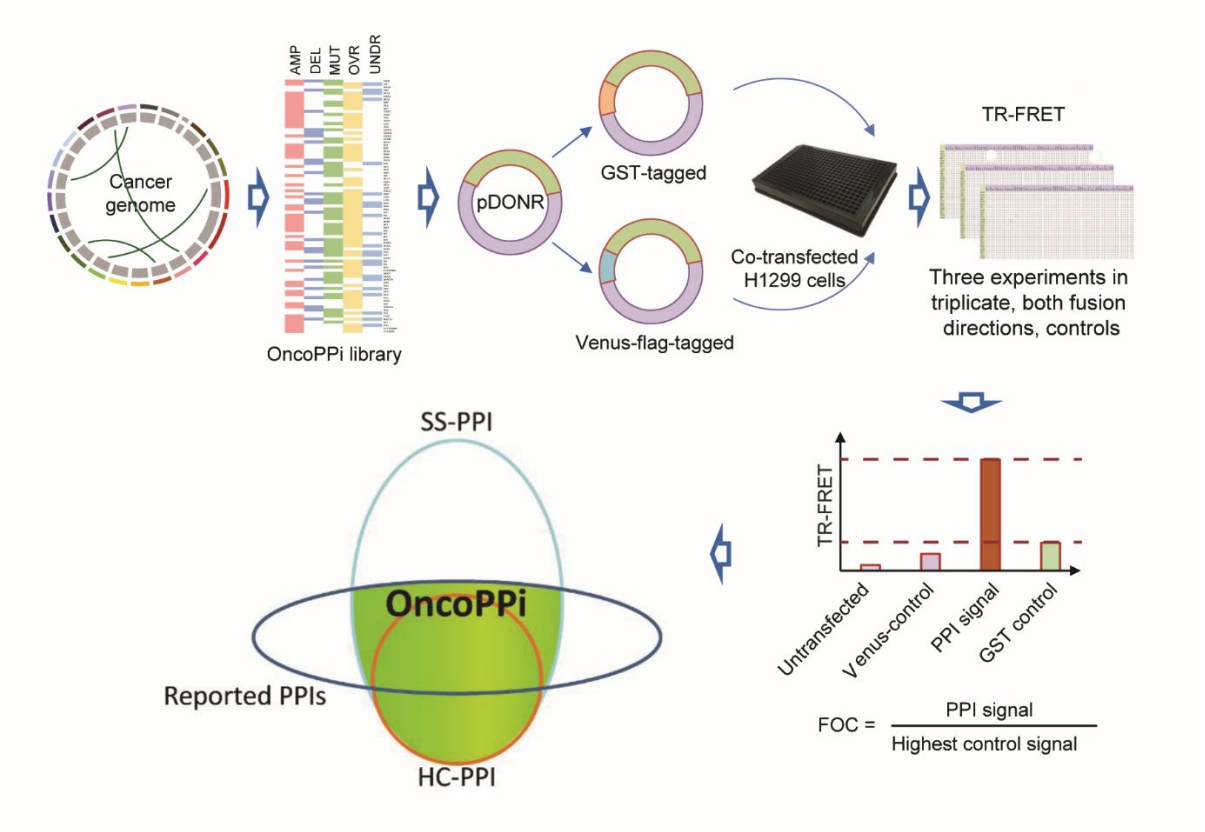
Cancer genome
AMP
DEL
MUT
OVR
UNDR
OncoPPi library
pDONR
GST-tagged
Venus-flag-tagged
Co-transfected H1299 cells
TR-FRET
Three experiments in triplicate, both fusion directions, controls
SS-PPI
OncoPPi
Reported PPIs
HC-PPI
TR-FRET
Untransfected
Venus-control
PPI signal
GST control
FOC = PPI signal / Highest control signal

Figure 2-2. Generation of OncoPPi network.

Genes altered in lung cancer were obtained from the cancer genome atlas (TCGA) to generate the OncoPPi expression vector library for pairwise TR-FRET-based high-throughput screening in H1299. Fold over control (FOC) was calculated for each interaction, by dividing the TR-FRET signal of the PPI by the highest negative control signal. Venn diagram representation of the OncoPPi network as a defined set of statistically significant PPIs (SS-PPI) or high confident PPI (HC-PPI). Reported PPIs, which served as positive controls, were also detected on our assay.

2.3.1 Defining MYC as a node for signaling pathway connection

Comparing degree and betweenness centrality (BC) index values for network nodes revealed MYC as a hub protein most critical for the OncoPPi network. On average, each protein in OncoPPi connects with nine protein partners, compared to an estimated median of five protein partners in the general proteome (153, 154), supporting the notion that proteins involved in the same disease, such as cancer, tend to interact with each other (162). The OncoPPi network also revealed prominent PPI hubs with novel connectivity exposing potentially critical biological insights for cancer genes such as MYC (Figure 2-3A). MYC contains multiple structural motifs that mediate interactions with a number of regulatory proteins (171). Our OncoPPi network confirmed reported MYC binders, such as GCN5 and SMAD2, and also revealed 23 new potential interaction partners for MYC, including NSD3S (Figure 2-3B). We used mutual exclusivity data to provide independent support for the involvement of the described PPIs in a common pathway. Mutual exclusivity analysis takes advantage of the observation that alterations in genes participating in the same biological process tend not to occur together in the same cancer patient (172). Mutual exclusivity analysis also supports the placement of MYC in signaling pathways with an epigenetic modulator NSD3 (WHSC1L1) (118) (Figure 2-3C), suggesting a new mechanism for MYC regulation. Interestingly, looking at genomic data, *NSD3* amplification correlates with upregulation of MYC target genes, *CCNE2*, *CCNA2*, and *CDK4*, in lung adenocarcinoma patients. To test an OncoPPi-generated hypothesis and gain mechanistic insights, the MYC/NSD3S interaction was further examined. NSD3 is a member of the nuclear receptor-binding SET domain (NSD) family of histone H3 lysine 36 (H3K36) methyltransferases. It is frequently amplified and functions as an oncoprotein in lung tumors and a range of other cancers (118). NSD3 has two isoforms, a long form with the methyltransferase domain and a short form (NSD3S) without the enzymatic activity. Interestingly, NSD3S serves as an adaptor to link BRD4 to the CHD8

chromatin remodeling protein (141). NSD3S binding to MYC as revealed in OncoPPi may regulate MYC's access to designated chromatin complexes in a methyltransferase-independent manner.

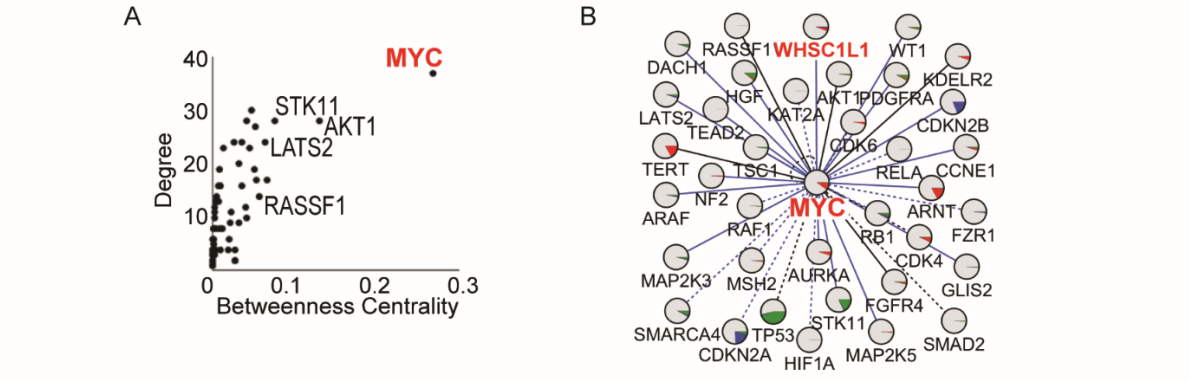
A
MYC
STK11
AKT1
LATS2
RASSF1
Degree
40
30
20
10
0
0.1
0.2
0.3
Betweenness Centrality
B
RASSF1
WHSC1L1
WT1
DACH1
KDELR2
HGF
AKT1
PDGFRA
LATS2
KAT2A
CDKN2B
TEAD2
CDK6
TERT
TSC1
RELA
CCNE1
NF2
MYC
ARNT
ARAF
RAF1
RB1
FZR1
CDK4
MAP2K3
MSH2
AURKA
GLIS2
FGFR4
STK11
SMARCA4
TP53
SMAD2
CDKN2A
HIF1A
MAP2K5

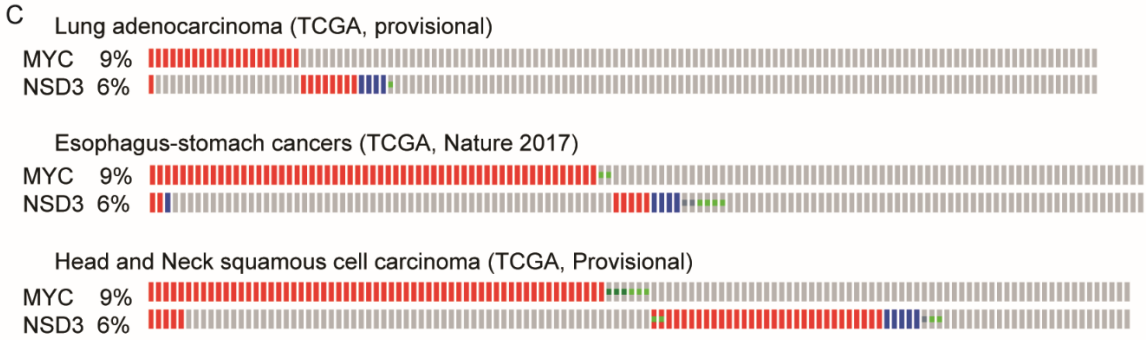
C
Lung adenocarcinoma (TCGA, provisional)
MYC 9%
NSD3 6%
Esophagus-stomach cancers (TCGA, Nature 2017)
MYC 9%
NSD3 6%
Head and Neck squamous cell carcinoma (TCGA, Provisional)
MYC 9%
NSD3 6%

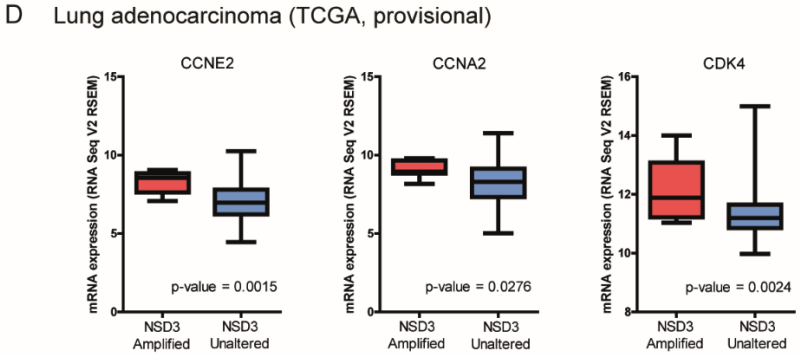
D
Lung adenocarcinoma (TCGA, provisional)
CCNE2
CCNA2
CDK4
mRNA expression (RNA Seq V2 RSEM)
p-value = 0.0015
p-value = 0.0276
p-value = 0.0024
NSD3 Amplified
NSD3 Unaltered

Figure 2-3. MYC as a hub in PPI and relevant for pathway connection.

A. MYC was found to have the highest betweenness centrality index and degree of interactors placing MYC as a relevant protein for pathway connection in lung cancer cell signaling. **B.** MYC interactors. The red, blue and green sectors inside the nodes represent the percent of LUAD cases (Lung adenocarcinoma, provisional dataset) with gene amplification, deletions or mutations, respectively. Already reported PPIs are indicated with dashed lines. Newly discovered PPIs are shown with solid lines. PPIs positive in mutual exclusivity analyses are highlighted with blue lines. **C.** Mutual exclusivity data for MYC and NSD3 in three different types of cancer, lung adenocarcinoma, esophagus-stomach cancers, and head and neck squamous cell carcinoma. For each cancer, the percentage of alteration for both genes are indicated and then on red, blue and green represents gene amplification, deletion or mutation, respectively, of the gene on a patient. **D.** Upregulation of MYC-target genes (*CCNE2*, *CCNA2*, and *CDK4*) are correlated with *NSD3* amplification in lung adenocarcinoma patients.

2.3.3 NSD3S is a novel MYC binding partner

To validate the interaction between MYC and NSD3S found in the OncoPPi network, we first used the solution-based TR-FRET assay. TR-FRET is the same assay that was used in the original OncoPPi screen, but instead of using a single point signal, we performed a dose-dependent TR-FRET. We transfected GST-MYC with Venus-flag-NSD3S in HEK293T cells. Indeed, dose-dependent TR-FRET gave a positive signal between MYC and NSD3S. As a background control, no TR-FRET signal was detected with the co-expression of either protein with the vector control (Figure 2-4A). To confirm the MYC/NSD3S interaction detected by TR-FRET, an affinity-based affinity assay was used, GST pull-down assay. GST-MYC was pull down with GST beads in HEK293T cells, and Venus-flag-NSD3S was found in the MYC complex. Binding of NSD3S to GST vector or Venus-flag-vector to MYC were both negative, demonstrating a specific association between MYC and NSD3S (Figure 2-4B). Finally, to evaluate if the two proteins interacted under physiological conditions in cancer cells, we performed endogenous co-immunoprecipitation. We utilized MYC antibody to isolate endogenous MYC protein, and we detected endogenous NSD3S on the MYC complex in H1299, H1944, MCF-7 and HT-29 cancer cell lines (Figure 2-4C). Orthogonal assays validated MYC/NSD3S interaction and detected under physiological conditions in lung, breast, and colon cancer cell lines.

NSD3S binds to BRD4 through the N-terminal region (amino acid 152-163) (141), we generated two truncations of NSD3S, residue 1 to 347 and 347 to 645, and tested the binding to GST-MYC by GST pull-down. A positive signal was found for full-length NSD3S and NSD3S 347-645, indicating that MYC interaction appears to be mediated by a region C-terminal to the PWWP motif of NSD3S, different to the part where BRD4 binds (Figure 2-5).

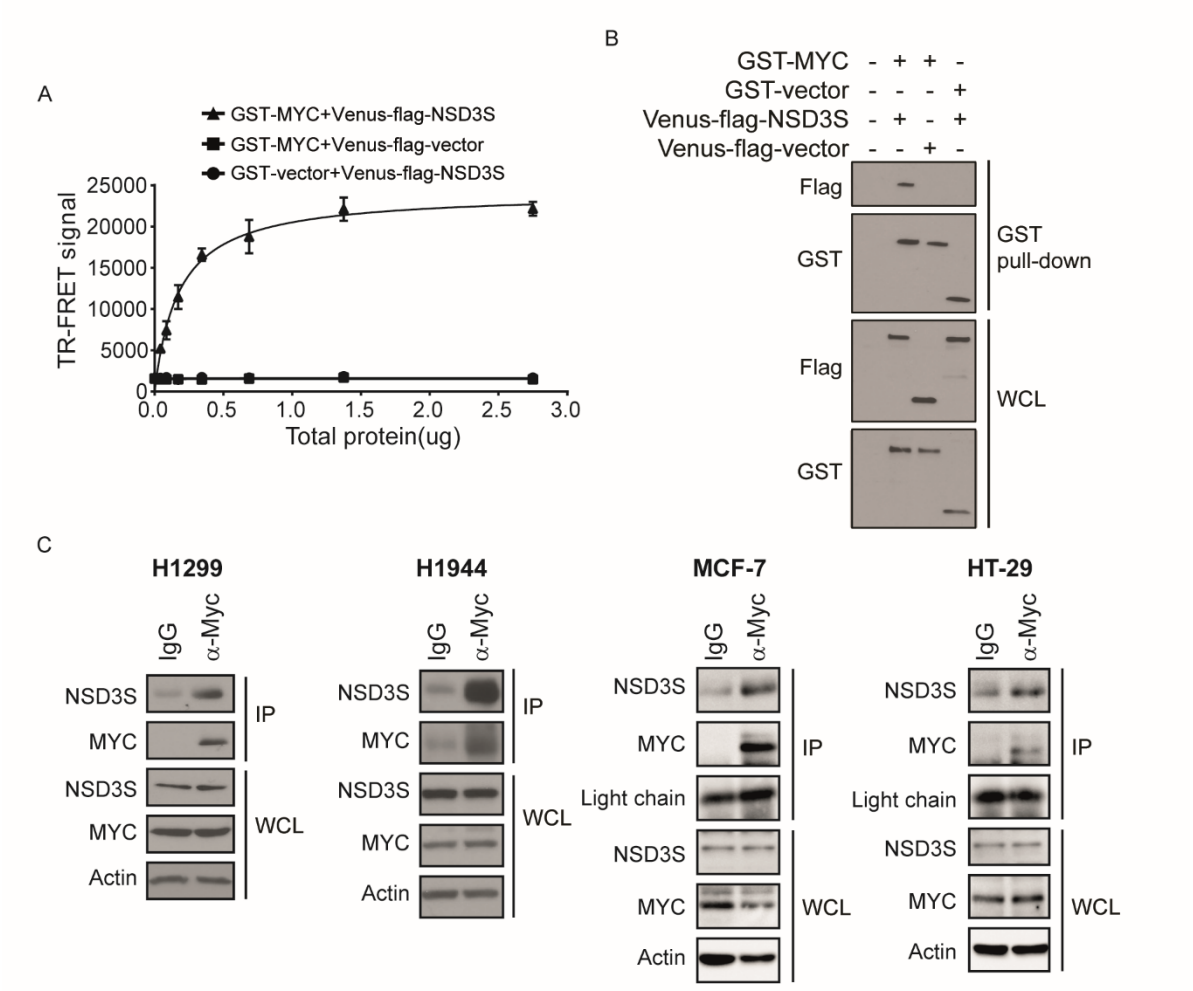
A
GST-MYC+Venus-flag-NSD3S
GST-MYC+Venus-flag-vector
GST-vector+Venus-flag-NSD3S
TR-FRET signal
25000
20000
15000
10000
5000
0
0.0
0.5
1.0
1.5
2.0
2.5
3.0
Total protein(ug)
B
GST-MYC - + + -
GST-vector - - - +
Venus-flag-NSD3S - + - +
Venus-flag-vector - - + -
Flag
GST
GST pull-down
Flag
GST
WCL
C
H1299
H1944
MCF-7
HT-29
IgG
α-Myc
NSD3S
MYC
Actin
Light chain
IP
WCL

Figure 2-4. Validation of MYC/NSD3S PPI.

A. TR-FRET assay performed using HEK293T cells lysates with overexpression of GST-MYC and Venus-flag-NSD3S or vectors controls. Tb-conjugated anti-GST-antibodies were incubated with cell lysates to detect GST-MYC. The TR-FRET signal is expressed as the FRET ratio (520nm/486nm * 10^4) Representative results of three independent experiments are shown. The error bars show the mean±s.d. of three replicates. **B.** GST-pull down assay performed to isolate GST-MYC complexes in lysate from HEK293T cells with Venus-flag-NSD3S co-expressed. The presence of NSD3S on the complex was evaluated with anti-flag antibody by western blot. GST antibody was used to control the amount of protein pull down. Expression in the whole cell lysate (WCL) was used as a control. **C.** Co-immunoprecipitation assay conducted in H1299, H1944, MCF-7 and HT-29 cancer cell lines using MYC antibody to isolate MYC complex, or anti-IgG as a negative control. Detection of endogenous NSD3S in the MYC complex was examined by western blot with an antibody against NSD3. Levels in the WCL were used as a control.

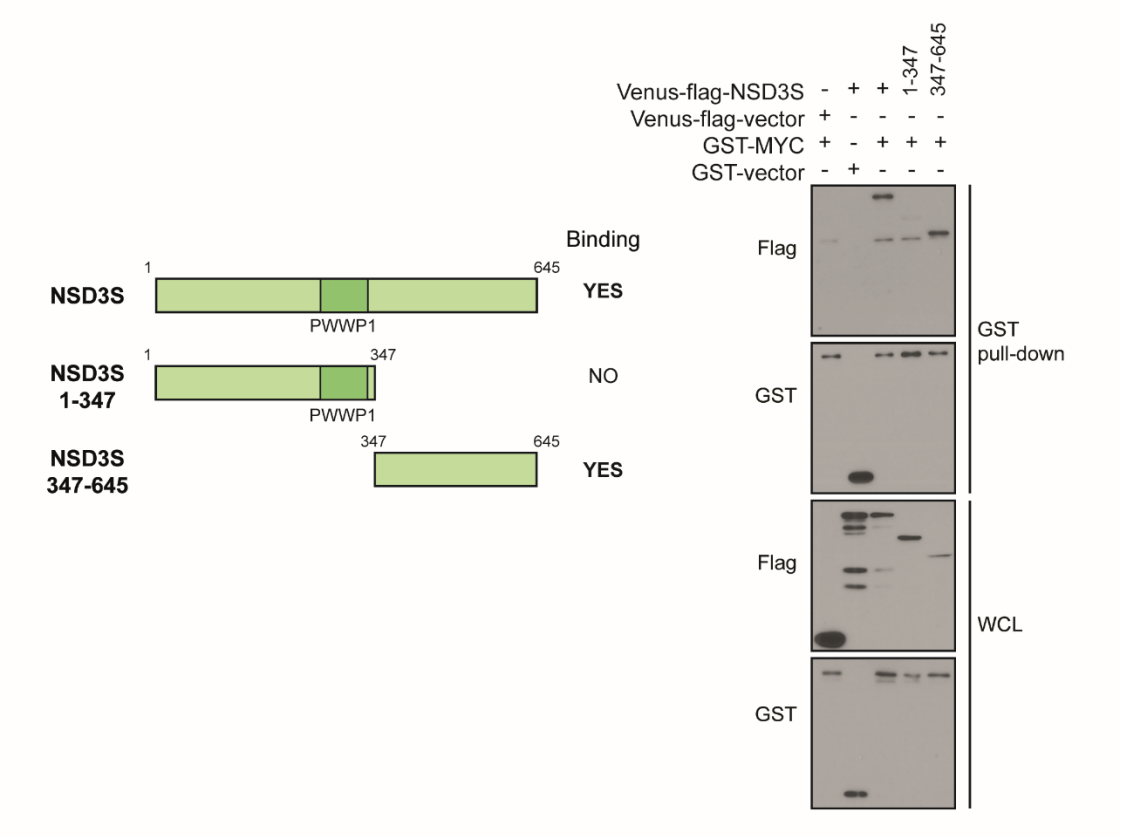
Binding
NSD3S
1
645
PWWP1
YES
NSD3S
1-347
1
347
PWWP1
NO
NSD3S
347-645
347
645
YES
Venus-flag-NSD3S
Venus-flag-vector
GST-MYC
GST-vector
1-347
347-645
Flag
GST
GST
pull-down
Flag
GST
WCL

Figure 2-5. Identification of binding region on NSD3S.

(Left) Diagram of NSD3S protein structure and the two truncations generated for deletion analyses, amino acids 1 to 347 and 347 to 645. Summary of binding to MYC on the side of each structure. (Right) GST-pull down assay in HEK293T cells overexpressing GST-MYC with Venus-flag-NSD3S full length or truncations. Binding of NSD3S plasmids to MYC was evaluated with anti-flag antibody. Levels of proteins in the WCL was used as a control.

2.3.4 NSD3S regulates MYC half-life and transcriptional activity

We sought to explore the effect of NSD3S in MYC function. As mentioned previously in Chapter 1, the MYC half-life is short, and there are numerous proteins which regulate MYC stability/degradation pathways, as levels of MYC are crucial for driving tumorigenesis. First, we examine the effect on MYC protein stability by performing a protein turnover assay, the cycloheximide assay. Cycloheximide (CHX) is a protein synthesis inhibitor; we added CHX to cells and collected cell lysate at different time points and observed endogenous MYC protein levels. With over-expression of Venus-flag-vector MYC half-life was approximately 45 min as expected. Addition of Venus-flag-NSD3S increases MYC half-life, demonstrating a stabilization effect in MYC protein. Interestingly, the MYC-binding defective fragment of NSD3S (residues 1 to 347) did not increase MYC half-life, suggesting that the binding between NSD3S to MYC is required for the stabilization effect (Figure 2-6A and 2-6B).

MYC is a transcription factor regulating the expression of a large number of genes involved in different oncogenic processes. To evaluate the effect of NSD3S in the transcriptional activity of MYC we used a MYC reporter assay, where luciferase expression is under the control of E-box promoter. We co-transfected Venus-flag-vector or -NSD3S along with E-box wild type (WT) or mutant (MUT), where MYC does and does not bind, respectively. Indeed, when NSD3S is overexpressed, there is an increase of luciferase expression compared to the negative controls, only with the E-box WT (Figure 2-6C), suggesting a specific increase of MYC transcriptional activity by NSD3S.

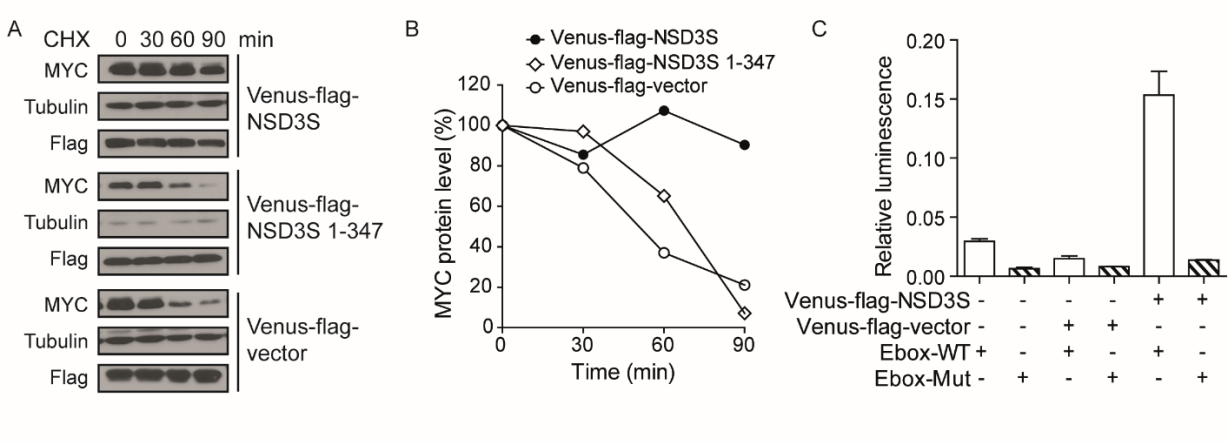
A
CHX 0 30 60 90 min
MYC
Tubulin
Flag
Venus-flag-NSD3S
MYC
Tubulin
Flag
Venus-flag-NSD3S 1-347
MYC
Tubulin
Flag
Venus-flag-vector
B
Venus-flag-NSD3S
Venus-flag-NSD3S 1-347
Venus-flag-vector
MYC protein level (%)
120
100
80
60
40
20
0
0
30
60
90
Time (min)
C
Relative luminescence
0.20
0.15
0.10
0.05
0.00
Venus-flag-NSD3S - - - - + +
Venus-flag-vector - - + + - -
Ebox-WT + - + - + -
Ebox-Mut - + - + - +

Figure 2-6. Effect of NSD3S on MYC protein stability and transcriptional activity.

A. Immunoblot showing endogenous MYC and tubulin levels in HEK293T cells at different time points after inhibition of protein synthesis with cycloheximide (CHX) with the expression of NSD3S, NSD3S 1-347 or vector control. **B.** Graph of MYC protein levels at indicated time points after CHX addition based on densitometric analysis of results in **(A)** 100% corresponds to the total MYC detected at the 0-time point. MYC levels are normalized to tubulin protein levels. **C.** HEK293T cells were co-transfected with Venus-flag-NSD3S or vector control and either wild-type (WT) or mutant (Mut) E-box luciferase reporter. Relative luciferase activity was measured, normalized to internal Renilla luciferase control. Representative results of three independent experiments are shown. The error bars show the mean±s.d. of three replicates.

2.3.5 Connection between MYC and BRD4 through NSD3S

The data shown on the previous sections led to the hypothesis that NSD3S functions as a new activator of MYC oncogenic activity by bridging MYC with BRD4 to allow the regulation of MYC function in response to epigenetic modulators. Indeed, by affinity-based GST pull-down assay, NSD3S can precipitate both MYC and BRD4 (Figure 2-7A). Concerning the binding, BRD4 and MYC bind to different regions on NSD3S (141).

NSD3S acts as an adaptor protein by bridging together BRD4 to CHD8 and promoting leukemia progression (141). BRD4 is an oncogene; it regulates MYC expression in cancer. However, the connection between BRD4 and MYC is not entirely understood. To evaluate the possibility if BRD4 is required for MYC/NSD3S interaction, we used a BRD4 degrader called ZBC260 (173). This compound uses the technology PROTAC (Protein-targeting chimeric molecules) that allows transiently to degrade the target protein by bringing them close to E3 ligase complex and promoting proteasomal degradation (174) (Figure 2-7B). Treatment of HEK293T cells with compound ZBC260 shows a concentration-dependent decrease in BRD4 protein expression over time (Figure 2-7C). The reduction is noticeable at 10 nM after 3 h of incubation, conditions used for further experiments. By GST pull-down assay in HEK293T cells the interaction between MYC and NSD3S was similar under the condition with DMSO, as control, and with ZBC260 treatment (Figure 2-7D). The binding pattern suggests that MYC/NSD3S interaction is independent of the presence of BRD4 in cells.

Our results led to a working model that BRD4 regulates MYC through a transcription-independent mechanism by means of the BRD4-NSD3S-MYC pathway, in addition to the well-established BRD4-pTEFb-mediated pathway (Figure 2-7E), which may have significant clinical implications for the response of MYC-driven tumors to BRD4 inhibitors that are currently in clinical trials.

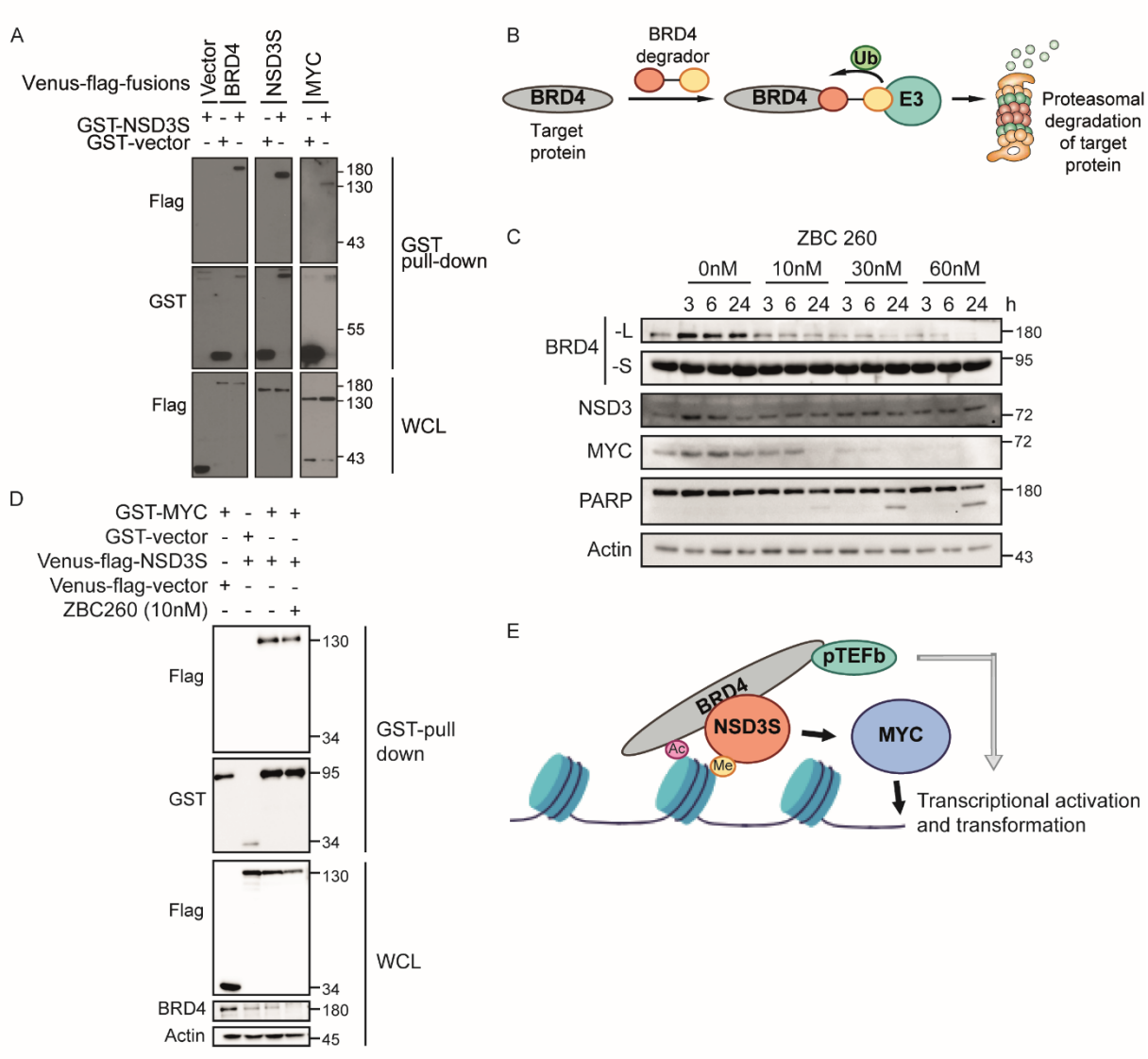
A
Venus-flag-fusions
Vector
BRD4
NSD3S
MYC
GST-NSD3S
GST-vector
Flag
GST
Flag
180
130
43
55
180
130
43
GST pull-down
WCL
B
BRD4 degrador
BRD4
Target protein
Ub
E3
Proteasomal degradation of target protein
C
ZBC 260
0nM
10nM
30nM
60nM
3 6 24 3 6 24 3 6 24 3 6 24 h
BRD4
-L
-S
NSD3
MYC
PARP
Actin
180
95
72
72
180
43
D
GST-MYC
GST-vector
Venus-flag-NSD3S
Venus-flag-vector
ZBC260 (10nM)
Flag
GST
Flag
BRD4
Actin
130
34
95
34
130
34
180
45
GST-pull down
WCL
E
pTEFb
BRD4
NSD3S
Ac
Me
MYC
Transcriptional activation and transformation

Figure 2-7. NSD3S binds both MYC and BRD4.

A. GST-NSD3S was co-transfected with Venus-flag-tagged constructs for MYC, NSD3S and BRD4 into HEK293T cells, followed by GST-pull down assay to isolate NSD3S complex. Western blot against flag proteins was used to detect the binding pattern. Levels of proteins in the WCL was used as a control. **B.** Diagram of the mechanism of action of BRD4 degrader using PROTAC technology. Target protein, BRD4 in this case, is brought to proximity to E3 ligase complex by the degrader, for subsequent ubiquitination and proteasomal degradation of BRD4. **C.** Treatment of HEK293T cells with BRD4 degrader ZBC260 (from Dr. Shaomeng Wang of the University of Michigan), at different time points and different concentrations. Levels of endogenous proteins in HEK293T cell lysate were evaluated by western blot with specific antibodies. **D.** GST-pull down assay with overexpressed GST-MYC and Venus-flag-NSD3S with or without ZBC260 treatment (10 nM for 3 h). Levels of proteins in the pull-down or WCL samples were examined with anti-flag or GST antibodies. **E.** Proposed working model. BRD4 utilizes its ET domain to regulate MYC through a transcription-independent mechanism via the BRD4-NSD3S-MYC pathway, in addition to the well-established BRD4-pTEFb-mediated pathway via the C-terminal fragment of BRD4. Both BRD4 and NSD3S interact with modified histones.

2.4 Discussion

This study reports the generation of an expanded lung cancer associated PPI network, termed OncoPPi (v.1), through the implementation of a TR-FRET-based high-throughput screening approach. The focused binary PPI screening coupled with a robust miniaturized screening platform allows a rigorous experimental design is generating 18 data points for each PPI to ensure high-confidence PPI data for future hypothesis-driven investigations. OncoPPi unveils important PPIs in cancer not detected in previous interactome studies. Previous large-scale interactome studies have indicated that much of the PPI landscape is still undescribed. Indeed, with our focused set of 83 lung cancer genes, we identify 4260 novel interactions, expanding the PPI landscape for this gene set by 4200%, including for well-studied cancer genes like MYC. Available to the community, OncoPPi is a valuable resource for discovery of cancer-associated PPIs as potential drug targets, examining network-informed signaling crosstalk, and predicting network-implicated tumor vulnerability, informative biomarkers and new strategies to target challenging cancer drivers. Usefulness of high-throughput-derived PPI data depends on its reproducibility, as well as the ability to detect true positive interactions. Overall, we found that 480% of tested OncoPPi interactions could be confirmed by GST pull-down. Of note, unlike the TR-FRET assay, GST pull-downs require stringent wash steps; thus, the 20% of PPIs not confirmed could represent both false positives and lower affinity interactions disrupted by wash steps. Despite transformative advances in cancer care towards precision oncology, clinical successes from genomics-based targeted cancer therapies remain largely focused on oncogenic enzymes, particularly protein kinases. Such enzymes offer druggable sites for therapeutic modulation of their catalytic activities. However, the majority of cancer driver genes identified through cancer genomics efforts encode 'undruggable' proteins such as (i) tumor suppressors with loss of function in cancer and (ii) adaptor proteins with no enzymatic activity, posing a major hurdle for therapeutic intervention (1). These challenging cancer drivers function by participating in protein complexes that

are involved in diverse cellular functions. Our approach addresses these challenges by placing cancer driver genes, both oncogenes and tumor suppressors, in the context of growth signaling PPI networks, offering unique opportunities to define promising therapeutic strategies for protein targets with or without enzymatic activity. It should be noted that our TR-FRET-based high throughput PPI screening method utilizes co-expression of exogenous protein pairs. The presence of these interactions under physiological and pathological conditions should be validated to examine their functional importance. As examples, we illustrate OncoPPi-generated new hypotheses for future pathway perturbagen discovery through interrogating MYC PPIs. Demonstration of selected PPI, MYC/NSD3S, under endogenous conditions in multiple cancer cell lines strongly supports the validity of the OncoPPi network data set for further examination. The MYC oncogene, which represents a highly validated and studied oncogenic cancer target, has no approved therapies that directly target the protein. This is due, in part, to the lack of enzymatic activity and defined catalytic site for structure-activity guided design of potent compounds. Thus, it is recognized that the MYC interactome may represent a viable option to inhibit this pathway for therapeutic benefit (171). Newly uncovered MYC binding partners in the OncoPPi network serve as examples to illustrate OncoPPi-inferred new signaling pathways for regulation of MYC-driven cell growth and oncogenic programs. We selected the physical interaction of MYC with NSD3S for validation and uncovered a potential positive regulatory function for NSD3S in activating MYC, implicating the BRD4/NSD3S/MYC pathway as a potential target for interrogating MYC-driven tumors. Because BRD4 inhibitors, such as JQ1, have been shown to be active against MYC-driven tumors, the intimate connection of NSD3S with BRD4 and with MYC supports the hypothesis that NSD3S may play a critical role in directing MYC-driven oncogenic programs and may recruit MYC to a chromatin location through NSD3S recognition of H3K36me3 and its association with acetylated lysine-BRD4, which warrants further investigation. The potential clinical importance of this connectivity is supported by the NSD3S/MYC interaction in the

NSD3-NUT fusion-driven NUT midline carcinoma (135). It is very likely that the NSD3–NUT fusion may be critical for the maintenance of MYC expression in these cancer cells. It is expected that other cancer drivers beyond MYC can also be exploited similarly to guide functional validation and therapeutic discoveries. To build on such success, our studies provide both potential PPI targets for manipulating oncogenic pathways, as well as highly sensitive high throughput screening (HTS) assays for PPI pathway perturbagen discovery. The TR-FRET assay format has been widely used in the HTS field for small molecule PPI modulator discovery (164). These HTS assays are readily applicable for future HTS campaigns to discover PPI modulators.

Chapter 3: NSD3S stabilizes MYC through hindering its interaction with FBXW7

This chapter was submitted to

Journal of Molecular Cell Biology (JMCB) (under review).

Valentina Gonzalez-Pecchi, Albert K. Kwan, Andrey A. Ivanov, Yuhong Du, and Haian Fu

3.1 Introduction

c-MYC (MYC) encodes a transcription factor and was one of the first oncogenes to be discovered in human cancers (9, 31). MYC functions by altering cellular characteristics associated with oncogenic transformation, such as proliferation (90, 175), apoptosis (93), metabolism (176, 177), and angiogenesis (103). Dysregulation of MYC activity, which occurs most commonly via MYC gene amplification, is found in a variety of human cancer types: on average, 50% of human cancers have increased expression of MYC. High MYC expression levels are furthermore correlated with increased tumor aggressiveness (25, 33).

The MYC protein is composed of four conserved regions known as MYC boxes (MBI, MBII, MBIII, MBIV). The C-terminal portion of MYC contains a basic-helix-loop-helix-leucine zipper domain (bHLH-LZ) that is responsible for heterodimerization with MYC-associated factor x (MAX) (67). The MYC/MAX complex binds to specific sequences in the DNA known as Enhancer box (E-box) sequences and recruits transcriptional co-activators to drive expression of MYC target genes (20, 178, 179).

MYC protein levels are tightly controlled by several mechanisms, including post-translational modifications (PTMs) and protein-protein interactions (PPIs). An example of such a PTM is phosphorylation of serine 62 (S62) by extracellular-regulated kinase 1,2 (ERK1, 2), which leads to the stabilization of MYC (47). This phosphorylation event creates a consensus region for subsequent phosphorylation of threonine 58 (T58) by glycogen synthase kinase 3 β (GSK3β) (58), which marks MYC for degradation (52). Ultimately, phosphorylation of T58 and dephosphorylation of S62 (180) provide a binding site for FBXW7, a substrate recognition subunit of SCF E3 ubiquitin ligase complexes that target MYC for ubiquitin-mediated proteasomal degradation (48, 49). Through its intricate interactions with FBXW7 and other regulatory proteins, MYC serves as a central node that

integrates upstream signaling events to control diverse intracellular transcriptional programs during normal physiological development. Dysregulation of MYC protein levels through MYC overexpression or reduced degradation may lead to multiple diseases, including cancer. Thus, understanding how the MYC protein stability is properly controlled through these molecular interactions has broad implications for the regulation of cell growth under physiological and pathological conditions. Our previous work on the establishment of the OncoPPi network revealed a new member of the MYC regulatory proteins, NSD3 (8, 181).

NSD3 is a lysine methyltransferase that belongs to the family of NSD proteins, including NSD1, NSD2, and NSD3 (117). NSD3 is thought to act as an oncogene, as it is frequently amplified in breast, lung and pancreatic cancers (128, 130). NSD3 has three isoforms: NSD3 long (NSD3L) that encodes the full-length protein with histone methyltransferase catalytic activity, NSD3 short (NSD3S) that lacks the catalytic SET domain-containing C-terminal fragment of the protein, and a testis-specific isoform named Whistle (117, 118). Interestingly, unique functions for the NSD3S isoforms have been reported, including a role in oncogenesis that is independent of methyltransferase activity. In leukemia cells, NSD3S has been shown to be essential for cancer progression by bridging the interaction between the bromodomain-containing protein 4 (BRD4) and chromodomain helicase DNA binding protein 8 (CHD8) (141). In NUT-midline carcinoma, NSD3 has been found to generate an oncogenic fusion with nuclear protein in testis (NUT) (NSD3-NUT), and the portion of NSD3 present in the fusion is almost the complete NSD3S sequence. The oncogenic fusion decreases cellular differentiation and increases proliferation of NUT-midline carcinoma cell lines (135, 136). We previously found that the same non-catalytic isoform of NSD3, NSD3S, was able to interact with MYC and promote its protein stability (8). However, the precise mechanism by which NSD3S regulates MYC stability remains unclear. To address this issue, we have defined the protein-protein interaction interfaces between NSD3S and MYC and revealed major binding sites on MYC and

NSD3S, respectively. Mechanistic studies showed that NSD3S competes with FBXW7 for binding to MYC, providing a potential model for the regulation of MYC stability through FBXW7 (182). This functional connection between MYC and NSD3S provides a novel link between two oncogenic proteins that are known to drive cancer cell survival and may serve as a promising target for therapeutic intervention in MYC-driven tumors.

3.2 Material and Methods

Plasmids and reagents

Plasmids for mammalian expression of Glutathione S-transferase- (GST), Venus-flag- and Human influenza hemagglutinin- (HA) tagged proteins were generated using the Gateway cloning system (Invitrogen, Waltham, MA, USA) according to the manufacturer´s protocol. Human MYC and NSD3S cDNA were used as previously described (8). FBXW7 and ERK cDNA were obtained from DNASU, and GSK3β was provided by Dr. Kenneth Scott. MYC and NSD3S truncations were generated by introducing a stop codon using a PCR-based mutagenesis protocol. All plasmids were confirmed by FastDigest Bsp1407I (ThermoScientific, Cat# FD0934) enzyme digestion and by sequencing analysis. The protein synthesis inhibitor, cycloheximide (CHX) (Cell Signaling, Cat# 2112), was used for the MYC stability assays at a final concentration of 100 μg/mL. The proteasome inhibitor, MG-132 (Cell Signaling, Cat# 2194), was used at a final concentration of 20 μM for 3 h before cell collection.

Cell culture

HEK293T embryonic kidney cells (ATCC CRL-3216) and NCI-H1299 lung cancer cells (ATCC CRL-5803) were obtained from American Type Cell Culture Collection (ATCC, Rockville, MD, USA) and maintained in Dulbecco´s modified Eagle´s medium (DMEM) (VWR, Cat# 45000-304) or RPMI

1640 containing L-glutamine (VWR, Cat# 45000-396), respectively. Culture media was supplemented with 10% fetal bovine serum and 1% penicillin/streptomycin solution (CellGro, Cat# 30-002-CI). Cells were cultured at 37°C with 5% CO_2 in a humidified incubator. Between passages, cells were detached with 0.25% trypsin with ethylenediaminetetraacetic acid (EDTA) (VWR, Cat# 45000-664).

Gene expression

HEK293T and H1299 cells were transfected with expression plasmids at a confluence of 60-70% using X-tremeGENE (Roche, Cat# 06366546001) or FuGENE HD (Promega, Cat# E2311) transfection reagent, respectively. A ratio of 3 µl transfection reagent to 1 µg of plasmid DNA was utilized in a volume of 100 µl of Opti-MEM reduced serum medium (Thermo Fisher, Cat# 31985070) for plasmid delivery, according to manufacturer's instructions. Expression of transfected genes was monitored by Western blotting with corresponding antibodies.

GST-pull down and immunoprecipitation

HEK293T or H1299 cells were seeded in 6-well plates and transfected. After 48 h, cells were collected and lysed with 200 µl of lysis buffer (150 mM NaCl, 10 mM HEPES pH 7.5, 0.25% Triton X-100, Phosphatase Inhibitor (Sigma, Cat# P5726) and Protease Inhibitor Cocktail (Sigma, Cat# P8340)) by sonication. The lysate was centrifuged to eliminate cellular debris. 20 µl was saved for an input control, and the rest was incubated either with, 20 µl of 50% glutathione-conjugated sepharose beads (GE, Cat# 17-0756-05) for GST-pull down experiments, 5 µl of EZview Red Anti-Flag M2 Affinity Gel (Sigma, Cat# F2426) for flag-immunoprecipitation, or 10 µl of EZview Red Anti-HA Affinity Gel (Sigma, Cat # E6779) for HA-immunoprecipitation, for 3 h rotating at 4°C. Beads were washed three times in 0.25% Triton X-100 lysis buffer and eluted by boiling for 5 minutes in sodium dodecyl sulfate (SDS) loading buffer. Samples were then analyzed by SDS-Polyacrylamide gel electrophoresis (SDS-PAGE) and Western blotting.

MYC reporter assay

HEK293T cells were seeded in 12-well plates. The next day, cells were transfected with Venus-flag-plasmids along with firefly luciferase reporter plasmid under the control of wild-type (GCCACGTGGCCACGTGGCCACGTGGC) or mutant (GCCTCGAGGCCTCGAGGCCTC GAGGC) E-box and renilla luciferase which served as an internal control. Cells were collected, centrifuged at 1200 rpm, and re-suspended in 50 µl of phosphate-buffered saline (PBS) (VWR, Cat# 45000-446). 10 µl of cells were transferred to a 384-well plate, and the MYC reporter assay was performed using the Dual-Glo luciferase kit (Promega, Cat# E2920) following the manufacturer's instructions. Firefly luciferase expression was normalized to the control of renilla expression. Data was analyzed on GraphPad Prism software.

Protein stability assay

HEK293T cells were seeded on 24-well plates and transfected. After 48 h, cells were treated with 100 µg/ml of CHX. At the indicated times, cells were collected with 80 µl of 2X SDS loading buffer, boiled for 10 minutes, and resolved by SDS- PAGE. Protein expression was detected by Western blotting and quantified using GelQuant software. Hsp60 protein levels were used as an internal control for MYC protein normalization.

Endogenous co-immunoprecipitation

HEK293T or H1299 cells were plated on 15 cm dishes and transfected. After 48 h, cells were collected and lysed with 0.25% Triton X-100 lysis buffer by sonication. The lysate was centrifuged, and 40 µl of the supernatant was saved for input control, the rest was incubated with MYC antibody (Santa Cruz, Cat# sc-40) overnight at 4°C. Then, protein A/G PLUS-agarose beads (Santa Cruz, Cat# sc-2003) were added to the mixture and were incubated at 4°C for another 4 h. Beads were washed three

times with 0.25% Triton X-100 lysis buffer, and proteins were eluted with SDS-PAGE loading buffer and analyzed by Western blot.

Antibodies

The following antibodies and conjugates were used for the western blotting: Flag-HRP (Sigma, Cat# A8592, dilution 1:2,000), GST-HRP (Sigma, Cat# A7340, dilution 1:3,000), HA-HRP (Sigma, Cat# H6533, dilution 1:3,000), goat anti-mouse IgG-HRP (Jackson ImmunoResearch, Cat# 115-035-003, dilution 1:3,000), and goat anti-rabbit IgG-HRP (Jackson ImmunoResearch, Cat# 111-035-003, dilution 1:3,000), and antibodies for MYC (Cell Signaling, Cat# 5605S, dilution 1:1,000), MYC (Santa Cruz, Cat# sc-40, dilution 1:1,000), FBXW7 (Abcam, Cat# ab109617, dilution 1:1,000), ERK (Cell Signaling, Cat# 4695, dilution 1:1,000), GSK3β (Cell Signaling, Cat# 9315, dilution 1:1,000), actin (Sigma, Cat# A5441, dilution 1:3,000), GFP (Abcam, Cat# ab290, 1:6,000), and Hsp60 (Cell Signaling, Cat# 4870, dilution 1:1,000).

Computational modeling

The model of NSD3S 356 to 426 region was built using the Schrodinger Prime software. The BLAST search was utilized to identify the template proteins with highest sequence similarity. The secondary structure (SS) analysis of NSD3S 356 to 426 was performed with the Prime program and matched with the secondary structures of the template proteins. The BLAST search of the crystallized proteins available in the Protein Data Bank has revealed that NSD3S 356 to 396 fragment demonstrate the highest sequence and structure similarity (Prime alignment score: 89, sequence similarity: 63%) with the crystallized region of PWWP1 domain of WHSC1 protein (PDB ID: 5VC8). Therefore, this structure was utilized as a template to construct NSD3 356 to 396 fragment. Since further residues of WHSC1 were not solved in the crystal structure, we sought for another template protein to build a model of NSD3 397 to 426. Through the BLAST and the SS analysis, the structure of Parkin E3 ligase

(PDB ID: 4I1H) was identified as the most suitable temple (Prime alignment score: 55.0, sequence similarity: 60%). Since the crystal structures of WHSC1 and the Parkin E3 ligases lack similar regions for structural alignment, the NSD3 356 to 396 and NSD3 356 to 426 were first built separately, and then connected using the Schrodinger Crosslink Proteins tool. The resulting structure of NSD3 356 to 426 was optimized by energy minimization in the OPLS2005 force field using the Polak-Ribier Conjugate Gradient algorithm. First, only the protein side chains were subjected to the energy minimization by 2,500 interactions and the convergence threshold of 0.05. Then, the constraints were released, and the whole structure of NSD3 356 to 426 was optimized by 10,000 interactions and the convergence threshold of 0.05.

The resulting model was further optimized by 100 ns molecular dynamics (MD) simulation performed with the Desmond program implemented in the Schrodinger Suite. The NSD3S model was placed in a box that contained 9,852 SPC water molecules and eight chloride anions. The resulting system contained a total of 30,791 atoms. The MD simulation was run for 100 ns under the Normal Temperature and Pressure (NTP) conditions, with the following parameters: Thermostate method: Nose-Hoover chain, relaxation time 1.0 ps; Barostate method: Martyna-Tobias-Klein, relaxation time: 2.0 ps; time step: 2 fs; Short range cutoff radius: 9.0Å, Energy recording time: 1.2 ps, Trajectory recording time: 10 ps. The energy of the resulting structure of NSD3S 356 to 426 obtained after the MD simulation was minimized as described above.

Data analysis

All data were performed and repeated three times. The data quantification of the MYC reporter and protein stability assays was performed using the GraphPad Prism software.

3.3 Results

3.3.1 NSD3S binds MYC at a distinct site

To understand the molecular basis of the MYC/NSD3S interaction, we examined MYC structural elements that are required for NSD3 binding through deletion analyses. MYC contains four conserved domains with defined functions for MYC regulation. Four large truncations of MYC were first generated: T1 containing MBI and MBII (1-185), T2 with only MBII (113-185), T3 spanning MBII to MBIV (130-338), and T4 with MBIII, MBIV and the basic helix loop helix domain (186-439) (Figure 3-1A). Co-expression of GST-MYC truncations with Venus-flag-tagged NSD3S was followed by immunoprecipitation with anti-Flag antibodies to pull down the NSD3S complex. Consistent with our previous report (8), full-length MYC was confirmed to interact with NSD3S (Figure 3-1B), which served as a positive control for binding site mapping. Fragments T3 (130-338) and T4 (186-439) of MYC showed similar strength of interaction with NSD3S as the full-length MYC (Figure 3-1B). Conversely, MYC truncations lacking regions T3 or T4 exhibited reduced binding to NSD3S (Figure 3-1B). These results suggest that the region shared between truncations T3 and T4, residues 186 to 338 of MYC, are required for binding to NSD3S (Figure 3-1A). To further narrow down the region of MYC that mediates the NSD3S/MYC interaction, we generated refined MYC fragments spanning residues 186 to 338 (Figure 3-1C) and performed further pulldown experiments. While full-length MYC and fragment 186-339 were found to interact with NSD3S, none of the smaller MYC truncations were detected in complex with NSD3S (Figure 3-1D). Together, these results suggest that the internal region, residues 186 to 338, between MBIII and MBIV of MYC are involved in the interaction with NSD3S.

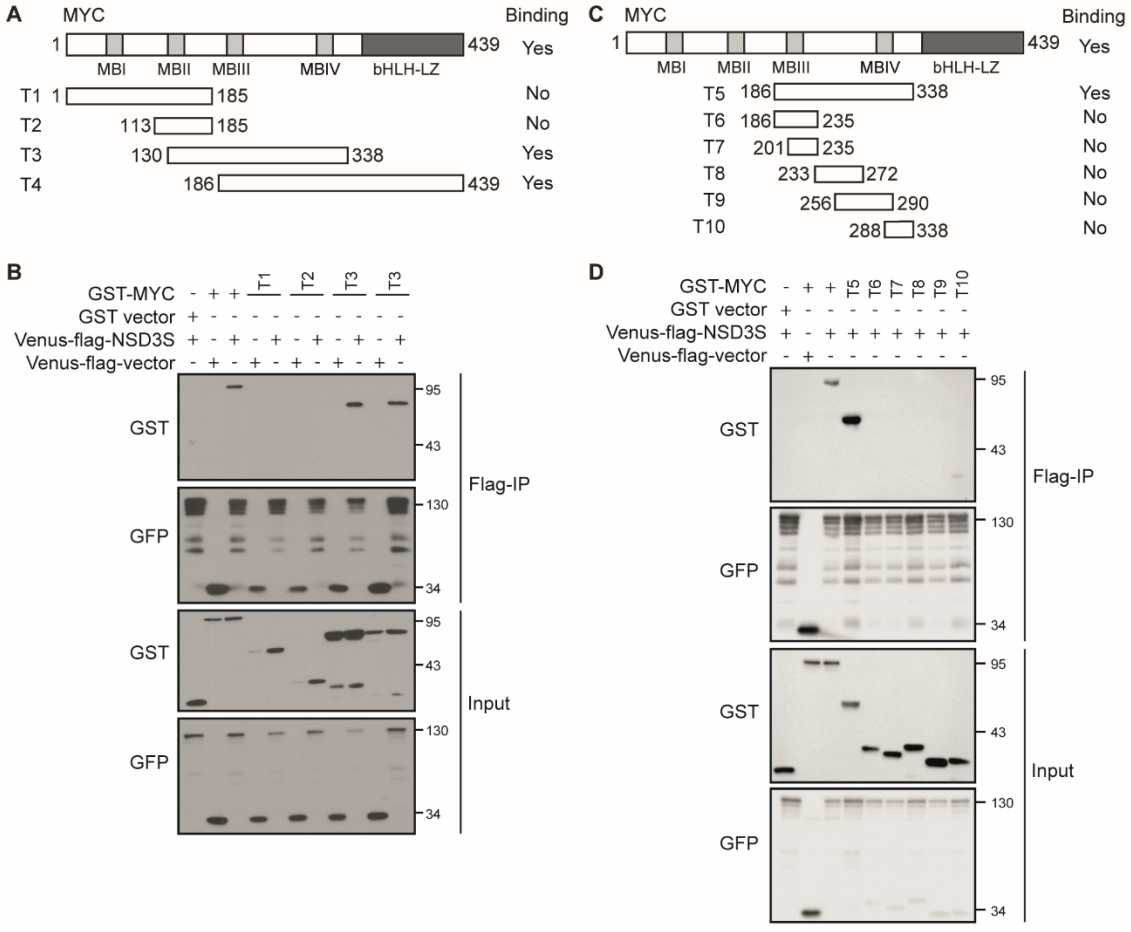
A
MYC
Binding
1
439
Yes
MBI
MBII
MBIII
MBIV
bHLH-LZ
T1 1 185 No
T2 113 185 No
T3 130 338 Yes
T4 186 439 Yes
C
MYC
Binding
1
439
Yes
MBI
MBII
MBIII
MBIV
bHLH-LZ
T5 186 338 Yes
T6 186 235 No
T7 201 235 No
T8 233 272 No
T9 256 290 No
T10 288 338 No
B
GST-MYC - + + T1 T2 T3 T3
GST vector + - - - - - - - - - -
Venus-flag-NSD3S + - + - + - + - + - +
Venus-flag-vector - + - + - + - + - + -
GST
GFP
GST
GFP
95
43
130
34
Flag-IP
Input
D
GST-MYC - + + T5 T6 T7 T8 T9 T10
GST vector + - - - - - - - - -
Venus-flag-NSD3S + - + + + + + + +
Venus-flag-vector - + - - - - - - -
GST
GFP
GST
GFP
95
43
130
34
Flag-IP
Input

Figure 3-1. Identification of MYC sequence that binds to NSD3S.

A. Diagram of MYC protein domains showing truncations used in the study labeled with residue numbers. **B.** Determination of MYC fragments involved in NSD3S binding. Venus-flag-NSD3S was co-expressed with GST-MYC and MYC truncations (T1 to T4) in HEK293T cells. The Venus-flag-NSD3S protein complex was immunoprecipitated with anti-Flag antibodies (Flag-IP). The presence of GST-MYC proteins in the NSD3S complex was detected by western blotting with an anti-GST antibody. Expression levels of Venus-flag-NSD3S and GST-MYC constructs were shown in input (WCL) cell lysates used for Flag-IP. **C.** Diagram of refined truncations of MYC (amino acids 186-338). **D.** Determination of MYC fragments (T5 to T10) for NSD3S binding. Flag-IP and western blotting were carried out as described in legend **B**.

3.3.2 A 15 amino acid peptide of NSD3S mediates MYC binding

The C-terminal 347 to 645 amino acid region of NSD3S was previously found to mediate binding to MYC (8). Further characterization of the residues on NSD3S involved in MYC binding may reveal the molecular basis for the interaction and identify strategies to manipulate the interaction for functional studies. We used a computational molecular modeling approach to guide the design of smaller C-terminal truncations of NSD3S shown in Figure 3-2A. Positive controls were first validated using the GST pull-down assay using glutathione-conjugated beads to isolate overexpressed GST-MYC and to identify NSD3S in the MYC complex. Indeed, full-length NSD3S and NSD3S fragment T-a (347 to 645) were found in complex with MYC (Figure 3-2B). Deletion of NSD3S residues 347 to 645 appeared to reduce, though not completely abolish, NSD3S interaction with MYC, suggesting a potential binding site within the region T-b (356 to 426). In support of this notion, NSD3S fragments lacking residues 356-426 exhibited no binding to MYC (Figure 3-2B). To test whether a MYC-binding site in the 356-426 region could be further delineated, we generated smaller truncations based on computational modeling predictions (Figure 3-2C). To guide the design of structural elements for testing, a computational molecular modeling approach was employed to define potential sub-structural regions within NSD3S fragment 356 to 426. The model obtained after a 100 ns molecular dynamics (MD) simulation suggested potential alpha-helical structures in regions W368 to K377 and R383 to Q389 of NSD3S, while the region encompassing Y390 to L426 is largely disordered (Figure 3-2C). The secondary structures (SS) observed for NSD3S region 356 to 426 in this model agrees with predictions made using Prime software [PMID 15048827]. Based on these secondary structure predictions, refined truncations within residues 356 to 426 (T-b) of NSD3S were generated (Figure 3-2D). Venus-flag-NSD3S truncations were tested for interaction with GST-MYC by GST pull-down with glutathione beads (Figure 3-2D). Positive binding signals were detected between full-length MYC and NSD3S truncations T-g (378 to 404) and T-i (378 to 426) (Figure 3-2E). In contrast, no binding

was observed between full-length MYC and NSD3S fragments T-f (356-378) and T-h (404-426), supporting a specific role for NSD3S residues 378 to 404 in mediating binding to MYC (Figure 3-2E). The 27-amino acid MYC-binding peptide of NSD3S was further divided into two segments (Figure 3-2F). Co-expression of GST-MYC and Venus-flag-NSD3S truncations was followed by GST pull-down assay as described above. NSD3S residues 389 to 404 demonstrated interaction with MYC, while the peptide containing residues 378-389 failed to show positive interaction (Figure 3-2G). Our results indicate that the 15-amino acid peptide spanning residues 389-404 on NSD3S (NSD3S-pep15) is sufficient to enable interaction with MYC protein.

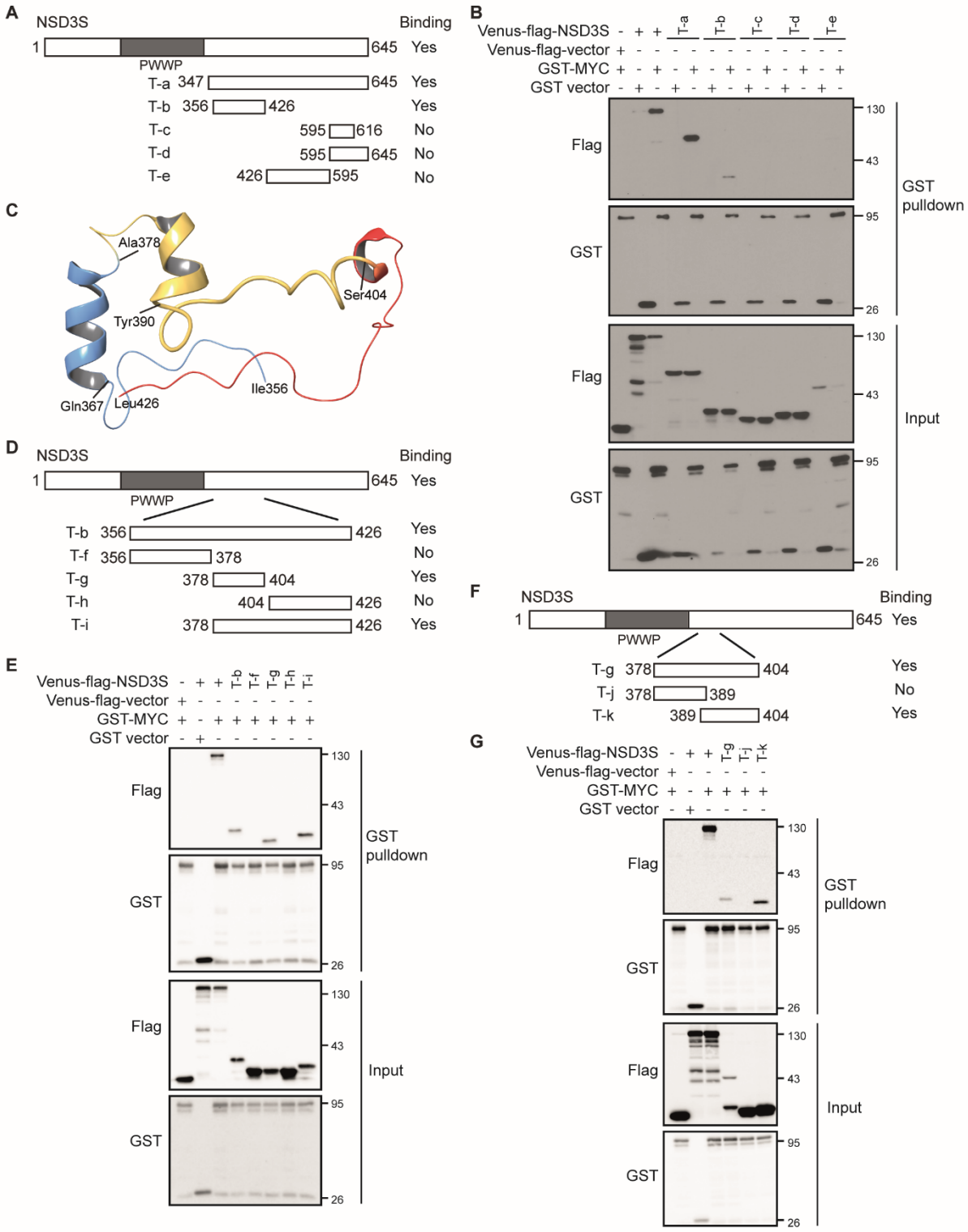
A
NSD3S
Binding
1
645
PWWP
T-a 347 645 Yes
T-b 356 426 Yes
T-c 595 616 No
T-d 595 645 No
T-e 426 595 No
B
Venus-flag-NSD3S
Venus-flag-vector
GST-MYC
GST vector
T-a
T-b
T-c
T-d
T-e
Flag
GST
GST pulldown
Input
130
43
95
26
C
Ala378
Tyr390
Ser404
Gln367
Leu426
Ile356
D
NSD3S
Binding
PWWP
T-b 356 426 Yes
T-f 356 378 No
T-g 378 404 Yes
T-h 404 426 No
T-i 378 426 Yes
E
Venus-flag-NSD3S
Venus-flag-vector
GST-MYC
GST vector
T-b
T-f
T-g
T-h
T-i
Flag
GST
GST pulldown
Input
F
NSD3S
Binding
PWWP
T-g 378 404 Yes
T-j 378 389 No
T-k 389 404 Yes
G
Venus-flag-NSD3S
Venus-flag-vector
GST-MYC
GST vector
T-g
T-j
T-k
Flag
GST
GST pulldown
Input

Figure 3-2. Determination of structural elements of NSD3S for MYC binding.

A. Diagram of NSD3S protein domains and truncations used for the study. Fragments (T-a to T-e) were labeled with residue numbers, and binding activity was indicated with plus signs. **B.** Determination of NSD3S fragments responsible for MYC binding by GST-pull down in HEK293T cells. GST-MYC protein was isolated with glutathione beads, and binding of Venus-flag-NSD3S truncations to GST-MYC was detected using anti-flag antibody. Binding of MYC to full-length NSD3S was included as a control. Expression of test proteins was shown as input (or WCL). **C.** A computational model of NSD3S 356 to 426 with predicted structural elements indicated: 356 to 378 (blue), 378 to 404 (yellow), and 404 to 426 (red). **D.** Diagram of NSD3S truncations (T-f to T-i) of fragment T-b (356 to 426) design according to the computational model generated. Truncations are labeled based on the residue number. **E.** Characterization of binding between Venus-flag-NSD3S and GST-MYC by GST pulldown in HEK293T cells. GST beads were used to pull down GST-MYC protein and detection of binding to NSD3S truncations was seen by western blot using flag antibody. Binding of MYC to full-length NSD3S and fragment T-b (356 to 426) was included as a control and expression of proteins was determined in the input. **F.** Diagram of refined truncations spanning residues T-g (378 to 404) of NSD3S. **G.** Characterization of refined NSD3S peptides responsible for binding to MYC by GST pull-down assay in HEK293T cells. GST-MYC was pulled down, and binding of Venus-flag-NSD3S peptides was detected by western blotting with flag antibody. Binding of MYC to full-length NSD3S and fragment T-g (378 to 404) was included as a control, expression of proteins was seen in the input.

3.3.3 NSD3S-pep15 is required for functional regulation of MYC

To understand the functional importance of MYC/NSD3S PPI, we tested the effect of NSD3S-pep15 in the interaction of NSD3S with MYC. By performing GST pull-down assay isolating GST-MYC protein, the binding of full-length Venus-flag-NSD3S to MYC was equal with or without NSD3S-pep15 (Figure 3-3A). These 15 residues appeared to be sufficient for MYC binding, but it was incapable of disrupting binding between these two full-length proteins. Our results suggest that NSD3S residues 389 to 404 may represent one, or a partial, interacting epitope to MYC.

The effect of the 15-residue deletion on NSD3S interaction with MYC was examined with the GST pull-down assay. The GST-MYC complex was found to contain NSD3SΔ15. The MYC binding signal for NSD3SΔ15 was similar to the one seen for the positive control, full-length NSD3S (Figure 3-3B). These data further support the model that region with amino acids 389 to 404 of NSD3S represents an interaction site, or a partial site, for MYC binding. More than one epitope may be involved in interacting with MYC (Figure 3-2G and 3-3B).

To probe for a functional role of NSD3S residues 389-404 in the regulation of MYC, we generated a deletion mutant of NSD3S lacking residues 389-404 (NSD3SΔ15). It has previously been demonstrated that NSD3S overexpression can extend the half-life of MYC (8). Thus, the effect of NSD3SΔ15 deletion on MYC protein half-life was evaluated. Cell treatment with a protein synthesis inhibitor, cycloheximide, allows the monitoring of half-life of the MYC protein over time (180), which was used for the study. Consistent with our previous results (8), overexpression of NSD3S stabilized MYC protein levels and increased MYC half-life. Compared to NSD3S, overexpression of NSD3SΔ15 exhibited a reduced stabilization effect on MYC, suggesting a partial role for this 15-residue NSD3S sequence in the stabilization of MYC (Figure 3-3C and 3-3D). Extended MYC protein half-life has been correlated with increased MYC transcriptional activity. To test the effect of NSD3SΔ15 on

MYC-driven transcription, an E-box-dependent luciferase-based MYC reporter assay was used (166, 183). Consistent with our previous report, overexpression of NSD3S was correlated with increased MYC transcriptional activity as shown by increased E-box dependent luciferase signal (8) (Figure 3-3E). In contrast, expression of NSD3SΔ15 failed to fully activate the MYC transcriptional activity, showing significantly decreased luciferase signal compared to that with NSD3S (Figure 3-3E). These data demonstrate that NSD3S residues 389-404 are crucial for NSD3S enhancement of MYC transcriptional activity. Together, these results suggest that amino acids 389 to 404 of NSD3S are required to regulate MYC function, increasing protein half-life and transcriptional activity.

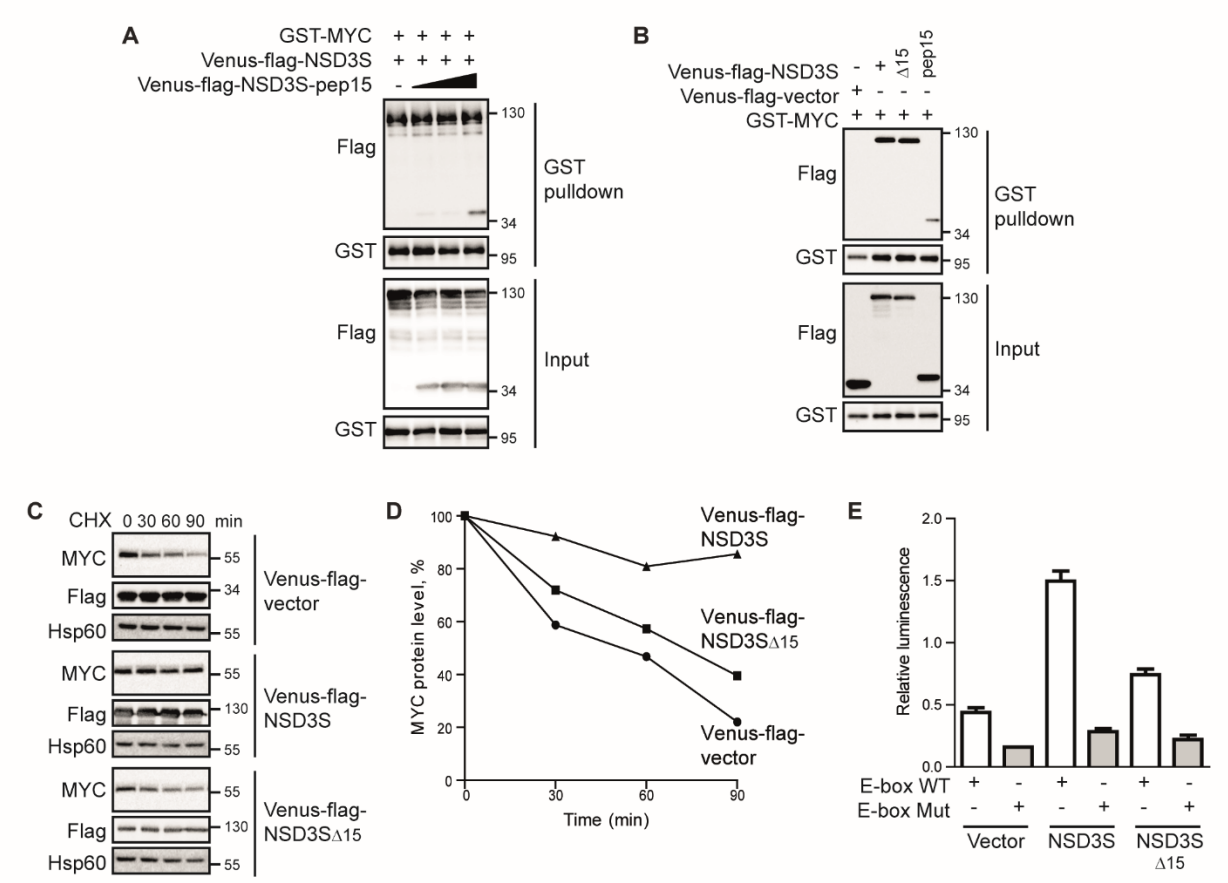
A
GST-MYC + + + +
Venus-flag-NSD3S + + + +
Venus-flag-NSD3S-pep15 -
Flag
GST
GST pulldown
Input
130
34
95
B
Venus-flag-NSD3S - + Δ15 pep15
Venus-flag-vector + - - -
GST-MYC + + + +
C
CHX 0 30 60 90 min
MYC
Flag
Hsp60
55
34
130
Venus-flag-vector
Venus-flag-NSD3S
Venus-flag-NSD3SΔ15
D
MYC protein level, %
Time (min)
Venus-flag-NSD3S
Venus-flag-NSD3SΔ15
Venus-flag-vector
E
Relative luminescence
E-box WT
E-box Mut
Vector
NSD3S
NSD3S Δ15

Figure 3-3. Deletion effect of NSD3S binding peptide on MYC transcriptional activity and stability.

A. Detection of the disrupting effect of MYC binding peptide, residues 389-404 of NSD3S in the interaction between full-length proteins by GST pull-down assay in HEK293T. Presence of NSD3S on the MYC complex was detected with flag antibody and compared to the expression in the input. **B.** Characterization of binding between Venus-flag-NSD3S deletion 389 to 404 and GST-MYC by GST pulldown assay in HEK293T cells. GST MYC was pull down with glutathione beads, and binding of the deletion was detected using flag antibody. NSD3S full length and truncation 389 to 404 were included as positive controls, expression of proteins was seen in the input. **C.** Effect of NSD3SΔ15 on MYC stability by cycloheximide (CHX) treatment in HEK293T cells. Levels of endogenous MYC protein were developed with a specific antibody, at different time points after inhibition of protein synthesis by CHX with Venus-flag-vector, -NSD3S or -NSD3SΔ15 overexpressed. **D.** Quantification of western blot showed in panel **C** of MYC levels at different time points of CHX treatment based on the densitometric analysis. MYC protein levels were normalized to Hsp60 protein levels as the loading control. **E.** Effect of NSD3SΔ15 on MYC reporter transcriptional assay in HEK293T cells. Luciferase activity was measured under conditions overexpressing Venus-flag-vector, Venus-flag-NSD3S or Venus-flag-NSD3SΔ15 and either wild-type (WT) or mutant (Mut) E-box luciferase reporter plasmid. Relative luminescence is the ratio between luciferase and the internal renilla activity control. Shown is a representative result of three independent experiments. The error bars indicate the mean ± s.d. of three replicates.

3.3.4 NSD3S stabilizes MYC by interfering with FBXW7-mediated proteasomal degradation

MYC is a transcription factor that acts as a master regulator of gene expression in cancer. Because of its significant role in regulating different characteristics of cancer cells to promote tumorigenesis, MYC activity is tightly controlled through intracellular protein-protein interactions (42, 184). To further understand the mechanism of MYC stabilization and activation by NSD3S, we investigated potential effects of NSD3S on MYC binding partners known to regulate MYC stability or transcriptional regulation. Overexpression of NSD3S along with some of the MYC binding partners (VHL, AURKA, SMAD3, SMAD2, BRCA1, SMARCA4, SMARCB1, RPL11, and FOXO3) does not significantly change MYC levels in the input sample, or the binding of either NSD3S or the MYC binding partner to MYC (Figure 3-4).

There was one protein that did show differences, FBXW7, a substrate recognition subunit of SCF E3 ubiquitin ligase complexes that are involved in one of the most extensively characterized proteolytic degradation pathways for MYC. For FBXW7 to associate with and mediate ubiquitination of MYC, MYC requires phosphorylation by two kinases, ERK, and GSK3β (72). Interestingly, expression of FBXW7 reduced MYC protein levels as expected, while co-expression of NSD3S with FBXW7 increased MYC levels, suggesting an antagonistic effect of NSD3S on FBXW7 function (Figure 3-5A). Because ERK and GSK3β are well-established regulators of MYC, the impact of NSD3S on MYC stability was examined under conditions with differential expression of ERK or GSK3β. As shown in Figure 3-5B, co-expression of NSD3S with either ERK or GSK3β exhibited MYC levels that were comparable to those under conditions of ERK, GSK3β or NSD3S overexpression alone.

Since NSD3S increases MYC protein stability and suppresses the action of FBXW7 on degrading MYC, we tested whether NSD3S expression could influence the interaction between

FBXW7 and MYC. We performed a GST pull-down assay against GST-MYC protein with overexpression of Venus-flag-NSD3S or Venus-flag-vector control. Overexpression of Venus-flag-NSD3S correlated with reduced interaction of endogenous FBXW7 with GST-MYC in HEK293T cells (Figure 3-5C). In H1299 lung cancer cells, we perform the same GST pull-down assay. Even though the band for FBXW7 in the MYC-pull down samples in both conditions is the same, the amount of MYC in the input and isolated by the beads is higher on the condition with NSD3S, indicating us that the levels of FBXW7 that are interacting to MYC are less with NSD3S overexpressed (Figure 3-5D). As in Figure 3-5B, NSD3S overexpression resulted in no changes in the interactions between MYC/ERK or MYC/GSK3β interactions (Figure 3-5C and 3-5D). We then evaluated whether NSD3S was able to disrupt endogenous binding between MYC and FBXW7. We performed an endogenous co-immunoprecipitation (co-IP) in HEK293T cells and H1299 cancer cell line using a MYC antibody, with overexpressed Venus-flag-NSD3S or Venus-flag-vector. In agreement with the results in the MYC overexpression system, NSD3S overexpression resulted in reduced interaction between endogenous FBXW7 and MYC but did not affect the association of ERK or GSK3β with MYC (Figure 3-5E and 3-5F). Again, as the GST pull-down assay in H1299 lung cancer cells, we see that NSD3S increases endogenous levels of MYC, so even though the band of FBXW7 bound to MYC in the IP samples is the same under both conditions, the levels of MYC are higher when NSD3S is overexpressed (Figure 3-5F). The effect of NSD3S overexpression in increasing MYC levels in H1299 lung cancer cells agrees with the stabilizing effect of NSD3S on MYC protein stability in HEK293T cells (Figure 3-3C and 3-3D).

FBXW7 is an SCF E3 ubiquitin ligase subunit that targets proteins for ubiquitination and proteasomal degradation (182). We thus investigated the effects of NSD3S expression on FBXW7-mediated ubiquitination of MYC. HA-tagged ubiquitin was overexpressed and immunoprecipitated using anti-HA antibodies, and ubiquitination of endogenous MYC was evaluated. NSD3S

overexpression resulted in reduced ubiquitin bound MYC on the IP samples in HEK293T cells and H1299 lung cancer cells (Figure 3-5G and 3-5H). Disruption of the interaction between MYC and FBXW7 by NSD3S thus correlates with decreased MYC ubiquitination and increased MYC protein levels in cells (Figure 3-6). Taken together, these results suggest a novel mechanism for how NSD3S stabilizes MYC protein levels by opposing FBXW7-mediated degradation pathway.

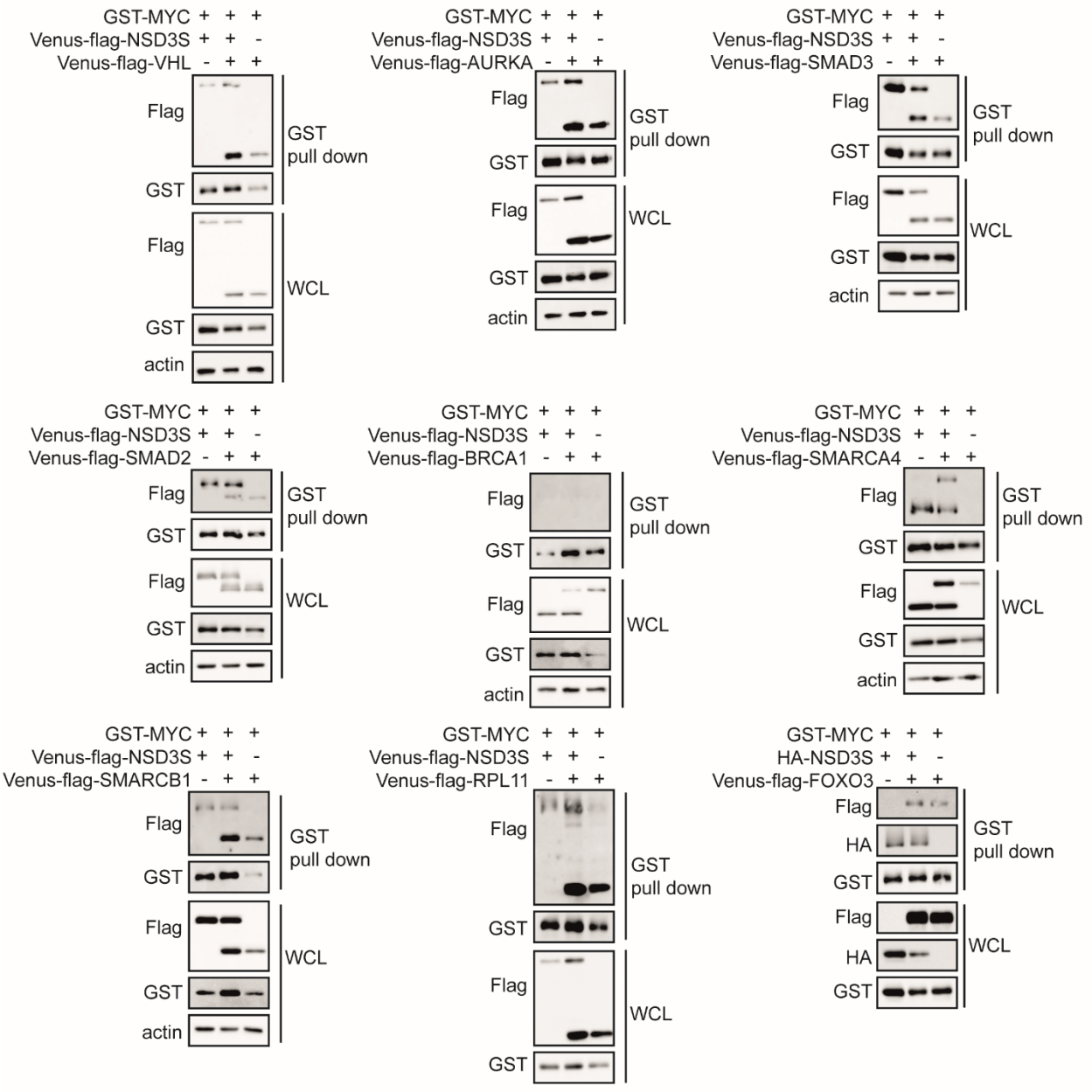
GST-MYC + + +
Venus-flag-NSD3S + + -
Venus-flag-VHL - + +
Flag
GST
pull down
GST
Flag
WCL
GST
actin
GST-MYC + + +
Venus-flag-NSD3S + + -
Venus-flag-AURKA - + +
Flag
GST
pull down
GST
Flag
WCL
GST
actin
GST-MYC + + +
Venus-flag-NSD3S + + -
Venus-flag-SMAD3 - + +
Flag
GST
pull down
GST
Flag
WCL
GST
actin
GST-MYC + + +
Venus-flag-NSD3S + + -
Venus-flag-SMAD2 - + +
Flag
GST
pull down
GST
Flag
WCL
GST
actin
GST-MYC + + +
Venus-flag-NSD3S + + -
Venus-flag-BRCA1 - + +
Flag
GST
pull down
GST
Flag
WCL
GST
actin
GST-MYC + + +
Venus-flag-NSD3S + + -
Venus-flag-SMARCA4 - + +
Flag
GST
pull down
GST
Flag
WCL
GST
actin
GST-MYC + + +
Venus-flag-NSD3S + + -
Venus-flag-SMARCB1 - + +
Flag
GST
pull down
GST
Flag
WCL
GST
actin
GST-MYC + + +
Venus-flag-NSD3S + + -
Venus-flag-RPL11 - + +
Flag
GST
pull down
GST
Flag
WCL
GST
GST-MYC + + +
HA-NSD3S + + -
Venus-flag-FOXO3 - + +
Flag
HA
GST
pull down
GST
Flag
HA
WCL
GST

Figure 3-4. Effect of NSD3S in MYC binding partners.

HEK293T GST pull-down assay for the detection of GST-MYC complexes with co-expression of NSD3S and some of MYC binding partners (VHL, AURKA, SMAD3, SMAD2, BRCA1, SMARCA4, SMARCB1, RPL11, and FOXO3). Levels of tagged-proteins in the WCL or input were used as controls.

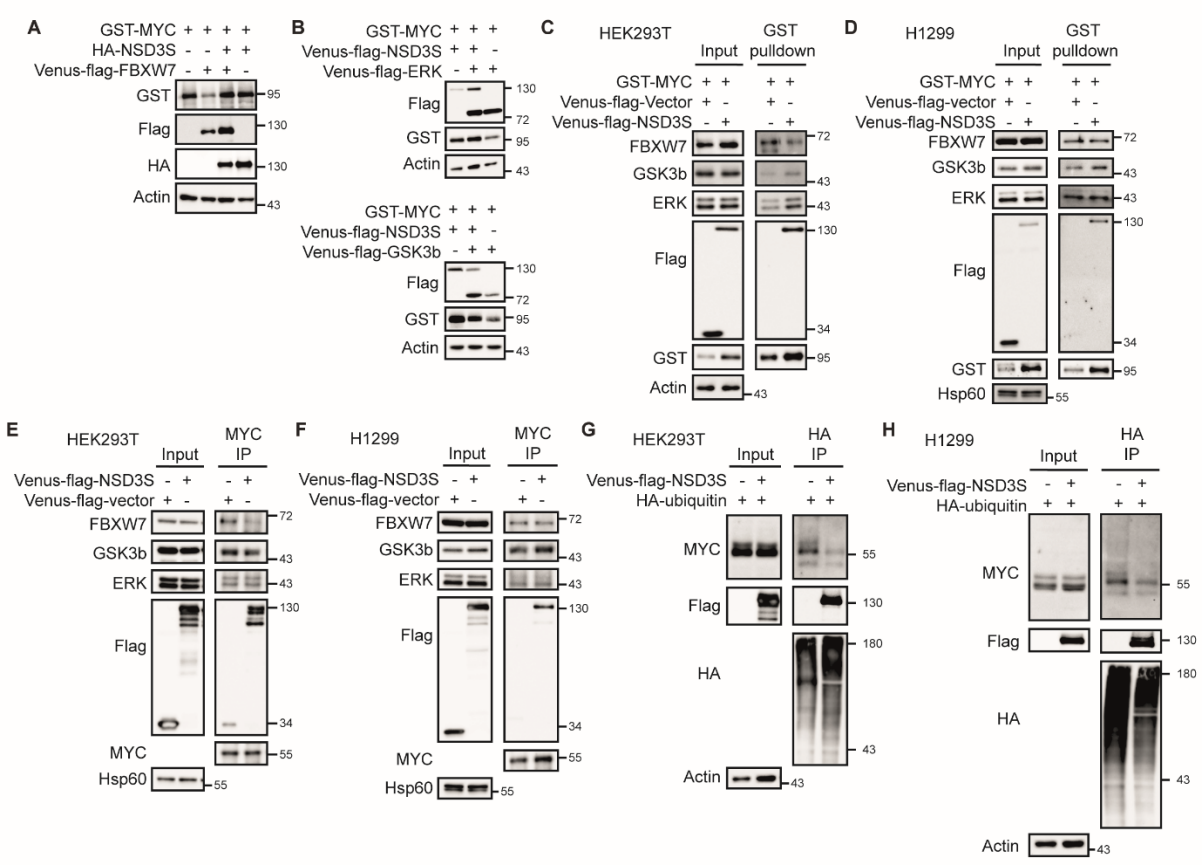
A
GST-MYC + + + +
HA-NSD3S - - + +
Venus-flag-FBXW7 - + + -
GST
Flag
HA
Actin
95
130
130
43
B
GST-MYC + + +
Venus-flag-NSD3S + + -
Venus-flag-ERK - + +
Flag
GST
Actin
130
72
95
43
GST-MYC + + +
Venus-flag-NSD3S + + -
Venus-flag-GSK3b - + +
Flag
GST
Actin
130
72
95
43
C
HEK293T
Input
GST pulldown
GST-MYC + + + +
Venus-flag-Vector + - + -
Venus-flag-NSD3S - + - +
FBXW7
GSK3b
ERK
Flag
GST
Actin
72
43
43
130
34
95
43
D
H1299
Input
GST pulldown
GST-MYC + + + +
Venus-flag-vector + - + -
Venus-flag-NSD3S - + - +
FBXW7
GSK3b
ERK
Flag
GST
Hsp60
72
43
43
130
34
95
55
E
HEK293T
Input
MYC IP
Venus-flag-NSD3S - + - +
Venus-flag-vector + - + -
FBXW7
GSK3b
ERK
Flag
MYC
Hsp60
72
43
43
130
34
55
55
F
H1299
Input
MYC IP
Venus-flag-NSD3S - + - +
Venus-flag-vector + - + -
FBXW7
GSK3b
ERK
Flag
MYC
Hsp60
72
43
43
130
34
55
55
G
HEK293T
Input
HA IP
Venus-flag-NSD3S - + - +
HA-ubiquitin + + + +
MYC
Flag
HA
Actin
55
130
180
43
43
H
H1299
Input
HA IP
Venus-flag-NSD3S - + - +
HA-ubiquitin + + + +
MYC
Flag
HA
Actin
55
130
180
43
43

Figure 3-5. Effect of NSD3S in MYC proteasomal degradation by FBXW7.

A. HEK293T cell lysate for the detection of GST-MYC levels with NSD3S in combination with FBXW7. Levels of MYC were compared against the NSD3S or FBXW7 alone, and actin was used as a loading control. **B.** Detection of MYC levels in cell lysate from HEK293T with NSD3S in combination with GSK3β or ERK. MYC levels were compared against the NSD3S, GSK3β or ERK alone and actin was used as a loading control **(C-D).** Detection of endogenous binding of FBXW7, GSK3β and ERK to GST-MYC in the presence of NSD3S by GST pulldown. Levels detected on the pulldown were compared to expression in the input and actin as a loading control in **C.** HEK293T cells. **D.** H1299 lung cancer cells. **(E-F).** Evaluation of FBXW7 binding to MYC by co-immunoprecipitation (co-IP) in the presence of NSD3S. Endogenous levels of FBXW7 were detected in complex with endogenous MYC that was immunoprecipitated with MYC antibody, levels were compared to those seen in the input samples, and Hsp60 protein was used as a loading control in **E.** HEK293T cells **F.** H1299 lung cancer cells **(G-H).** Determination of ubiquitinated MYC levels by HA-immunoprecipitation of HA-ubiquitin in the presence or absence of NSD3S. Levels of endogenous MYC detected on the HA-ubiquitin complex were quantified and compared to the expression of proteins in the input sample and actin as a loading control in **G.** HEK293T cells. **H.** H1299 lung cancer cells.

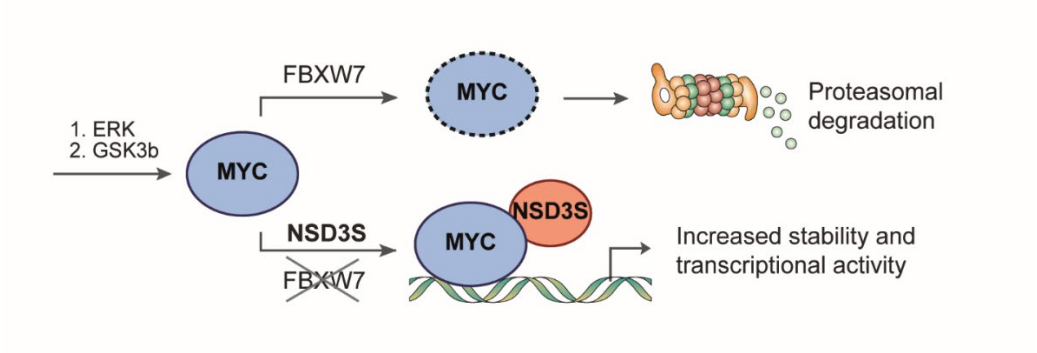
FBXW7
MYC
Proteasomal
degradation
1. ERK
2. GSK3b
MYC
NSD3S
MYC
NSD3S
Increased stability and
transcriptional activity
FBXW7

Figure 3-6. Proposed model for NSD3S role in MYC protein stability.

NSD3S impacts a major pathway, the FBXW7-mediated proteasomal degradation pathway, that regulates MYC half-life. NSD3S binds to MYC and suppresses the FBXW7 activity by disrupting the interaction with MYC, increasing MYC protein half-life and transcriptional activity.

3.4 Discussion

MYC is a master regulator of cell growth, and its activity is tightly regulated by diverse mechanisms (185). Here we present evidence in support of a novel mechanism by which NSD3S stabilizes MYC through disruption of the FBXW7/MYC interaction.

To gain insights into the molecular interaction between NSD3S and MYC, we identified an internal region of MYC that extends through MBIII and MBIV as an NSD3S binding site (Figure 3-1D). In contrast to the MBI and MBII regions that are localized in the transactivation domain (TAD) and are essential for cell transformation (186), and the C-terminal bHLH-LZ domain that is important for MAX dimerization and DNA binding, the internal segment of MYC is highly disordered, and the functions of MBIII and MBIV have not been extensively characterized. Also, most of MYC binding partners bind the N- or C-terminus of the protein (21, 42, 187). For example, these binding sites include ERK (N-terminal) (47, 53), GSK3β (residues 1-100) (52, 53), and FBXW7 (MBI, residue phospho-T58) (48, 49). Thus, mapping the binding site for NSD3S reveals a new functional site on MYC with a potential regulatory role for MYC stabilization.

On NSD3S, we narrowed down the MYC binding site to a 15-amino acid peptide. NSD3S has one defined structural domain, termed the PWWP domain, which has been shown to mediate binding to methylated H3K36me2/3 (188) and other proteins (116). Currently, only two NSD3 binding proteins have been mapped: BRD4, which binds to amino acids 152 to 163, and CHD8, which binds to C-terminal amino acids 384 to 645 (141). Here, we add MYC as a binding partner of NSD3S that specifically binds to residues 389 to 404. Those 15 amino acids are sufficient but not required for MYC binding and not able to disrupt the PPI, implying that more than one epitope or a conformational change on NSD3S may be important for interacting to MYC. Importantly, our data

reveal a critical role for NSD3S-pep15 in the regulation of MYC function, as deletion of this segment leads to decreased MYC transcriptional activity and degradation.

MYC is an "immediate early gene" (25, 189) known to be a serum-activated protein with a short half-life of about 30 minutes in proliferating cells (28). Different regulatory mechanisms have been reported to alter MYC protein stability that could directly impact MYC signaling under physiological and pathological conditions (30). One well-established mechanism is the priming of MYC by two kinases, ERK and GSK3β, that leads to the binding of FBXW7, a protein that directly regulates MYC degradation (190). Previously, we reported that NSD3S increases MYC protein stability and that the stabilization effect is possibly through binding (8). Our current findings reveal that NSD3S stabilizes MYC by interfering with the interaction between MYC and FBXW7, an E3 ligase subunit known to mediate MYC ubiquitination and degradation (48, 49). NSD3S does not influence ERK or GSK3β activity, but it appears to suppress FBXW7 function (Figure 3-5). Interestingly, NSD3S interferes with FBXW7 binding to MYC, preventing ubiquitination and proteasomal degradation of MYC. GSK3β phosphorylation of MYC at T58 allows interaction of FBXW7 with MYC through its MBI domain (191). Here we show that NSD3S binds to the internal region of MYC (residues 186-338). Although NSD3S and FBXW7 do not compete for binding to the same fragment of MYC, it is possible that the binding of NSD3S alters the three-dimensional protein structure of MYC, thus reducing MYC binding to FBXW7.

NSD3S belongs to the NSD family of proteins that have been implicated in oncogenesis (114). Specifically, NSD3S, a short isoform of the NSD3 histone lysine methyltransferase, lacking methyltransferase activity, has been linked with progression of leukemia (141) and NUT-midline carcinoma (135, 136). Here, we report a novel mechanism for how NSD3S may contribute to tumorigenesis by acting as a positive regulator of the MYC oncogene. Moreover, this regulation shows

a broader mechanism of action of NSD3S, as MYC acts as a driver in multiple solid and hematological cancers (33) and this study suggests regulation of MYC by NSD3S in various cellular environments.

Results from this paper defined a binding interface between NSD3S and MYC, which may provide a basis for further understanding of the interaction for functional manipulation. This study also revealed the importance of NSD3 residues 389 to 404 in MYC regulation, which may lead to future strategies to regulate MYC function. Furthermore, we uncovered a novel regulatory mechanism of MYC by NSD3S binding, adding a novel regulatory element to the well-characterized FBXW7 proteasomal degradation pathway for MYC. This regulatory circuit between FBXW7/MYC/NSD3S makes the MYC/NSD3S PPI an interesting target for therapeutic exploration in MYC-driven tumors, as it impacts both transcriptional activity and the half-life of MYC protein. Targeting the MYC/NSD3S PPI interface may prove beneficial for patients with MYC amplification, as their disruption may restore the binding between MYC and the tumor suppressor FBXW7.

Chapter 4: Discussion and future directions

4.1 MYC as a central node in the PPI network

Cancer is a multistep disease, meaning multiple alterations of genes are required for its development (192). In a cell, PPIs regulates many signaling pathways. Cancer cells are no exception, and the generation of OncoPPi (v.1) revealed 397 lung cancer associated-PPIs (8). Genetic and epigenetic changes may alter the normal PPI network of a cell, as genes are amplified, deleted or mutated. With the information obtained from OncoPPi (v.1), MYC was identified as a hub in PPIs and as important for pathway connectivity (8). MYC itself is a disordered protein. This characteristic, along with its many interaction partners, may suggest MYC engages different conformations depending on the protein which it interacts. Also, MYC PPIs may be regulated in a temporal and spatial dimension; all of MYC binding partners are unlikely to interact simultaneously. Most of the PPIs might be transient interactions, depending on when the proteins are expressed or induced in a cell (193). In addition to being a disordered protein, MYC also lacks enzymatic activity, and most cancer therapeutics are being developed against proteins with catalytic activity (1). Here, we characterized the PPI formed by two proteins lacking enzymatic activity, MYC oncogene, and NSD3S isoform, belonging to the HMTs family of proteins.

The connection between MYC and HMTs have been reported previously. The SMYD3 methyltransferase that maintains H3K4me3 at promoters, a mark that correlates with the higher presence of MYC on those regions of the chromatin (194). MYC also has an inhibitory action on KDM5A/B demethylase, maintaining H3K4me3 permissive-MYC binding state (195). Interestingly, however, our data revealed a connection between MYC and NSD3S. An isoform that lacks the methyltransferase activity, NSD3S contains the PWWP domain, thus acting only as a chromatin "reader" protein.

Support for direct crosstalk between MYC and NSD3S signaling has not been provided in previous work; yet, a study published in 2014 linked co-amplification of the genomic region 8p11-12 (NSD3 included) and the MYC oncogene on 8q24.21 in primary invasive breast carcinoma (196). Indirect work has supported the connection between these two proteins through BRD4, which increases MYC transcriptional activity and also interacts with NSD3S (140, 141, 197). Our work placed NSD3S upstream of MYC signaling, and the PPI is formed with or without BRD4 presence. Whether MYC/NSD3S/BRD4 signaling functions together to promote tumor progression remains to be tested.

4.2 Elements of MYC and NSD3S relevant for binding

Here we characterized the binding interface between MYC and NSD3S. Identification of the structural elements involved in binding not only describes the nature of the interaction but also provides a basis for the design of PPI disruptors that can be used as functional probes or therapeutic agents. As described above, MYC interacts with a variety of proteins that regulate its function; it predominantly does so through its N- and C-terminal domains (42, 171). We described NSD3S as a novel MYC interactor, binding to the internal portion of MYC. About NSD3S, a 15 amino acid peptide (residues 378 to 404), labeled as NSD3S-pep15, seems to be relevant for binding to MYC. Both the short and full-length protein contained in the sequence those 15 residues. By affinity overexpressed assays, we were able to detect the binding between MYC and NSD3L (data not shown). However, we failed to detect under endogenous levels of proteins by co-immunoprecipitation. The reason for the inconclusive result might be that the sensitivity of the antibody was not enough or due to the higher expression of NSD3S on cancer cell lines, as reported previously (117, 125). Deletion of those 15 amino acids, NSD3SΔ15, still binds to MYC, implying that more than one NSD3S epitope may be involved in MYC interaction. These findings suggest that NSD3S-pep15 is sufficient, but not

required for MYC binding. However, those 15 residues are important for the functional regulation of MYC oncogene.

4.3 NSD3S regulates MYC function through a well-defined degradation pathway

The findings of this dissertation discovered NSD3S as a positive regulator of MYC protein stability and uncovered the molecular mechanism behind the increased half-life of MYC, by interfering with FBXW7 binding. Our study adds knowledge of a molecular player, NSD3S, that acts on FBXW7 proteasomal degradation pathway, specifically in the last step, the binding of FBXW7 to MYC. NSD3S seems not to affect the proteins involved in the phosphorylation events leading to the proteasomal degradation of MYC. Our data also revealed that NSD3S and FBXW7 bind to different regions on MYC. What remains to be determined is how NSD3S interferes with MYC/FBXW7 binding. The region where FBXW7 and NSD3 bind on MYC structure (residues 58-62 and 186-338, respectively) have not been crystallized. It would be interesting to solve the MYC crystal structure and study how those domains connect. Another possibility is that NSD3S binding to MYC generates a conformational change in MYC; it may be affecting the binding of Pin1 or PP2A, therefore reducing binding of FBXW7. However, this remains to be tested. While the findings reported here begin to uncover the mechanism of regulation that NSD3S has in increasing MYC half-life, it does not directly address the effect of NSD3S on MYC proteasomal degradation. The work presented shows a decrease of ubiquitylated-MYC when NSD3S is overexpressed, suggesting a role for the proteasome. Further studies are required to fully characterize the action of NSD3S on proteasomal degradation of MYC.

Through our work, we expanded the set of proteins known to control MYC stability by adding NSD3S. MYC is an oncogene overexpressed in nearly every human cancer. However, only a third of them have MYC locus amplification or translocation (10). Thus, deregulation of NSD3S

(amplification) or FBXW7 (deletion), could partially contribute and explain the increase in MYC overexpression without having MYC loci amplification.

NSD3S, described here, is not the only protein belonging to the NSD family to impact MYC stability. Indeed, overexpression of NSD2 can upregulate MYC protein expression indirectly by silencing the miR-126* tumor suppressor, inducing cell growth in multiple myeloma cell lines. In the study, increased binding of NSD2 to the miR-126* promoter was not associated with increased H3K36 methylation, suggesting a methyltransferase independent activity (198).

4.4 Potential mechanisms for the increase of MYC transcriptional activity by NSD3S

In this dissertation, we presented NSD3S as a positive regulator of MYC transcriptional activity. We reported that deletion of residues 378 to 404, NSD3SΔ15, cannot increase luciferase expression on a MYC reporter assay, suggesting a critical role for that NSD3S short segment. However, the mechanism by which NSD3S generates this effect on MYC remains to be elucidated. NSD3S could contribute to MYC transcriptional activity in a number of manners, three of which I will discuss below.

First, it is known that chromatin "readers," "writers" and "erasers" usually associate with large protein complexes to act together on chromatin regulation (199). It remains to be determined if NSD3S directly binds to MYC. Our studies suggest direct binding, due to TR-FRET assay, as a positive signal is only read when proteins are within 10 nm of distance (200). However, we cannot rule out the possibility that NSD3S is forming a protein complex and thereby binding to MYC and increasing transcriptional activity. According to the knowledge we have on NSD3S and MYC, BRD4 could be postulated as one of the proteins that could be involved in the protein complex, through binding to acetylated lysine on the chromatin. In addition, there could also be a sequential event on

MYC transcriptional activity through BRD4-MYC-NSD3S protein axis, meaning that binding between them could promote binding in certain regions of the chromatin.

Second, considering that NSD3S, through the PWWP domain, binds to active marks for transcription (H3K36me) and that MYC preferentially binds to euchromatin state, NSD3S could be an adaptor protein that brings MYC to active portions of the chromatin, therefore increasing gene transcription. To test this hypothesis, we could generate a PWWP mutant, unable to bind to chromatin (PWWP W284A on NSD3S) (141), and see the effect of the wild-type and mutant NSD3S on regulating MYC transcriptional activity.

Finally, another potential mechanism worthy of consideration is through MAX. MYC by itself cannot bind to DNA; it needs to dimerize with MAX to be able to bind to chromatin (21). Since NSD3S and MAX interact in different regions of MYC structure (186-338 and bHLH-LZ, respectively), it is not altogether surprising that NSD3S does not compete with MAX for MYC binding. Moreover, MAX seems to enhance the binding between MYC and NSD3S (Appendix A.1). Also, Figure A-1A and A-1B show that NSD3S can also bind to MAX protein. However, the consequence of this cooperation between MAX/MYC/NSD3S proteins remains to be tested. Further biochemical characterization of the MYC/NSD3S PPI may help distinguish between the mechanisms discussed here or other alternative mechanisms not explored in this section.

4.5 Therapeutic implications

Precision medicine proposes a therapy that is targeted to specific individual´s cancer depending on their genetic background. Our work adds on this notion, as we study how genetic alterations in oncogenes or tumor suppressor genes changes PPI networks in cancer, and finally signaling pathways. Specifically, here we discovered novel PPIs for MYC oncogene and characterized

in detail MYC/NSD3S PPI. Centering at MYC and NSD3S proteins, we discuss their therapeutic implications.

4.5.1 MYC

MYC has emerged as a viable therapeutic target in cancer (108). Indeed, MYC is amplified and a driver in different tumor types. Therefore, finding a small molecule to disrupt MYC/NSD3S PPI (Preliminary results on Appendix A.2), will represent an indirect approach to target this oncoprotein in a broad spectrum of MYC-dependent tumor types.

4.5.2 NSD3S

NSD3S is amplified in different cancers; however, reviewing the studies, it is not entirely established if it acts as a driver or passenger in cancer progression. On one cancer type that NSD3S may be relevant, is in NUT midline carcinoma. NSD3-NUT oncofusion contains almost the complete sequence of NSD3S isoform, including the 15 amino acids required for the increase on MYC stability and transcriptional activity. Therefore, by targeting NSD3S/MYC PPI, we may be disrupting one of the mechanisms that the fusion protein may have to promote tumorigenesis. Interestingly, in NUT midline carcinomas driven by BRD4-NUT oncofusion, NSD3S/MYC PPI may also be relevant, due to the potential connection between BRD4, MYC and NSD3S protein, already discussed before. Also, BRD4-NUT fusion may bind to NSD3S/MYC complex and by that mechanism promote tumorigenesis. In Appendix A.3 we also show preliminary data for the identification of inhibitors for NSD3S/BRD4 PPI.

4.6 Summary and future directions

In summary, the work presented in this dissertation provides a novel mechanism of regulation of the MYC oncogene. We described and characterized a new PPI between MYC and NSD3S, therefore connecting an oncogenic pathway to an epigenetic regulator. We also uncover an oncogenic

function for NSD3S isoform, increasing MYC half-life and transcriptional activity. Overall, the dual effect that NSD3S has in MYC may be driven by different signaling molecules (Figure 4-1). The impact in MYC stability, as we show here, might be in part by acting through the FBXW7 pathway. The MYC transcriptional activity effect could be through MAX or involving other proteins. It is also possible that the increased transcriptional activity of MYC is due to the increased amount of MYC half-life with reduced degradation induced by NSD3S. This work adds knowledge for the development of a PPI disruptor for MYC/NSD3S, that could benefit cancer patients with MYC or NSD3S amplification or oncofusions.

Future directions of this work would advance MYC/NSD3S knowledge to a translational aspect of cancer biology. First, it is important to determine the connection between MYC/NSD3S PPI with the different hallmarks of cancer. This will allow us to understand the functional importance of the PPI and give us insights into what steps of cancer progression this PPI could be linked. Next, studying deeper the mechanism by which NSD3S increases the transcriptional activity of MYC. MYC as a transcription factor acts through the activation/repression of target genes, so understanding how NSD3S achieves the enhancement could be relevant for developing small molecule inhibitors. Similarly, there is more to discover on the regulation of FBXW7 pathway. Lastly, the development of small molecule inhibitors for MYC/NSD3S PPI (Appendix A.2) and testing those inhibitors in MYC-driven tumors and NUT midline carcinoma cell lines may have significant therapeutic implications.

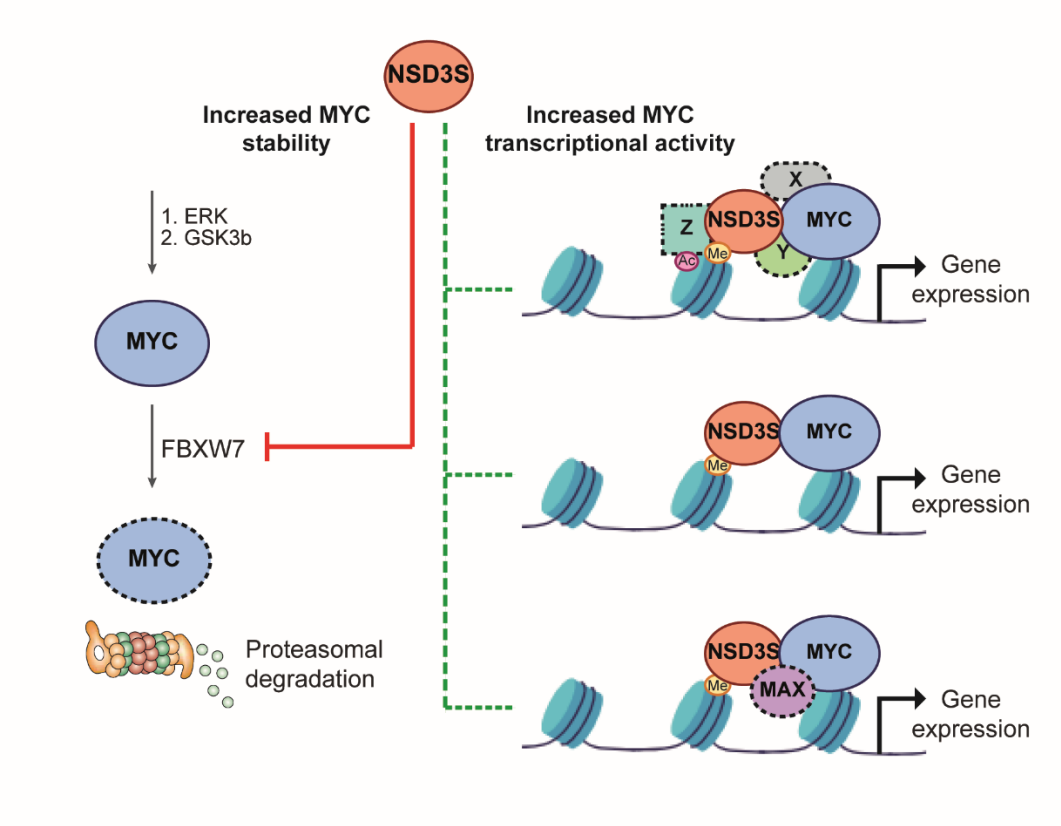
NSD3S
Increased MYC stability
Increased MYC transcriptional activity
1. ERK
2. GSK3b
MYC
FBXW7
MYC
Proteasomal degradation
X
Z
NSD3S
MYC
Y
Ac
Me
Gene expression
NSD3S
MYC
Me
Gene expression
NSD3S
MYC
Me
MAX
Gene expression

Figure 4-1. Proposed model.

NSD3S increases MYC stability and transcriptional activity. The enhancement of MYC half-life is partially through the interruption of FBXW7/MYC binding. The effect of NSD3S in MYC transcriptional activity may be due to numerous mechanisms. Here we illustrate just three of them. First, forming a complex with other epigenetic regulators (labeled as protein "X," "Y" or "Z"), second, by binding to H3K36me through the PWWP domain, and finally by interacting to MAX.

References

1. Vogelstein B, Papadopoulos N, Velculescu VE, Zhou S, Diaz LA, Jr., Kinzler KW. Cancer genome landscapes. Science. 2013;339(6127):1546-58.

2. Hanahan D, Weinberg RA. The hallmarks of cancer. Cell. 2000;100(1):57-70.

3. Hanahan D, Weinberg RA. Hallmarks of cancer: the next generation. Cell. 2011;144(5):646-74.

4. Ivanov AA, Khuri FR, Fu H. Targeting protein-protein interactions as an anticancer strategy. Trends in pharmacological sciences. 2013;34(7):393-400.

5. Wells JA, McClendon CL. Reaching for high-hanging fruit in drug discovery at protein-protein interfaces. Nature. 2007;450(7172):1001-9.

6. Oltersdorf T, Elmore SW, Shoemaker AR, Armstrong RC, Augeri DJ, Belli BA, et al. An inhibitor of Bcl-2 family proteins induces regression of solid tumours. Nature. 2005;435(7042):677-81.

7. Vassilev LT, Vu BT, Graves B, Carvajal D, Podlaski F, Filipovic Z, et al. In vivo activation of the p53 pathway by small-molecule antagonists of MDM2. Science. 2004;303(5659):844-8.

8. Li Z, Ivanov AA, Su R, Gonzalez-Pecchi V, Qi Q, Liu S, et al. Corrigendum: The OncoPPi network of cancer-focused protein-protein interactions to inform biological insights and therapeutic strategies. Nature communications. 2017;8:15350.

9. Vennstrom B, Sheiness D, Zabielski J, Bishop JM. Isolation and characterization of c-myc, a cellular homolog of the oncogene (v-myc) of avian myelocytomatosis virus strain 29. Journal of virology. 1982;42(3):773-9.

10. Nesbit CE, Tersak JM, Prochownik EV. MYC oncogenes and human neoplastic disease. Oncogene. 1999;18(19):3004-16.

11. Tansey WP. Mammalian MYC Proteins and Cancer. New Journal of Science. 2014;2014:27.

12. Andresen C, Helander S, Lemak A, Fares C, Csizmok V, Carlsson J, et al. Transient structure and dynamics in the disordered c-Myc transactivation domain affect Bin1 binding. Nucleic acids research. 2012;40(13):6353-66.

13. Stone J, de Lange T, Ramsay G, Jakobovits E, Bishop JM, Varmus H, et al. Definition of regions in human c-myc that are involved in transformation and nuclear localization. Molecular and cellular biology. 1987;7(5):1697-709.

14. Hemann MT, Bric A, Teruya-Feldstein J, Herbst A, Nilsson JA, Cordon-Cardo C, et al. Evasion of the p53 tumour surveillance network by tumour-derived MYC mutants. Nature. 2005;436(7052):807-11.

15. Zhang XY, DeSalle LM, McMahon SB. Identification of novel targets of MYC whose transcription requires the essential MbII domain. Cell cycle. 2006;5(3):238-41.

16. Li LH, Nerlov C, Prendergast G, MacGregor D, Ziff EB. c-Myc represses transcription in vivo by a novel mechanism dependent on the initiator element and Myc box II. The EMBO journal. 1994;13(17):4070-9.

17. Herbst A, Hemann MT, Tworkowski KA, Salghetti SE, Lowe SW, Tansey WP. A conserved element in Myc that negatively regulates its proapoptotic activity. EMBO reports. 2005;6(2):177-83.

18. Kurland JF, Tansey WP. Myc-mediated transcriptional repression by recruitment of histone deacetylase. Cancer research. 2008;68(10):3624-9.

19. Cowling VH, Chandriani S, Whitfield ML, Cole MD. A conserved Myc protein domain, MBIV, regulates DNA binding, apoptosis, transformation, and G2 arrest. Molecular and cellular biology. 2006;26(11):4226-39.

20. Blackwell TK, Kretzner L, Blackwood EM, Eisenman RN, Weintraub H. Sequence-specific DNA binding by the c-Myc protein. Science. 1990;250(4984):1149-51.

21. Blackwood EM, Eisenman RN. Max: a helix-loop-helix zipper protein that forms a sequence-specific DNA-binding complex with Myc. Science. 1991;251(4998):1211-7.

22. Waters CM, Littlewood TD, Hancock DC, Moore JP, Evan GI. c-myc protein expression in untransformed fibroblasts. Oncogene. 1991;6(5):797-805.

23. Lin CY, Loven J, Rahl PB, Paranal RM, Burge CB, Bradner JE, et al. Transcriptional amplification in tumor cells with elevated c-Myc. Cell. 2012;151(1):56-67.

24. Kelly K, Cochran BH, Stiles CD, Leder P. Cell-specific regulation of the c-myc gene by lymphocyte mitogens and platelet-derived growth factor. Cell. 1983;35(3 Pt 2):603-10.

25. Spencer CA, Groudine M. Control of c-myc regulation in normal and neoplastic cells. Advances in cancer research. 1991;56:1-48.

26. Culjkovic B, Topisirovic I, Skrabanek L, Ruiz-Gutierrez M, Borden KL. eIF4E is a central node of an RNA regulon that governs cellular proliferation. The Journal of cell biology. 2006;175(3):415-26.

27. Dani C, Blanchard JM, Piechaczyk M, El Sabouty S, Marty L, Jeanteur P. Extreme instability of myc mRNA in normal and transformed human cells. Proceedings of the National Academy of Sciences of the United States of America. 1984;81(22):7046-50.

28. Hann SR, Eisenman RN. Proteins encoded by the human c-myc oncogene: differential expression in neoplastic cells. Molecular and cellular biology. 1984;4(11):2486-97.

29. Vervoorts J, Luscher-Firzlaff J, Luscher B. The ins and outs of MYC regulation by posttranslational mechanisms. The Journal of biological chemistry. 2006;281(46):34725-9.

30. Farrell AS, Sears RC. MYC degradation. Cold Spring Harbor perspectives in medicine. 2014;4(3).

31. Land H, Parada LF, Weinberg RA. Cellular oncogenes and multistep carcinogenesis. Science. 1983;222(4625):771-8.

32. Arvanitis C, Felsher DW. Conditional transgenic models define how MYC initiates and maintains tumorigenesis. Seminars in cancer biology. 2006;16(4):313-7.

33. Vita M, Henriksson M. The Myc oncoprotein as a therapeutic target for human cancer. Seminars in cancer biology. 2006;16(4):318-30.

34. He TC, Sparks AB, Rago C, Hermeking H, Zawel L, da Costa LT, et al. Identification of c-MYC as a target of the APC pathway. Science. 1998;281(5382):1509-12.

35. Dave SS, Fu K, Wright GW, Lam LT, Kluin P, Boerma EJ, et al. Molecular diagnosis of Burkitt's lymphoma. The New England journal of medicine. 2006;354(23):2431-42.

36. Taub R, Kirsch I, Morton C, Lenoir G, Swan D, Tronick S, et al. Translocation of the c-myc gene into the immunoglobulin heavy chain locus in human Burkitt lymphoma and murine plasmacytoma cells. Proceedings of the National Academy of Sciences of the United States of America. 1982;79(24):7837-41.

37. Dalla-Favera R, Bregni M, Erikson J, Patterson D, Gallo RC, Croce CM. Human c-myc onc gene is located on the region of chromosome 8 that is translocated in Burkitt lymphoma cells. Proceedings of the National Academy of Sciences of the United States of America. 1982;79(24):7824-7.

38. Bhatia K, Spangler G, Gaidano G, Hamdy N, Dalla-Favera R, Magrath I. Mutations in the coding region of c-myc occur frequently in acquired immunodeficiency syndrome-associated lymphomas. Blood. 1994;84(3):883-8.

39. Clark HM, Yano T, Otsuki T, Jaffe ES, Shibata D, Raffeld M. Mutations in the coding region of c-MYC in AIDS-associated and other aggressive lymphomas. Cancer research. 1994;54(13):3383-6.

40. Love C, Sun Z, Jima D, Li G, Zhang J, Miles R, et al. The genetic landscape of mutations in Burkitt lymphoma. Nature genetics. 2012;44(12):1321-5.

41. Salghetti SE, Kim SY, Tansey WP. Destruction of Myc by ubiquitin-mediated proteolysis: cancer-associated and transforming mutations stabilize Myc. The EMBO journal. 1999;18(3):717-26.

42. Tu WB, Helander S, Pilstal R, Hickman KA, Lourenco C, Jurisica I, et al. Myc and its interactors take shape. Biochimica et biophysica acta. 2015;1849(5):469-83.

43. Arnold HK, Zhang X, Daniel CJ, Tibbitts D, Escamilla-Powers J, Farrell A, et al. The Axin1 scaffold protein promotes formation of a degradation complex for c-Myc. The EMBO journal. 2009;28(5):500-12.

44. Wang Q, Zhang H, Kajino K, Greene MI. BRCA1 binds c-Myc and inhibits its transcriptional and transforming activity in cells. Oncogene. 1998;17(15):1939-48.

45. Popov N, Schulein C, Jaenicke LA, Eilers M. Ubiquitylation of the amino terminus of Myc by SCF(beta-TrCP) antagonizes SCF(Fbw7)-mediated turnover. Nature cell biology. 2010;12(10):973-81.

46. Cheng AS, Jin VX, Fan M, Smith LT, Liyanarachchi S, Yan PS, et al. Combinatorial analysis of transcription factor partners reveals recruitment of c-MYC to estrogen receptor-alpha responsive promoters. Molecular cell. 2006;21(3):393-404.

47. Sears R, Nuckolls F, Haura E, Taya Y, Tamai K, Nevins JR. Multiple Ras-dependent phosphorylation pathways regulate Myc protein stability. Genes & development. 2000;14(19):2501-14.

48. Welcker M, Orian A, Jin J, Grim JE, Harper JW, Eisenman RN, et al. The Fbw7 tumor suppressor regulates glycogen synthase kinase 3 phosphorylation-dependent c-Myc protein degradation. Proceedings of the National Academy of Sciences of the United States of America. 2004;101(24):9085-90.

49. Yada M, Hatakeyama S, Kamura T, Nishiyama M, Tsunematsu R, Imaki H, et al. Phosphorylation-dependent degradation of c-Myc is mediated by the F-box protein Fbw7. The EMBO journal. 2004;23(10):2116-25.

50. Chandramohan V, Mineva ND, Burke B, Jeay S, Wu M, Shen J, et al. c-Myc represses FOXO3a-mediated transcription of the gene encoding the p27(Kip1) cyclin dependent kinase inhibitor. Journal of cellular biochemistry. 2008;104(6):2091-106.

51. McMahon SB, Wood MA, Cole MD. The essential cofactor TRRAP recruits the histone acetyltransferase hGCN5 to c-Myc. Molecular and cellular biology. 2000;20(2):556-62.

52. Gregory MA, Qi Y, Hann SR. Phosphorylation by glycogen synthase kinase-3 controls c-myc proteolysis and subnuclear localization. The Journal of biological chemistry. 2003;278(51):51606-12.

53. Lutterbach B, Hann SR. Hierarchical phosphorylation at N-terminal transformation-sensitive sites in c-Myc protein is regulated by mitogens and in mitosis. Molecular and cellular biology. 1994;14(8):5510-22.

54. Koshiji M, Kageyama Y, Pete EA, Horikawa I, Barrett JC, Huang LE. HIF-1alpha induces cell cycle arrest by functionally counteracting Myc. The EMBO journal. 2004;23(9):1949-56.

55. Staller P, Peukert K, Kiermaier A, Seoane J, Lukas J, Karsunky H, et al. Repression of p15INK4b expression by Myc through association with Miz-1. Nature cell biology. 2001;3(4):392-9.

56. Gargano B, Amente S, Majello B, Lania L. P-TEFb is a crucial co-factor for Myc transactivation. Cell cycle. 2007;6(16):2031-7.

57. Kanazawa S, Soucek L, Evan G, Okamoto T, Peterlin BM. c-Myc recruits P-TEFb for transcription, cellular proliferation and apoptosis. Oncogene. 2003;22(36):5707-11.

58. Yeh E, Cunningham M, Arnold H, Chasse D, Monteith T, Ivaldi G, et al. A signalling pathway controlling c-Myc degradation that impacts oncogenic transformation of human cells. Nature cell biology. 2004;6(4):308-18.

59. Dai MS, Arnold H, Sun XX, Sears R, Lu H. Inhibition of c-Myc activity by ribosomal protein L11. The EMBO journal. 2007;26(14):3332-45.

60. Kim SY, Herbst A, Tworkowski KA, Salghetti SE, Tansey WP. Skp2 regulates Myc protein stability and activity. Molecular cell. 2003;11(5):1177-88.

61. von der Lehr N, Johansson S, Wu S, Bahram F, Castell A, Cetinkaya C, et al. The F-box protein Skp2 participates in c-Myc proteosomal degradation and acts as a cofactor for c-Myc-regulated transcription. Molecular cell. 2003;11(5):1189-200.

62. Feng XH, Liang YY, Liang M, Zhai W, Lin X. Direct interaction of c-Myc with Smad2 and Smad3 to inhibit TGF-beta-mediated induction of the CDK inhibitor p15(Ink4B). Molecular cell. 2002;9(1):133-43.

63. Pal S, Yun R, Datta A, Lacomis L, Erdjument-Bromage H, Kumar J, et al. mSin3A/histone deacetylase 2- and PRMT5-containing Brg1 complex is involved in transcriptional repression of the Myc target gene cad. Molecular and cellular biology. 2003;23(21):7475-87.

64. McMahon SB, Van Buskirk HA, Dugan KA, Copeland TD, Cole MD. The novel ATM-related protein TRRAP is an essential cofactor for the c-Myc and E2F oncoproteins. Cell. 1998;94(3):363-74.

65. Liu X, Tesfai J, Evrard YA, Dent SY, Martinez E. c-Myc transformation domain recruits the human STAGA complex and requires TRRAP and GCN5 acetylase activity for transcription activation. The Journal of biological chemistry. 2003;278(22):20405-12.

66. Hwang IY, Roe JS, Seol JH, Kim HR, Cho EJ, Youn HD. pVHL-mediated transcriptional repression of c-Myc by recruitment of histone deacetylases. Molecules and cells. 2012;33(2):195-201.

67. Luscher B, Larsson LG. The basic region/helix-loop-helix/leucine zipper domain of Myc proto-oncoproteins: function and regulation. Oncogene. 1999;18(19):2955-66.

68. Guccione E, Martinato F, Finocchiaro G, Luzi L, Tizzoni L, Dall' Olio V, et al. Myc-binding-site recognition in the human genome is determined by chromatin context. Nature cell biology. 2006;8(7):764-70.

69. James L, Eisenman RN. Myc and Mad bHLHZ domains possess identical DNA-binding specificities but only partially overlapping functions in vivo. Proceedings of the National Academy of Sciences of the United States of America. 2002;99(16):10429-34.

70. Eilers M, Eisenman RN. Myc's broad reach. Genes & development. 2008;22(20):2755-66.

71. Nie Z, Hu G, Wei G, Cui K, Yamane A, Resch W, et al. c-Myc is a universal amplifier of expressed genes in lymphocytes and embryonic stem cells. Cell. 2012;151(1):68-79.

72. Thomas LR, Tansey WP. Proteolytic control of the oncoprotein transcription factor Myc. Advances in cancer research. 2011;110:77-106.

73. Small GW, Chou TY, Dang CV, Orlowski RZ. Evidence for involvement of calpain in c-Myc proteolysis in vivo. Archives of biochemistry and biophysics. 2002;400(2):151-61.

74. Conacci-Sorrell M, Ngouenet C, Eisenman RN. Myc-nick: a cytoplasmic cleavage product of Myc that promotes alpha-tubulin acetylation and cell differentiation. Cell. 2010;142(3):480-93.

75. Schrader EK, Harstad KG, Matouschek A. Targeting proteins for degradation. Nature chemical biology. 2009;5(11):815-22.

76. Herbst A, Salghetti SE, Kim SY, Tansey WP. Multiple cell-type-specific elements regulate Myc protein stability. Oncogene. 2004;23(21):3863-71.

77. Gregory MA, Hann SR. c-Myc proteolysis by the ubiquitin-proteasome pathway: stabilization of c-Myc in Burkitt's lymphoma cells. Molecular and cellular biology. 2000;20(7):2423-35.

78. Farrell AS, Pelz C, Wang X, Daniel CJ, Wang Z, Su Y, et al. Pin1 regulates the dynamics of c-Myc DNA binding to facilitate target gene regulation and oncogenesis. Molecular and cellular biology. 2013;33(15):2930-49.

79. Adhikary S, Marinoni F, Hock A, Hulleman E, Popov N, Beier R, et al. The ubiquitin ligase HectH9 regulates transcriptional activation by Myc and is essential for tumor cell proliferation. Cell. 2005;123(3):409-21.

80. Schwamborn JC, Berezikov E, Knoblich JA. The TRIM-NHL protein TRIM32 activates microRNAs and prevents self-renewal in mouse neural progenitors. Cell. 2009;136(5):913-25.

81. Koch HB, Zhang R, Verdoodt B, Bailey A, Zhang CD, Yates JR, 3rd, et al. Large-scale identification of c-MYC-associated proteins using a combined TAP/MudPIT approach. Cell cycle. 2007;6(2):205-17.

82. Choi SH, Wright JB, Gerber SA, Cole MD. Myc protein is stabilized by suppression of a novel E3 ligase complex in cancer cells. Genes & development. 2010;24(12):1236-41.

83. Paul I, Ahmed SF, Bhowmik A, Deb S, Ghosh MK. The ubiquitin ligase CHIP regulates c-Myc stability and transcriptional activity. Oncogene. 2013;32(10):1284-95.

84. Moberg KH, Mukherjee A, Veraksa A, Artavanis-Tsakonas S, Hariharan IK. The Drosophila F box protein archipelago regulates dMyc protein levels in vivo. Current biology : CB. 2004;14(11):965-74.

85. Popov N, Wanzel M, Madiredjo M, Zhang D, Beijersbergen R, Bernards R, et al. The ubiquitin-specific protease USP28 is required for MYC stability. Nature cell biology. 2007;9(7):765-74.

86. Vervoorts J, Luscher-Firzlaff JM, Rottmann S, Lilischkis R, Walsemann G, Dohmann K, et al. Stimulation of c-MYC transcriptional activity and acetylation by recruitment of the cofactor CBP. EMBO reports. 2003;4(5):484-90.

87. Zhang K, Faiola F, Martinez E. Six lysine residues on c-Myc are direct substrates for acetylation by p300. Biochemical and biophysical research communications. 2005;336(1):274-80.

88. Patel JH, Du Y, Ard PG, Phillips C, Carella B, Chen CJ, et al. The c-MYC oncoprotein is a substrate of the acetyltransferases hGCN5/PCAF and TIP60. Molecular and cellular biology. 2004;24(24):10826-34.

89. Soucek L, Evan G. Myc-Is this the oncogene from Hell? Cancer cell. 2002;1(5):406-8.

90. Karn J, Watson JV, Lowe AD, Green SM, Vedeckis W. Regulation of cell cycle duration by c-myc levels. Oncogene. 1989;4(6):773-87.

91. Kaczmarek L, Hyland JK, Watt R, Rosenberg M, Baserga R. Microinjected c-myc as a competence factor. Science. 1985;228(4705):1313-5.

92. Oster SK, Ho CS, Soucie EL, Penn LZ. The myc oncogene: MarvelouslY Complex. Advances in cancer research. 2002;84:81-154.

93. Evan GI, Wyllie AH, Gilbert CS, Littlewood TD, Land H, Brooks M, et al. Induction of apoptosis in fibroblasts by c-myc protein. Cell. 1992;69(1):119-28.

94. Eischen CM, Packham G, Nip J, Fee BE, Hiebert SW, Zambetti GP, et al. Bcl-2 is an apoptotic target suppressed by both c-Myc and E2F-1. Oncogene. 2001;20(48):6983-93.

95. Egle A, Harris AW, Bouillet P, Cory S. Bim is a suppressor of Myc-induced mouse B cell leukemia. Proceedings of the National Academy of Sciences of the United States of America. 2004;101(16):6164-9.

96. Leone G, Sears R, Huang E, Rempel R, Nuckolls F, Park CH, et al. Myc requires distinct E2F activities to induce S phase and apoptosis. Molecular cell. 2001;8(1):105-13.

97. Hermeking H, Eick D. Mediation of c-Myc-induced apoptosis by p53. Science. 1994;265(5181):2091-3.

98. Schmidt EV. The role of c-myc in cellular growth control. Oncogene. 1999;18(19):2988-96.

99. Shim H, Chun YS, Lewis BC, Dang CV. A unique glucose-dependent apoptotic pathway induced by c-Myc. Proceedings of the National Academy of Sciences of the United States of America. 1998;95(4):1511-6.

100. Wise DR, DeBerardinis RJ, Mancuso A, Sayed N, Zhang XY, Pfeiffer HK, et al. Myc regulates a transcriptional program that stimulates mitochondrial glutaminolysis and leads to glutamine

addiction. Proceedings of the National Academy of Sciences of the United States of America. 2008;105(48):18782-7.

101. Dang CV. MYC, metabolism, cell growth, and tumorigenesis. Cold Spring Harbor perspectives in medicine. 2013;3(8).

102. Vafa O, Wade M, Kern S, Beeche M, Pandita TK, Hampton GM, et al. c-Myc can induce DNA damage, increase reactive oxygen species, and mitigate p53 function: a mechanism for oncogene-induced genetic instability. Molecular cell. 2002;9(5):1031-44.

103. Baudino TA, McKay C, Pendeville-Samain H, Nilsson JA, Maclean KH, White EL, et al. c-Myc is essential for vasculogenesis and angiogenesis during development and tumor progression. Genes & development. 2002;16(19):2530-43.

104. Smith AP, Verrecchia A, Faga G, Doni M, Perna D, Martinato F, et al. A positive role for Myc in TGFbeta-induced Snail transcription and epithelial-to-mesenchymal transition. Oncogene. 2009;28(3):422-30.

105. Soucek L, Whitfield J, Martins CP, Finch AJ, Murphy DJ, Sodir NM, et al. Modelling Myc inhibition as a cancer therapy. Nature. 2008;455(7213):679-83.

106. Soucek L, Whitfield JR, Sodir NM, Masso-Valles D, Serrano E, Karnezis AN, et al. Inhibition of Myc family proteins eradicates KRas-driven lung cancer in mice. Genes & development. 2013;27(5):504-13.

107. Fletcher S, Prochownik EV. Small-molecule inhibitors of the Myc oncoprotein. Biochimica et biophysica acta. 2015;1849(5):525-43.

108. Soucek L, Jucker R, Panacchia L, Ricordy R, Tato F, Nasi S. Omomyc, a potential Myc dominant negative, enhances Myc-induced apoptosis. Cancer research. 2002;62(12):3507-10.

109. Follis AV, Hammoudeh DI, Wang H, Prochownik EV, Metallo SJ. Structural rationale for the coupled binding and unfolding of the c-Myc oncoprotein by small molecules. Chemistry & biology. 2008;15(11):1149-55.

110. Follis AV, Hammoudeh DI, Daab AT, Metallo SJ. Small-molecule perturbation of competing interactions between c-Myc and Max. Bioorganic & medicinal chemistry letters. 2009;19(3):807-10.

111. Prochownik EV, Vogt PK. Therapeutic Targeting of Myc. Genes & cancer. 2010;1(6):650-9.

112. Kouzarides T. Histone methylation in transcriptional control. Current opinion in genetics & development. 2002;12(2):198-209.

113. Kim SM, Kee HJ, Eom GH, Choe NW, Kim JY, Kim YS, et al. Characterization of a novel WHSC1-associated SET domain protein with H3K4 and H3K27 methyltransferase activity. Biochemical and biophysical research communications. 2006;345(1):318-23.

114. Morishita M, di Luccio E. Cancers and the NSD family of histone lysine methyltransferases. Biochimica et biophysica acta. 2011;1816(2):158-63.

115. Lucio-Eterovic AK, Carpenter PB. An open and shut case for the role of NSD proteins as oncogenes. Transcription. 2011;2(4):158-61.

116. Stec I, Nagl SB, van Ommen GJ, den Dunnen JT. The PWWP domain: a potential protein-protein interaction domain in nuclear proteins influencing differentiation? FEBS letters. 2000;473(1):1-5.

117. Stec I, van Ommen GJ, den Dunnen JT. WHSC1L1, on human chromosome 8p11.2, closely resembles WHSC1 and maps to a duplicated region shared with 4p16.3. Genomics. 2001;76(1-3):5-8.

118. Angrand PO, Apiou F, Stewart AF, Dutrillaux B, Losson R, Chambon P. NSD3, a new SET domain-containing gene, maps to 8p12 and is amplified in human breast cancer cell lines. Genomics. 2001;74(1):79-88.

119. Wang Y, Reddy B, Thompson J, Wang H, Noma K, Yates JR, 3rd, et al. Regulation of Set9-mediated H4K20 methylation by a PWWP domain protein. Molecular cell. 2009;33(4):428-37.

120. Maurer-Stroh S, Dickens NJ, Hughes-Davies L, Kouzarides T, Eisenhaber F, Ponting CP. The Tudor domain 'Royal Family': Tudor, plant Agenet, Chromo, PWWP and MBT domains. Trends in biochemical sciences. 2003;28(2):69-74.

121. Rona GB, Almeida DSG, Pinheiro AS, Eleutherio ECA. The PWWP domain of the human oncogene WHSC1L1/NSD3 induces a metabolic shift toward fermentation. Oncotarget. 2017;8(33):54068-81.

122. Morishita M, Mevius D, di Luccio E. In vitro histone lysine methylation by NSD1, NSD2/MMSET/WHSC1 and NSD3/WHSC1L. BMC structural biology. 2014;14:25.

123. Allali-Hassani A, Kuznetsova E, Hajian T, Wu H, Dombrovski L, Li Y, et al. A Basic Post-SET Extension of NSDs Is Essential for Nucleosome Binding In Vitro. Journal of biomolecular screening. 2014;19(6):928-35.

124. Li Y, Trojer P, Xu CF, Cheung P, Kuo A, Drury WJ, 3rd, et al. The target of the NSD family of histone lysine methyltransferases depends on the nature of the substrate. The Journal of biological chemistry. 2009;284(49):34283-95.

125. Yang ZQ, Liu G, Bollig-Fischer A, Giroux CN, Ethier SP. Transforming properties of 8p11-12 amplified genes in human breast cancer. Cancer research. 2010;70(21):8487-97.

126. Han X, Piao L, Zhuang Q, Yuan X, Liu Z, He X. The role of histone lysine methyltransferase NSD3 in cancer. OncoTargets and therapy. 2018;11:3847-52.

127. Mann KM, Ward JM, Yew CC, Kovochich A, Dawson DW, Black MA, et al. Sleeping Beauty mutagenesis reveals cooperating mutations and pathways in pancreatic adenocarcinoma. Proceedings of the National Academy of Sciences of the United States of America. 2012;109(16):5934-41.

128. Tonon G, Wong KK, Maulik G, Brennan C, Feng B, Zhang Y, et al. High-resolution genomic profiles of human lung cancer. Proceedings of the National Academy of Sciences of the United States of America. 2005;102(27):9625-30.

129. Adelaide J, Chaffanet M, Imbert A, Allione F, Geneix J, Popovici C, et al. Chromosome region 8p11-p21: refined mapping and molecular alterations in breast cancer. Genes, chromosomes & cancer. 1998;22(3):186-99.

130. Garcia MJ, Pole JC, Chin SF, Teschendorff A, Naderi A, Ozdag H, et al. A 1 Mb minimal amplicon at 8p11-12 in breast cancer identifies new candidate oncogenes. Oncogene. 2005;24(33):5235-45.

131. Gelsi-Boyer V, Orsetti B, Cervera N, Finetti P, Sircoulomb F, Rouge C, et al. Comprehensive profiling of 8p11-12 amplification in breast cancer. Molecular cancer research : MCR. 2005;3(12):655-67.

132. Mahmood SF, Gruel N, Nicolle R, Chapeaublanc E, Delattre O, Radvanyi F, et al. PPAPDC1B and WHSC1L1 are common drivers of the 8p11-12 amplicon, not only in breast tumors but also in pancreatic adenocarcinomas and lung tumors. The American journal of pathology. 2013;183(5):1634-44.

133. Bernard-Pierrot I, Gruel N, Stransky N, Vincent-Salomon A, Reyal F, Raynal V, et al. Characterization of the recurrent 8p11-12 amplicon identifies PPAPDC1B, a phosphatase protein, as a new therapeutic target in breast cancer. Cancer research. 2008;68(17):7165-75.

134. Rosati R, La Starza R, Veronese A, Aventin A, Schwienbacher C, Vallespi T, et al. NUP98 is fused to the NSD3 gene in acute myeloid leukemia associated with t(8;11)(p11.2;p15). Blood. 2002;99(10):3857-60.

135. French CA, Rahman S, Walsh EM, Kuhnle S, Grayson AR, Lemieux ME, et al. NSD3-NUT fusion oncoprotein in NUT midline carcinoma: implications for a novel oncogenic mechanism. Cancer discovery. 2014;4(8):928-41.

136. Suzuki S, Kurabe N, Minato H, Ohkubo A, Ohnishi I, Tanioka F, et al. A rare Japanese case with a NUT midline carcinoma in the nasal cavity: a case report with immunohistochemical and genetic analyses. Pathology, research and practice. 2014;210(6):383-8.

137. Suzuki S, Kurabe N, Ohnishi I, Yasuda K, Aoshima Y, Naito M, et al. NSD3-NUT-expressing midline carcinoma of the lung: first characterization of primary cancer tissue. Pathology, research and practice. 2015;211(5):404-8.

138. Stevens TM, Morlote D, Xiu J, Swensen J, Brandwein-Weber M, Miettinen MM, et al. NUTM1-rearranged neoplasia: a multi-institution experience yields novel fusion partners and expands the histologic spectrum. Modern pathology : an official journal of the United States and Canadian Academy of Pathology, Inc. 2019.

139. Fang R, Barbera AJ, Xu Y, Rutenberg M, Leonor T, Bi Q, et al. Human LSD2/KDM1b/AOF1 regulates gene transcription by modulating intragenic H3K4me2 methylation. Molecular cell. 2010;39(2):222-33.

140. Rahman S, Sowa ME, Ottinger M, Smith JA, Shi Y, Harper JW, et al. The Brd4 extraterminal domain confers transcription activation independent of pTEFb by recruiting multiple proteins, including NSD3. Molecular and cellular biology. 2011;31(13):2641-52.

141. Shen C, Ipsaro JJ, Shi J, Milazzo JP, Wang E, Roe JS, et al. NSD3-Short Is an Adaptor Protein that Couples BRD4 to the CHD8 Chromatin Remodeler. Molecular cell. 2015;60(6):847-59.

142. Saloura V, Vougiouklakis T, Zewde M, Deng X, Kiyotani K, Park JH, et al. WHSC1L1-mediated EGFR mono-methylation enhances the cytoplasmic and nuclear oncogenic activity of EGFR in head and neck cancer. Scientific reports. 2017;7:40664.

143. Wang C, Wang Q, Xu X, Xie B, Zhao Y, Li N, et al. The methyltransferase NSD3 promotes antiviral innate immunity via direct lysine methylation of IRF3. The Journal of experimental medicine. 2017;214(12):3597-610.

144. Turner-Ivey B, Smith EL, Rutkovsky AC, Spruill LS, Mills JN, Ethier SP. Development of mammary hyperplasia, dysplasia, and invasive ductal carcinoma in transgenic mice expressing the 8p11 amplicon oncogene NSD3. Breast cancer research and treatment. 2017;164(2):349-58.

145. Guffanti A, Iacono M, Pelucchi P, Kim N, Solda G, Croft LJ, et al. A transcriptional sketch of a primary human breast cancer by 454 deep sequencing. BMC genomics. 2009;10:163.

146. Liu Z, Piao L, Zhuang M, Qiu X, Xu X, Zhang D, et al. Silencing of histone methyltransferase NSD3 reduces cell viability in osteosarcoma with induction of apoptosis. Oncology reports. 2017;38(5):2796-802.

147. Saloura V, Vougiouklakis T, Zewde M, Kiyotani K, Park JH, Gao G, et al. WHSC1L1 drives cell cycle progression through transcriptional regulation of CDC6 and CDK2 in squamous cell carcinoma of the head and neck. Oncotarget. 2016;7(27):42527-38.

148. Kang D, Cho HS, Toyokawa G, Kogure M, Yamane Y, Iwai Y, et al. The histone methyltransferase Wolf-Hirschhorn syndrome candidate 1-like 1 (WHSC1L1) is involved in human carcinogenesis. Genes, chromosomes & cancer. 2013;52(2):126-39.

149. Ferrell CM, Dorsam ST, Ohta H, Humphries RK, Derynck MK, Haqq C, et al. Activation of stem-cell specific genes by HOXA9 and HOXA10 homeodomain proteins in CD34+ human cord blood cells. Stem cells. 2005;23(5):644-55.

150. Zhou Z, Thomsen R, Kahns S, Nielsen AL. The NSD3L histone methyltransferase regulates cell cycle and cell invasion in breast cancer cells. Biochemical and biophysical research communications. 2010;398(3):565-70.

151. Kim SM, Kee HJ, Choe N, Kim JY, Kook H, Kook H, et al. The histone methyltransferase activity of WHISTLE is important for the induction of apoptosis and HDAC1-mediated transcriptional repression. Experimental cell research. 2007;313(5):975-83.

152. Hunter T. Signaling--2000 and beyond. Cell. 2000;100(1):113-27.

153. Huttlin EL, Ting L, Bruckner RJ, Gebreab F, Gygi MP, Szpyt J, et al. The BioPlex Network: A Systematic Exploration of the Human Interactome. Cell. 2015;162(2):425-40.

154. Rolland T, Tasan M, Charloteaux B, Pevzner SJ, Zhong Q, Sahni N, et al. A proteome-scale map of the human interactome network. Cell. 2014;159(5):1212-26.

155. Rual JF, Venkatesan K, Hao T, Hirozane-Kishikawa T, Dricot A, Li N, et al. Towards a proteome-scale map of the human protein-protein interaction network. Nature. 2005;437(7062):1173-8.

156. Chatr-Aryamontri A, Breitkreutz BJ, Oughtred R, Boucher L, Heinicke S, Chen D, et al. The BioGRID interaction database: 2015 update. Nucleic acids research. 2015;43(Database issue):D470-8.

157. Warde-Farley D, Donaldson SL, Comes O, Zuberi K, Badrawi R, Chao P, et al. The GeneMANIA prediction server: biological network integration for gene prioritization and predicting gene function. Nucleic acids research. 2010;38(Web Server issue):W214-20.

158. Woods NT, Mesquita RD, Sweet M, Carvalho MA, Li X, Liu Y, et al. Charting the landscape of tandem BRCT domain-mediated protein interactions. Science signaling. 2012;5(242):rs6.

159. Kandoth C, McLellan MD, Vandin F, Ye K, Niu B, Lu C, et al. Mutational landscape and significance across 12 major cancer types. Nature. 2013;502(7471):333-9.

160. Govindan R, Ding L, Griffith M, Subramanian J, Dees ND, Kanchi KL, et al. Genomic landscape of non-small cell lung cancer in smokers and never-smokers. Cell. 2012;150(6):1121-34.

161. Imielinski M, Berger AH, Hammerman PS, Hernandez B, Pugh TJ, Hodis E, et al. Mapping the hallmarks of lung adenocarcinoma with massively parallel sequencing. Cell. 2012;150(6):1107-20.

162. Barabasi AL, Gulbahce N, Loscalzo J. Network medicine: a network-based approach to human disease. Nature reviews Genetics. 2011;12(1):56-68.

163. Pinero J, Berenstein A, Gonzalez-Perez A, Chernomoretz A, Furlong LI. Uncovering disease mechanisms through network biology in the era of Next Generation Sequencing. Scientific reports. 2016;6:24570.

164. Du Y, Havel J. Chemical Genomics. 2012.

165. Li S, Jiang C, Pan J, Wang X, Jin J, Zhao L, et al. Regulation of c-Myc protein stability by proteasome activator REGgamma. Cell death and differentiation. 2015;22(6):1000-11.

166. Yin X, Giap C, Lazo JS, Prochownik EV. Low molecular weight inhibitors of Myc-Max interaction and function. Oncogene. 2003;22(40):6151-9.

167. Brambilla E, Gazdar A. Pathogenesis of lung cancer signalling pathways: roadmap for therapies. The European respiratory journal. 2009;33(6):1485-97.

168. Collisson EA, Campbell JD, Brooks AN, Berger AH, Lee W, Chmielecki J, et al. Comprehensive molecular profiling of lung adenocarcinoma. Nature. 2014;511(7511):543-50.

169. Lawrence MS, Stojanov P, Mermel CH, Robinson JT, Garraway LA, Golub TR, et al. Discovery and saturation analysis of cancer genes across 21 tumour types. Nature. 2014;505(7484):495-501.

170. Ivanov AA, Revennaugh B, Rusnak L, Gonzalez-Pecchi V, Mo X, Johns MA, et al. The OncoPPi Portal: an integrative resource to explore and prioritize protein-protein interactions for cancer target discovery. Bioinformatics. 2018;34(7):1183-91.

171. Conacci-Sorrell M, McFerrin L, Eisenman RN. An overview of MYC and its interactome. Cold Spring Harbor perspectives in medicine. 2014;4(1):a014357.

172. Ciriello G, Cerami E, Sander C, Schultz N. Mutual exclusivity analysis identifies oncogenic network modules. Genome research. 2012;22(2):398-406.

173. Zhou B, Hu J, Xu F, Chen Z, Bai L, Fernandez-Salas E, et al. Discovery of a Small-Molecule Degrader of Bromodomain and Extra-Terminal (BET) Proteins with Picomolar Cellular Potencies and Capable of Achieving Tumor Regression. Journal of medicinal chemistry. 2018;61(2):462-81.

174. Huang X, Dixit VM. Drugging the undruggables: exploring the ubiquitin system for drug development. Cell research. 2016;26(4):484-98.

175. Iritani BM, Eisenman RN. c-Myc enhances protein synthesis and cell size during B lymphocyte development. Proceedings of the National Academy of Sciences of the United States of America. 1999;96(23):13180-5.

176. Shim H, Lewis BC, Dolde C, Li Q, Wu CS, Chun YS, et al. Myc target genes in neoplastic transformation. Current topics in microbiology and immunology. 1997;224:181-90.

177. Hu S, Balakrishnan A, Bok RA, Anderton B, Larson PE, Nelson SJ, et al. 13C-pyruvate imaging reveals alterations in glycolysis that precede c-Myc-induced tumor formation and regression. Cell metabolism. 2011;14(1):131-42.

178. Amati B, Brooks MW, Levy N, Littlewood TD, Evan GI, Land H. Oncogenic activity of the c-Myc protein requires dimerization with Max. Cell. 1993;72(2):233-45.

179. Eisenman RN. Deconstructing myc. Genes & development. 2001;15(16):2023-30.

180. Liu L, Eisenman RN. Regulation of c-Myc Protein Abundance by a Protein Phosphatase 2A-Glycogen Synthase Kinase 3beta-Negative Feedback Pathway. Genes & cancer. 2012;3(1):23-36.

181. Mo XL, Luo Y, Ivanov AA, Su R, Havel JJ, Li Z, et al. Enabling systematic interrogation of protein-protein interactions in live cells with a versatile ultra-high-throughput biosensor platform. Journal of molecular cell biology. 2016;8(3):271-81.

182. Yeh CH, Bellon M, Nicot C. FBXW7: a critical tumor suppressor of human cancers. Molecular cancer. 2018;17(1):115.

183. Jung KY, Wang H, Teriete P, Yap JL, Chen L, Lanning ME, et al. Perturbation of the c-Myc-Max protein-protein interaction via synthetic alpha-helix mimetics. Journal of medicinal chemistry. 2015;58(7):3002-24.

184. Mo X, Qi Q, Ivanov AA, Niu Q, Luo Y, Havel J, et al. AKT1, LKB1, and YAP1 Revealed as MYC Interactors with NanoLuc-Based Protein-Fragment Complementation Assay. Molecular pharmacology. 2017;91(4):339-47.

185. Chakravorty D, Jana T, Das Mandal S, Seth A, Bhattacharya A, Saha S. MYCbase: a database of functional sites and biochemical properties of Myc in both normal and cancer cells. BMC bioinformatics. 2017;18(1):224.

186. Kato GJ, Barrett J, Villa-Garcia M, Dang CV. An amino-terminal c-myc domain required for neoplastic transformation activates transcription. Molecular and cellular biology. 1990;10(11):5914-20.

187. Kalkat M, Resetca D, Lourenco C, Chan PK, Wei Y, Shiah YJ, et al. MYC Protein Interactome Profiling Reveals Functionally Distinct Regions that Cooperate to Drive Tumorigenesis. Molecular cell. 2018.

188. Wu H, Zeng H, Lam R, Tempel W, Amaya MF, Xu C, et al. Structural and histone binding ability characterizations of human PWWP domains. PloS one. 2011;6(6):e18919.

189. Marcu KB. Regulation of expression of the c-myc proto-oncogene. BioEssays : news and reviews in molecular, cellular and developmental biology. 1987;6(1):28-32.

190. Adhikary S, Eilers M. Transcriptional regulation and transformation by Myc proteins. Nature reviews Molecular cell biology. 2005;6(8):635-45.

191. Salghetti SE, Muratani M, Wijnen H, Futcher B, Tansey WP. Functional overlap of sequences that activate transcription and signal ubiquitin-mediated proteolysis. Proceedings of the National Academy of Sciences of the United States of America. 2000;97(7):3118-23.

192. Vogelstein B, Kinzler KW. The multistep nature of cancer. Trends in genetics : TIG. 1993;9(4):138-41.

193. Tsai CJ, Ma B, Nussinov R. Protein-protein interaction networks: how can a hub protein bind so many different partners? Trends in biochemical sciences. 2009;34(12):594-600.

194. Liu C, Fang X, Ge Z, Jalink M, Kyo S, Bjorkholm M, et al. The telomerase reverse transcriptase (hTERT) gene is a direct target of the histone methyltransferase SMYD3. Cancer research. 2007;67(6):2626-31.

195. Secombe J, Eisenman RN. The function and regulation of the JARID1 family of histone H3 lysine 4 demethylases: the Myc connection. Cell cycle. 2007;6(11):1324-8.

196. Parris TZ, Kovacs A, Hajizadeh S, Nemes S, Semaan M, Levin M, et al. Frequent MYC coamplification and DNA hypomethylation of multiple genes on 8q in 8p11-p12-amplified breast carcinomas. Oncogenesis. 2014;3:e95.

197. Zhang Q, Zeng L, Shen C, Ju Y, Konuma T, Zhao C, et al. Structural Mechanism of Transcriptional Regulator NSD3 Recognition by the ET Domain of BRD4. Structure. 2016;24(7):1201-8.

198. Min DJ, Ezponda T, Kim MK, Will CM, Martinez-Garcia E, Popovic R, et al. MMSET stimulates myeloma cell growth through microRNA-mediated modulation of c-MYC. Leukemia. 2013;27(3):686-94.

199. Torres IO, Fujimori DG. Functional coupling between writers, erasers and readers of histone and DNA methylation. Current opinion in structural biology. 2015;35:68-75.

200. Du Y, Fu RW, Lou B, Zhao J, Qui M, Khuri FR, et al. A time-resolved fluorescence resonance energy transfer assay for high-throughput screening of 14-3-3 protein-protein interaction inhibitors. Assay and drug development technologies. 2013;11(6):367-81.

201. Xiong J, Pecchi VG, Qui M, Ivanov AA, Mo X, Niu Q, et al. Development of a Time-Resolved Fluorescence Resonance Energy Transfer Ultrahigh-Throughput Screening Assay for Targeting the NSD3 and MYC Interaction. Assay and drug development technologies. 2018;16(2):96-106.

Appendix

A.1 Connection between NSD3S/MYC/MAX

Introduction

MYC and MAX are transcription factors that belong to the bHLH-LZ family of proteins. We have already shown that NSD3S increases MYC transcriptional activity. For MYC to bind E-box promoters, it needs to heterodimerize with MAX protein. We sought to investigate the connection or collaboration between NSD3S, MYC, and MAX.

Results

We examined if NSD3S can also bind to MAX, and indeed by TR-FRET and GST pull-down, we could detect a positive signal for GST-MAX and Venus-flag-NSD3S (Figure A-1A and A-1B). Interestingly, when co-expressing the three proteins together and isolating GST-MYC, we can see that NSD3S binding to MYC is enhanced under the presence of MAX (Figure A-1C). Also, when isolating GST-MAX, the binding of NSD3S to MAX is increased when MYC is co-expressed together (Figure A-1D). On both assays, the binding between MYC and MAX seems to be similar with or without NSD3S (Figure A-1C and A1-D). Furthermore, the increase was seen between NSD3S/MYC with MAX, and NSD3S/MAX with MYC, tend to be dose-dependent (Figure A-1E and A-1F).

Conclusions

The data shown here, suggest a positive collaboration between MYC/MAX with NSD3S interactions. Additionally, results presented could explain the increase of MYC transcriptional activity by NSD3S, maybe forming a complex and bringing it to active transcription sites by the chromatin reader, the PWWP domain.

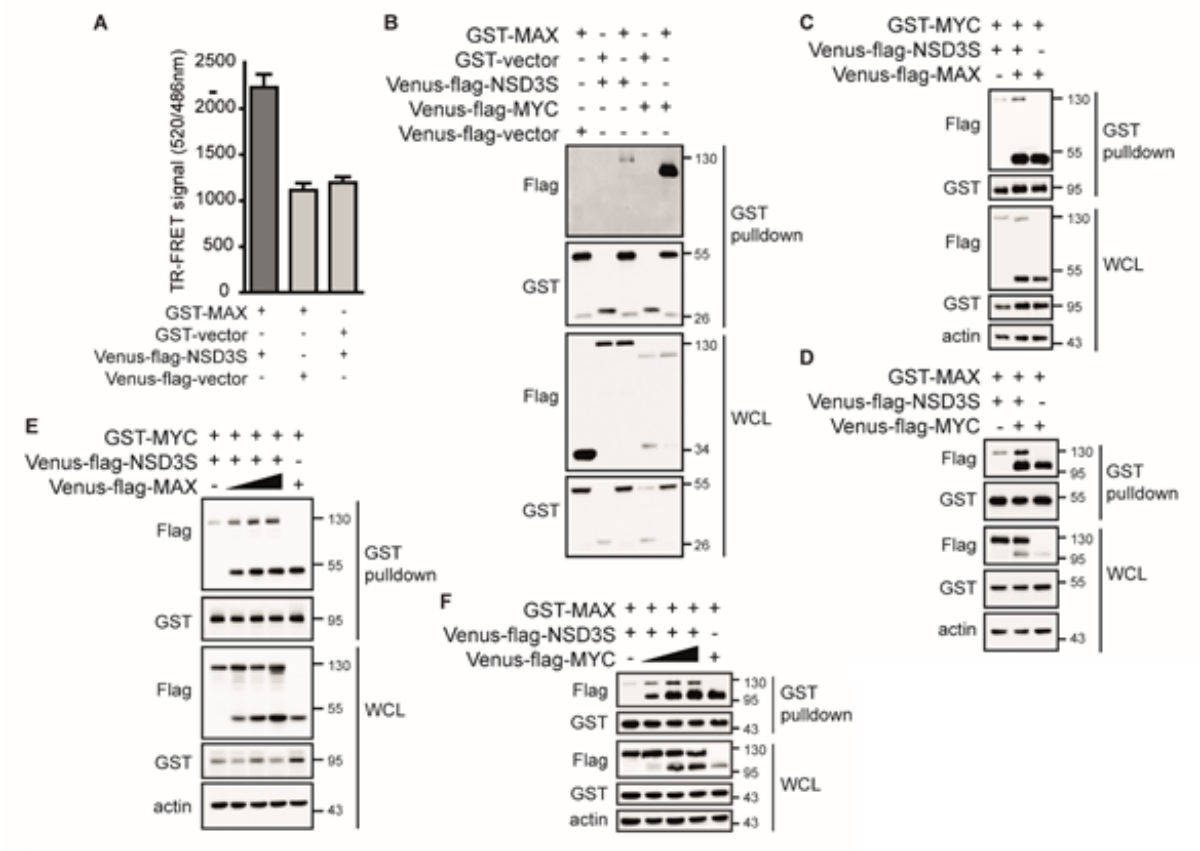
A
TR-FRET signal (520/486nm)
2500
2000
1500
1000
500
0
GST-MAX + + -
GST-vector - - +
Venus-flag-NSD3S + - +
Venus-flag-vector - + -
B
GST-MAX + - + - +
GST-vector - + - + -
Venus-flag-NSD3S - + + - -
Venus-flag-MYC - - - + +
Venus-flag-vector + - - - -
Flag
GST
GST pulldown
WCL
130
55
26
34
C
GST-MYC + + +
Venus-flag-NSD3S + + -
Venus-flag-MAX - + +
Flag
GST
actin
GST pulldown
WCL
130
95
55
43
D
GST-MAX + + +
Venus-flag-NSD3S + + -
Venus-flag-MYC - + +
E
GST-MYC + + + + +
Venus-flag-NSD3S + + + + -
Venus-flag-MAX - +
F
GST-MAX + + + + +
Venus-flag-NSD3S + + + + -
Venus-flag-MYC - +

Figure A-1. Examination of the interplay between NSD3S, MYC and MAX proteins.

A. TR-FRET assay performed using HEK293T cell lysate with overexpression of GST-MAX and Venus-flag-NSD3S or vector controls. Tb-conjugated anti-GST-antibodies were used to detect GST-MAX. The TR-FRET signal is expressed as the FRET ratio. Representative results of three independent experiments are shown. **B.** GST-pull down assay performed to isolate GST-MYC complexes in lysate from HEK293T cells with Venus-flag-NSD3S and/or -MAX overexpressed. The presence of NSD3S and/or MAX on the complex was evaluated with anti-flag antibody by western blot. GST antibody was used to control the amount of protein pull down. Expression in the whole cell lysate (WCL) was used as a control. **C.** GST pull-down assay performed as panel **B** to isolate GST-MAX with Venus-flag-NSD3S or-MYC overexpressed. **D.** GST pull-down same as panel **B**, only that increasing amounts of Venus-flag-MAX were overexpressed (different amount of plasmid transfected). **E.** GST pull-down with same conditions as panel **C**, only that increasing amounts of Venus-flag-MYC were overexpressed.

A.2 Ultra-high-throughput screening of small molecules for MYC/NSD3S PPI

Introduction

MYC is a well-validated oncoprotein. It has been extensively studied as a potential target for cancer therapy due to its demonstrated functions in processes that drive cell transformation. This dissertation revealed the novel interaction between MYC and NSD3S. NSD3S is sufficient to increase MYC transcriptional activity and stabilizes MYC protein levels, indicating a potential oncogenic role for MYC/NSD3S PPI.

Results

In collaboration with Jinglin Xiong and others in the lab, we published an assay paper of the development of a time-resolved fluorescence resonance energy transfer (TR-FRET) assay for ultra-high-throughput screening (uHTS) to find disruptors for MYC/NSD3S PPI. The experimental details on the development and optimization of the TR-FRET assay have been published in Assay and drug development technologies (2018) doi:10-1089. To validate the assay for screening in a 1,536-well uHTS format, a pilot screening was carried out using the Spectrum library containing 2,000 pharmacologically active compounds with a final compound concentration of 20 mM (201) (Figure A-2A). To validate the positive compounds identified in the pilot screening, we optimized a GST pull-down assay. Finally using sonication with lysis buffer of 0.25% Triton X-100 and adding 120 µl of lysate for the isolation of GST-MYC (Figure A-2B). After the optimization of the orthogonal GST pull-down assay, we tested 15 compounds that showed promising results in the pilot screening (Figure A-2C).

Conclusions

Together, the results show the development and validation of a cell lysate based TR-FRET assay for screening small molecule inhibitors for the MYC/NSD3S interaction.

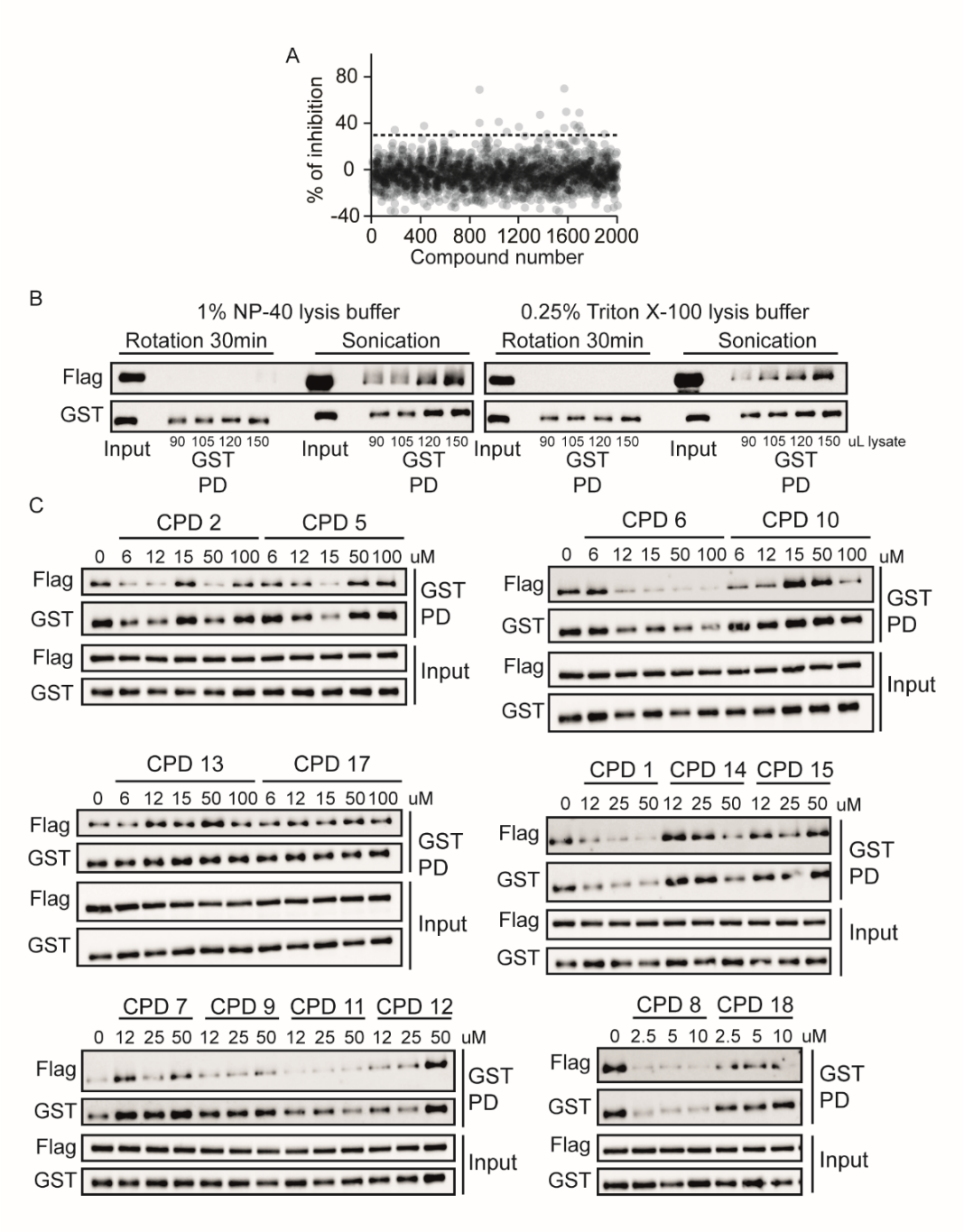
A
% of inhibition
80
40
0
-40
0 400 800 1200 1600 2000
Compound number
B
1% NP-40 lysis buffer
0.25% Triton X-100 lysis buffer
Rotation 30min
Sonication
Rotation 30min
Sonication
Flag
GST
Input
90 105 120 150
GST PD
Input
90 105 120 150
GST PD
Input
90 105 120 150
GST PD
Input
90 105 120 150
GST PD
uL lysate
C
CPD 2
CPD 5
0 6 12 15 50 100 6 12 15 50 100 uM
Flag
GST
Flag
GST
GST PD
Input
CPD 6
CPD 10
0 6 12 15 50 100 6 12 15 50 100 uM
Flag
GST
Flag
GST
GST PD
Input
CPD 13
CPD 17
0 6 12 15 50 100 6 12 15 50 100 uM
Flag
GST
Flag
GST
GST PD
Input
CPD 1
CPD 14
CPD 15
0 12 25 50 12 25 50 12 25 50 uM
Flag
GST
Flag
GST
GST PD
Input
CPD 7
CPD 9
CPD 11
CPD 12
0 12 25 50 12 25 50 12 25 50 12 25 50 uM
Flag
GST
Flag
GST
GST PD
Input
CPD 8
CPD 18
0 2.5 5 10 2.5 5 10 uM
Flag
GST
Flag
GST
GST PD
Input

Figure A-2. Development and validation of a uHTS for MYC/NSD3S PPI.

A. Pilot screening in an uHTS format with Spectrum library of 2,000 compounds. Percentage of inhibition was calculated for each compound. A hit cut-off of 40% was used, leading to the identification of hit compounds. **B.** GST pull-down assay optimization with lysis buffer of 1%NP-40 and 0.25% Triton X-100. Optimization also of lysate method for HEK-293T cells with rotation for 30°C or sonication for 5 second. Finally, different amounts of lysate were tested for detection of GST-MYC and Venus-flag-NSD3S PPI. **C.** Validation of positive hit compounds by GST-pull down assay for GST-MYC/Venus-flag-NSD3S PPI in the presence of different concentrations of the compound.

A.3 Ultra-high-throughput screening of small molecules for NSD3S/BRD4 PPI.

Introduction

NSD3S/BRD4 PPI has been studied previously and shown to be an important interaction for the progression of leukemia. Both NSD3S and BRD4 have been validated as oncogenes and BRD4 as a therapeutic target for cancer. We postulate here NSD3S/BRD4 PPI as a potential target for cancer therapy due to its demonstrated functions in processes that drive cell transformation.

Results

In collaboration with Dr. Du and others, we developed a time-resolved fluorescence resonance energy transfer (TR-FRET) assay for ultra-high-throughput screening (uHTS) to find disruptors for NSD3S/BRD4 PPI, having a positive signal for the interaction (Figure A-3A). To validate the assay for screening in a 1,536-well uHTS format, a pilot screening was carried out using the LOPAC library containing 1,280 compounds with a final concentration of 20 mM (Figure A-3B). Work published in 2016 showed the structural mechanism of NSD3S recognition by the BRD4 ET domain (Figure A-3C). Further, it shows, that interacting sequence 152-163 of NSD3S it is similar to MLV integrase peptide (Figure A-3C). We tested the synthesized MLV peptide in TR-FRET and flag-immunoprecipitation, in both seeing a dose-dependent disruption of NSD3S/BRD4 interaction (Figure A-3D and A-3E).

Conclusions

Together, the results show the development of a uHTS assay for NSD3S/BRD4 PPI and the validation of MLV peptide as a disruptor, which can be used a positive control for later compound validation.

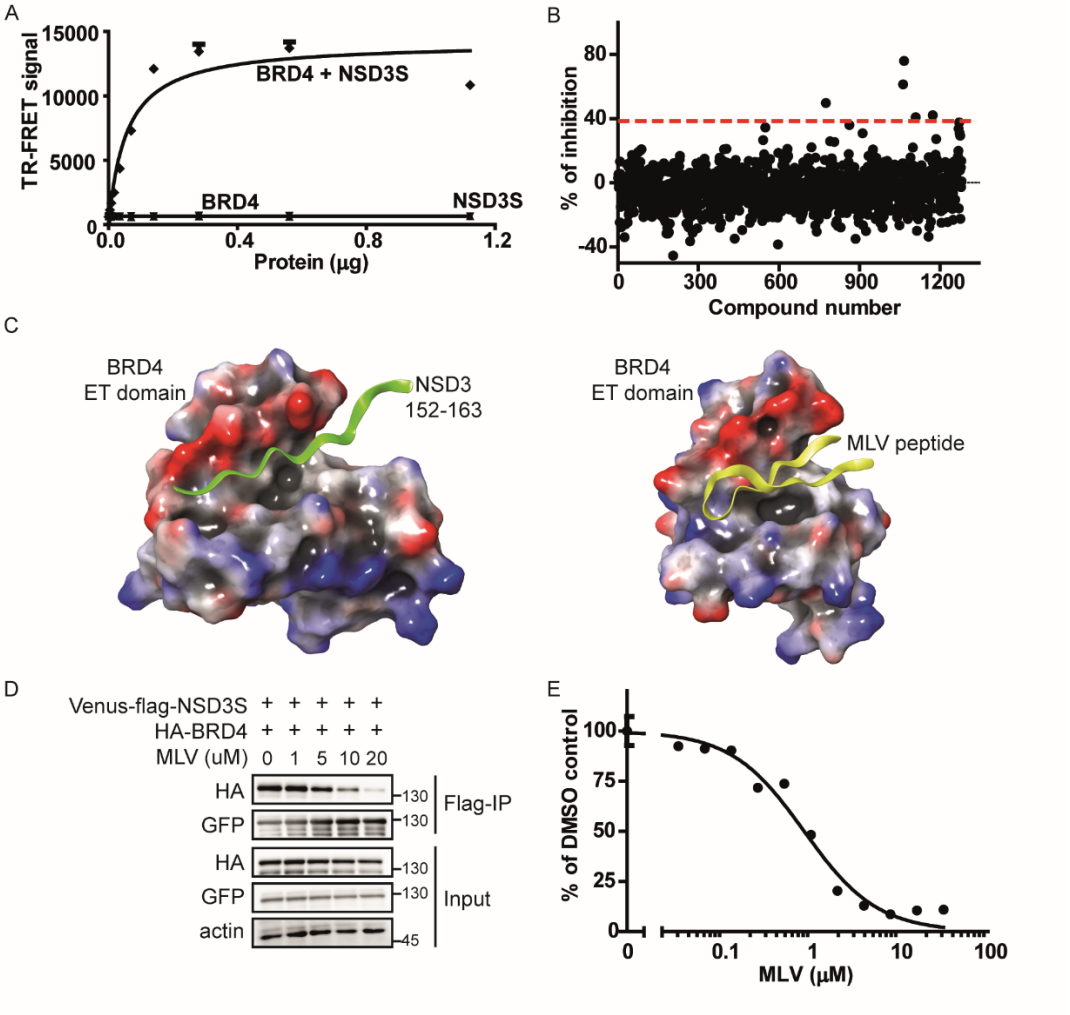
A
TR-FRET signal
15000
10000
5000
0
BRD4 + NSD3S
BRD4
NSD3S
0.0
0.4
0.8
1.2
Protein (μg)
B
% of inhibition
80
40
0
-40
0
300
600
900
1200
Compound number
C
BRD4
ET domain
NSD3
152-163
BRD4
ET domain
MLV peptide
D
Venus-flag-NSD3S + + + + +
HA-BRD4 + + + + +
MLV (uM) 0 1 5 10 20
HA
GFP
130
130
Flag-IP
HA
GFP
actin
130
130
45
Input
E
% of DMSO control
100
75
50
25
0
0
0.1
1
10
100
MLV (μM)

Figure A-3. Development of a uHTS for NSD3S/BRD4.

A. HEK-293T cells were transfected with HA-BRD4 and Venus-flag-NSD3S. The cell lysate was used for TR-FRET assay. **B.** Pilot uHTS was carried out in a 1,536-well plate using 1,280 compounds of LOPAC library. Percentage (%) of inhibition was calculated. A hit cut-off of 40% was used. **C.** Structure of BRD4 ET domain and NSD3S linear binding peptide (on green) and MLV β-sheet peptide (on yellow). **(E-F).** Co-expression of HA-BRD4, Venus-flag-NSD3S and increasing concentrations of MLV peptide on **E.** Flag-immunoprecipitation. **F.** TR-FRET assay.